Confidential

For 5 years from 16th August 2018

Please delete the file and report to kenwcheng@hotmail.com if you receive this document by accident

Optimal Wind Farm Lifetime Power Production

Department of Wind Energy Master Report

Wai Hang Cheng

DTU Wind Energy-M-0205

August 2018

DTU Wind Energy
Department of Wind Energy

Authors: Wai Hang Cheng

Title: Optimal Wind Farm Lifetime Power Production

DTU Wind Energy-M-0205
August 2018

Project Period:
November 2017 – August 2018

ECTS: 45

Education: Master of Science

Supervisors:

Taeseong Kim
DTU Wind Energy

John Bagterp Jørgensen
DTU Compute

Wim Bierbooms
TU Delft

Peter Fogh Odgaard
Goldwind Energy

Remarks:
This report is submitted as partial fulfillment of the requirements for graduation in the above education at the Technical University of Denmark.

DTU Wind Energy is a department of the Technical University of Denmark with a unique integration of research, education, innovation and public/private sector consulting in the field of wind energy. Our activities develop new opportunities and technology for the global and Danish exploitation of wind energy. Research focuses on key technical-scientific fields, which are central for the development, innovation and use of wind energy and provides the basis for advanced education at the education.

We have more than 240 staff members of which approximately 60 are PhD students. Research is conducted within nine research programmes organized into three main topics: Wind energy systems, Wind turbine technology and Basics for wind energy.

Technical University of Denmark
Department of Wind Energy
Frederiksborgvej 399
2800 Kgs. Lyngby
Denmark

www.vindenergi.dtu.dk

Danmarks
Tekniske
Universitet


Optimal Wind Farm Lifetime Power Production

- Master Thesis Report -

in partial fulfillment of the requirements for the degree of Master of Science

in Wind Energy at Technical University of Denmark and
in Aerospace Engineering at Delft University of Technology.

Ken Cheng Wai Hang

August 16, 2018

Student Number: S161026 (DTU)
4596986 (TU Delft)

Supervisors:	Prof. Dr. Simon Watson	TU Delft, chair of the thesis committee
	Dr. Ir. Wim Bierbooms	TU Delft, supervisor
	Dr. Taeseong Kim	DTU, supervisor
	Dr. John Bagterp Jørgensen	DTU, supervisor
	Dr. Peter Fogh Odgaard	Goldwind, supervisor

Contents

List of Figures

List of Tables

List of Symbols and Abbreviations

σ_u	Standard deviation of wind fluctuation	S_i	Fatigue loads
$\lambda_o pt$	Optimal tip-speed-ratio	U	Annual mean wind speed
Ω	Rotational speed	U_{mean}	Annual mean wind speed
A	Weibull scale parameter	V_{ref}	Reference Velocity
$C_{p,opt}$	Optimal power coefficient	x	10-minute mean wind speed
D	Accumulative fatigue damage	CPC	Collective Pitch Control
D_{total}	Total fatigue damage	$CapEx$	Capital Expenditure
$D(t)$	Debt/ Profit	EPC	Envelope Protection Control
E	Electricity price	IPC	Individual Pitch Control
$F_{eq,L,accu}$	Accumulated equivalent load	MPC	Model Predictive Control
i_{annual}	Annual interest rate	$MxMB$	Main bearing moment (x-axis)
i_{daily}	Daily interest rate	$MxMB$	Main bearing moment (x-axis)
$I_u(z)$	Turbulence intensity	$MxTB$	Tower base moment (x-axis)
k	Weibull shape parameter	$MxTT$	Tower top moment (x-axis)
m	Slope of S-N curve (material properties)	$MyBR$	Blade root moment (y-axis)
n	Number of cycles	$MyMB$	Main bearing moment (y-axis)
n_{eq}	Equivalent cycles	$MyTB$	Tower base moment (y-axis)
$n_{eq,L}$	Life-time equivalent cycles	$MyTT$	Tower top moment (y-axis)
n_T	Turbine life-time	$MzBR$	Blade root moment (z-axis)
$P(V)$	Rayleigh distribution	$MzTT$	Tower top moment (z-axis)
R	Load Range/ Radius	$O\&M$	Operations and Maintenance
R_{eq}	Equivalent Load	$OpEx$	Operating Expenses
S_0	Ultimate strength of material	RFC	Rainflow Counting

Table 1: List of symbols

Acknowledgement

I am most grateful to my thesis supervisor from Goldwind, Dr. Peter Fogh Odgaard for his valuable review of previous revisions of this thesis report and this opportunity in discovering the potential of optimizing project revenue through wind turbine life-time fatigue control. I am also thankful to Dr. Taeseong Kim and Dr. John Bagterp Jørgensen, for their contribution at various stages of the project. I would also like to thank my supervisor from TU Delft Dr. Ir. Wim Bierbooms for taking an active interest in the thesis and advising me from time to time. I would also like to thank Marianne Hjorthede Arbirk for her help on the EWEM thesis administration.
A special thanks to all the EWEM students who have spent the past two years together going through the program together.
I would also like to thank my family and girlfriend for their continuous support. The journey would be different without their unwavering support.

Abstract

This project is a collaboration between Goldwind, Technical University of Denmark (DTU) and Delft University of Technology (TUDelft), of which focusing in developing an optimization model that could determinate the optimal operation schedule for wind turbine under the uncertainty of the electricity price and limitation in life-time equivalent fatigue loads, for the purpose of improving and maximizing the revenue or cash flow for wind farm project.

The project comprises of two main parts, including the design and validation of up- and de-rated operation modes, and the model development and optimization of the revenue. The design of the different operation modes provide varies rated power without sacrificing the life-time structural integrity, as such offer extra flexibility in wind turbine operation schedule according to the fluctuation in electricity price. Life-time equivalent loads would be calculated for the different operation modes design and a weighting factor, that indicate the rate of fatigue consumption relatively to the normal operation, would be computed and used in the optimization process. An optimization model is developed based on the turbine structural constraints as well as the financial profile. The optimization model processes the electricity price data and other wind turbine data, for example the fatigue consumption, to reproduce the optimal operation schedule and operation price thresholds that would yield utmost financial benefits.

The optimizer has a proven performance improvement in revenue generation of 1.5% and 5% reduction in the project related interest payment under one of the case study under electricity price uncertainty. The model is effective in scheduling the turbine operation upon the varying electricity price. This optimization model is providing game changing insights and operation strategies that could be used throughout the turbine life-time under the ever changing electricity price of the energy market. And further drive down the cost of energy in the highly competitive market.

By improvising continuous input to the optimizer including bending moment sensors inputs, the optimization process could reproduce a more accurate revenue improvement.

1 Introduction

Normally wind farms are designed and financed with their life-time, 20 years. Projects are usually financed at the early stage of the development, when construction take place. The capital cost is tremendous for a wind farm project as well as the interests financing the project. This thesis investigate the feasibility by frontloading the power production of the wind turbine/ farm, such that more power is generated at the beginning of the wind farm life-time, in order to pay less interests and improve the net present value of the wind farm.

A frontloaded or up-rated power production mode is beneficial to project management because it provides extra flexibility on how the turbine generate power. However, the overload on the turbine components could result in a shorter components life-time and contribute to a de-rated turbine. In order to ensure the turbine could serve its 20 years life-time, a fatigue load analysis would be necessary in determining and managing the distribution of fatigue load generation under different operation modes under assumptions, for example, that the generator and converter would be able to manage the specified extra workload. Through the fatigue load analysis, a detail profile of the turbine operation limit under the up-rated operation mode could be determined and vice versa for a de-rated operation mode.

The designed turbine operation scheme would then be evaluated by their cost of energy, loan principle based on project assumptions and electricity prices accordingly. The objective of the evaluation is to optimize the operation scheme such that the optimal operation schedule of the wind turbine could yield the most revenue in operation management at the end of the project, in another words earn the most money.

Furthermore, few extensions could be leveraged under the designed operation modes. Operation and maintenance (O&M) is one major field in wind farm operation, few expected maintenance schedule of the turbine could be adjusted according to the shifted fatigue load of the turbine. The correlation between the O&M cost and the fatigue load is an invaluable analysis. Other correlations, for example with the turbulence intensity, could also be insightful. However, only the coupling between the electricity price uncertainty with the fatigue load of the turbine under different operation mode would be considered under this thesis. And a great portion of the project will be spent on explaining how the optimization model could calculate or continuous monitor the optimal operation schedule.

The thesis will explain in details how the up- and de- rated operation modes are made and how the two operation modes could make a different in maximizing revenue in section 5. The section would also covers the life-time equivalent fatigue load calculations, of which provides the important weighting factors during the optimization process. With the weighting factors, section 7 would cover how the financial calculation formulate the mathematical model for the optimization. The section would also cover some benchmark examples and illustrate how the optimizer can maximize the profit. At the end, a closed-loop optimization model is also discussed and illustrated how the system can continuously be applied under the daily varying electricity price with uncertainty.

2 Literature Review

In the literature review, three aspects related to the project, namely the fatigue and operation design, financial and optimization, are looked into. The purpose of doing so is to investigate the current state-of-the-art methodologies in relation to the project.
On the turbine technology side, the fatigue load calculations and operation control design, literature that are related to deriving new power level operation for existing turbines are investigated.
On the financial side, literature that calculated technology financial comparison are reviewed. Few literature that provide important parameters for financial model realization are reviewed as well.
Lastly, optimization related literature that provides deterministic optimization are studied as a mathematical model for the turbine life-time fatigue financial calculation has to be developed in this project.

2.1 Controller Design

As part of the project is to design a specific operation for the wind turbine such that it could operate at different designed power level, the controller designs strategies are important.

Until now in wind turbine control, torque controller are utilized before rated wind speed, in order to maintain the optimal lambda, tip-speed-ratio, for the operation. After rated wind speed, the turbine start to behave with constant power output, it is because the pitch controller toke over the controlling algorithm so that a smooth power level could be maintained after the rated wind speed. Most of the control system, at the moment, are using more traditional Collective Pitch Control (CPC) or more recently researched Individual Pitch Control (IPC) after rated wind speed. PID control with gain scheduling is the classic control system for CPC. However, fatigue loads could be further reduced and improve wind turbine life-time by introducing advance adaptive control, for example Model Predictive Control (MPC), or IPC, [Menezes et al., 2018]. The use of IPC emphasize on reducing individual blade root bending or to damp blade structural modes in order to reduce fatigue loads. One of the objectives in the literature review is to investigate more possible ways in reducing fatigue load and yield more frontloaded operation.

As the project is not going to design a new controller, different commonly used controller strategies are discussed and determined if it is feasible to be implemented in the project.

For torque controller, many commercial turbines have adopted the Maximum Power Point Tracking (MPPT) strategy, which aims to optimize the efficiency. One of them is the Optimal Torque Control (OTC), the OTC is a standard algorithm that imposing the torque accoding to a quadratic law based on the rotor speed [Menezes et al., 2018].

$$T_g = k\Omega^2$$

$$k = \frac{1}{2}\rho\pi R^5 \frac{C_{p,opt}}{\lambda_{opt}^3}$$

where we have k as a constant, which is commonly known as the torque controller gain; T_g is the generator torque; Ω is the rotational speed; ρ is the air density; R is the radius; $C_{p,opt}$ is the optimal power coefficient; λ_{opt} is the optimal tip speed ratio. It is derived based on the aerodynamic characteristic of the wind turbine in order to obtain the optimal value for power coefficient and tip-speed-ratio. By further implementing additional torque control loop, the controller could dampen drive-train torsion mode and resonant loads. While, the OTC requires only a shaft rotational speed sensor, according to the equation shown above, it's simplicity to the control algorithm is considered as a big advantage.

On the other hand, for pitch controller, most of the commercial wind turbine nowadays uses the proportional-integral (PI) collective blade-pitch controller, CPC,to regulate rotor speed above rated wind speed regime, where the controlling algorithm is listed below [Jackson and Dirk, 2016],

$$\beta_c(t) = K_p\Omega_e(t) + K_i \int_0^t \Omega_e(\tau)d\tau$$

where $\Omega_e = \Omega_d - \Omega$ is the error in rotor speed between the desired and current rotor speed; While K_p and K_i denote the proportional and integral controller gain constant. Traditionally, the controller gain employ a schedule method, which aims to cope with the non-linearities of the pitch actuation. However, using CPC has a draw back, which is the assumption of similar loads and behavior on the usually unbalanced loads and stresses on the three blades.

For a more advanced methodology, the pitch controller can adopt individual pitch controller, IPC. Similar to CPC, IPC also ensure power generation to be maintained within its nominal value by reducing wind turbine aerodynamic efficiency with individual blade pitching under varies wind speed in the region 3. While the change in aerodynamic efficiency and blade pitching, has significant influences on the structural loading on the turbine, literature [Vlaho et al., 2015] has proved that IPC has been able to reduce the structural loads including blade harmonics as well as tower loads.

Show in figure 1, referenced from [Vlaho et al., 2015], it demonstrated the logic of the IPC. It is a closed-loop time dependent controlling process. Moments and rotational speed were used as the inputs for the IPC. Each parameters are sent into the control algorithm with different harmonics or load reduction strategies as well as the nominal power controller, such that the controlling values would no longer be the same for each blade, like the gain schedule from CPC.

Since wind turbine has to deal with extra external forces like gravity and stochastic profile of the incoming wind, blade structural loads have significant effect in contributing to fatigue and shorten wind turbine life-time. Advanced control algorithms have to be adopted.

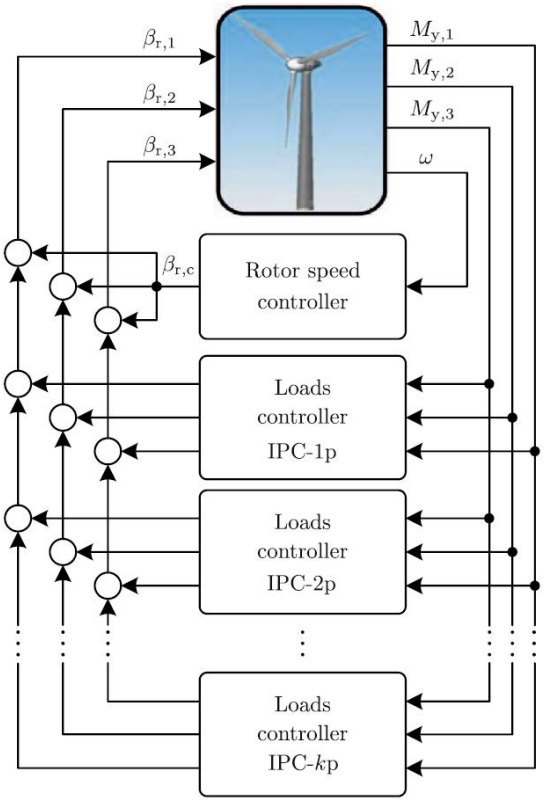

Figure 1: IPC working principle in load reduction

2.2 Power Production

In this section, few aspects of research related to the power production of wind turbine are being investigated. The findings would be beneficial in making assumption for the wind turbine operation condition in this thesis.

Icing is one of the limitation that would cause under performance of the turbine. In cold climate regions, turbines have to adapt effective ice mitigation design to withstand the performance loss due to the ice accretion. It has been found that aerodynamic performance would be deteriorated up to 30% lift reduction and 50% drag increase of the blade [Zanon et al., 2018]. This could be translated into 22% loss of the power production. A finding from the paper also demonstrated that up to 6% of the power production could be improved by reducing the rotational speed during icing event. Meanwhile, 3% loss would happen by keeping the same rotational speed.

Wake effect is another aspect that would alter the power production and fatigue loads. The higher turbulence intensity and wind shear, increased by wake effect from upwind wind turbine, could cause 7% reduction in annual energy production (AEP), and increase fatigue loads by up to 20% under a case study in Korea [Hyun et al., 2015].

2.3 Fatigue Load Reduction and Life-time Fatigue Analysis

As one of the main parameters is to determine the life-time of the wind turbine. By reducing fatigue loads, the wind turbine will have a longer life-span and as such result in more power production potential. A lot researches has been done in reducing fatigue load and improving the reliability of wind turbine through control system.

In controlling fatigue load, a novel Envelope Protection Control (EPC) has been proposed by [Vlaho and L, 2017]. The EPC based on the concept of envelope riding. An online numerical optimization method is used to predict the extreme wind speed that cause the turbine to encounter the envelope of its safe operation range in each time instant. Based on the extreme weather condition, controller inputs are computed such that the response would always maintain within the safety region at all time and at most riding on the envelope boundaries without leaving it. The EPC is capable in ensuring the entire range of wind speed. With comparison between the EPC and the standard control algorithm, for example, peak-shaving and soft cut-out schemes, the EPC illustrated in reducing loads and improving power output.

Researches have been done in discovering more methods in reducing the fatigue loads for wind turbine. A distributed flap control system has been implemented and tested [Bernhammer et al., 2016]. It demonstrated that the smart rotor would be able to reduce the fatigue load for 5-15%. The research has also taken into different load cases, including power production and start-up mode, normal and extreme turbulence, extreme gust and wind direction changes.

Similar research [Mingming et al., 2016], has also shown the implementation of smart rotor is able to reduce fatigue loadings by 12.0-22.5% in contrast to the collective pitch control method. The smart rotor shown modification of the in-phased flow-blade interaction in to an anti-phased one for 1P mode. This means that by doing so, the damping of the structure is enhanced, subsequently it contribute to the reduction in fatigue load accumulation.

In terms of the influence of fatigue load into one of the components of the wind turbine, [Niesłony, 2009] has performed analysis for turbine components at early designing stage. The purpose is to perform calculation through algorithm to determine the fragments of different service loading part that is utmost important to normal wind turbine operation under fatigue loads. This multiaxial loading calculation results has an influence to smoothing fatigue damage accumulation on the components, such that improve the performance resisting fatigue load.

Regarding fatigue assessment for wind farm, [Bouty et al., 2017] has proposed an extrapolation methodology in determining fatigue damage profile through out the life-time. The study intended to step towards an effective and efficient assessment methodology for lifetime extension for offshore wind farms. The literature has proved that for given environmental data commonly available during the design stage, the fatigue reassessment result indicated that the extrapolation in feasible for selected parameters when the environmental condition changes are small. The environmental condition changes could consist of the soil conditions, wind & waves conditions as well as the water depth. The

methodology is especially useful when offshore projects can make use of the fatigue re-assessment result as a closed loop algorithm integrating with accumulated fatigue damage sensor. This could be beneficial in extending the life-time of offshore wind turbines or more power production in the sense of this project.

Moreover, literature regarding fatigue load calculation with S-N curves for typical turbine materials are reviewed. [Boyer, 1985] is a solid literature that provided massive range of fatigue calculation details from different governing equation to comparison of fatigue characteristic.

Literature from [Romans and Peter, 2015] also employed the state-of-the-art methodology in calculating life-time equivalent fatigue load. It further makes comparison with different power rating wind turbines in order to make comparison on the developing trend on fatigue load and power rating of wind turbines. Nonetheless, its methodology in life-time equivalent fatigue load is reviewed for the project. An value of exponents of trend equation has been developed in the literature as well in translating the relationship between the fatigue and power rating.

A case study on the fatigue load calculation has been conducted under New Zealand conditions [Noda and Flay, 1999]. The literature investigated the fatigue load difference due to the non similar wind resources behavior in Denmark and New Zealand. The results concluded that typical overseas turbine site has 2 to 2.5 fold of damage increase than the New Zealand site. Although the result of the literature is location specific, the idea of different wind resources within a wind farm could cause increased or decreased fatigue load is important.

2.4 Optimization

Researches in both academic and industrial field have shown increasing published paper using control system to reduce fatigue load and improve the power production efficiency. As mentioned before, more advanced control system, for example, MPC system has been implemented and researched over the recent years. MPC is an feedback-feedforward optimization algorithm that make use of the wind turbine system that could predict the wind speed at the next instant. Such that turbine control system could adjust accordingly. [Sanchez et al., 2015] has conducted a case study and demonstrated that 26% of the accumulated fatigue load could be mitigated through using MPC system with minimal power production reduction of 1.9% by coupling MPC system with the wind turbine control system. A state-of-the-art fatigue load analysis is also demonstrated in this paper.

The benefit of using MPC in wind turbine is that it could maximize the power production while maintaining with minimal fatigue loads. When the job of the controller gets more complicated and has to deal with multiple objectives, commercially used PI controller could become inefficient or hard to be tuned in a way to work effectively. By developing a mathematical model, the MPC can handle it systematically under the Multiple-input-multiple-output (MIMO) environment. As mentioned in literature [Lio et al., 2014], there

are three major MPC methodologies, namely Linear MPC, Scheduled MPC and Nonlinear MPC. For linear MPC, the controller is based on a linearized wind turbine model. It require less computational power than nonlinear model, however the linearization part has to be justified. For Scheduled MPC, it is a method in between linearity and non linearity. Few operating points, that might not have good performance under the linearization are operated differently. Lastly for nonlinear MPC, it is not as common as the other two method at the moment in the industry due to its higher computational cost, of which has to solve extra optimization constraints and the model would be more complicated.

Another literature has covered the use of MPC with the yaw drive mechanism [Song et al., 2018]. The literature proposed to integrate the yaw controller with MPC methodology, and aims to take advantage of the prediction in incoming wind direction so that yaw controller could adjust the rotor to wind direction alignment with minimal difference, by doing so, more power could be extracted. The controller algorithm has used discrete data obtained at every sampling time for prediction (10s, 30s and 60s mean values by hybrid ARIMA-KF model). The model has been applied to in a wind farm in China with the available the wind resources data and shown an extra 1% of power extraction capability. Figure2, referenced from [Song et al., 2018], shown the block diagram of the MPC algorithm in dealing yaw alignment control.

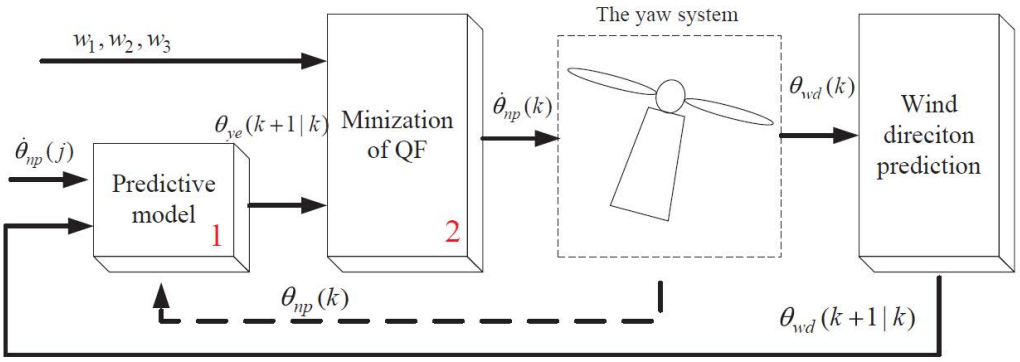

Figure 2: Proposed MPC Block Diagram

where w_1, w_2 and w_3 are three different weighting value to be used in the Quality Function (QF). $\dot{\theta}_{np}(j)$ represents the permissible yaw speed. $\theta_{ye}(k+1|k)$ represents the predicted yaw error at the kth sampling period. $\dot{\theta}_{np}(k)$ represents the yaw speed during the kth control period. $\theta_{wd}(k)$ represents the measured wind direction sampled at the kth sampling period. $\theta_{wd}(k+1|k)$ represents the predicted mean values of wind direction at the kth sampling period. $\theta_{np}(k)$ represents the nacelle position measured at kth sampling period The primary control objective in this algorithm is to track the predicted wind direction, also to decrease the yaw error. The secondary control objective is to avoid the overuse of the yaw actuator. The control algorithm with MPC is similar to normal control logic, but with the addition prediction to feed-back into the minimization of yaw errors.

Even though a lot of researches have been done in controller for optimization, many other literature shows different approaches in wind turbine optimization due to the extra com-

petitiveness that optimization could bring to wind farms. Optimization for the wind farm layout in coupling with the controller strategies were covered by [Mahmood et al., 2015]. The paper developed three models of a wind farm based on three different control strategies. The constant rotational speed after rated were proved to be the best strategy in power production.

Researches focus not only on controller within wind turbine itself, but also shed light on the feasibility in controlling fatigue loads throughout the whole wind farm. [Schram and Vyas, 2007] has patented the idea of a central controller, which collect loads data from each wind turbines within the wind farm and send feedback signals to each individual turbine to reduce load in compliance to the power generation limit of the wind farm. [PF and PB, 2013]

Optimization tool is also applied to deal with wind power ramping events, when wind speed is reduced significantly under a short period of time. A two-stage optimization tool is designed to smoothen the output power and reducing the ramping rate by utilizing power rate limit and energy storage system collaboration. The two stage optimization tool aims to minimize the ramping rate, maximize the power generation and load reduction. With a case study in Korea, the tool has proven to reduce wind turbine load and reduce the risk of ramping events. [Weipeng et al., 2017]

Although there are a lot of optimization in wind turbine in order to reduce fatigue load on the rotor design, there are no research being done in optimizing the operation mode base on the financial consideration. This shows the novelty of the simulator model in this thesis.

Model Development

Another part of the project is to develop a mathematical model, which translate the relationship between the fatigue loads with the financial side of the wind turbine operation. The model is further optimized such that a optimal solution is computed for the turbine operation. As a result, literature study on the model development is conducted.

Optimization under uncertainty is not a recent topic in the optimization field, a large number of problems nowadays in relation to production planning or scheduling, transportation, finance and engineering design require a decision to be made with the presence of a level of uncertainty. In this project, the uncertainty is the electricity price. Stochastic programming is one of the ways in coping with optimization problem. [Sahinidis, 2003]. The literature cover different theory and methodologies in how stochastic programming are developed.

Stochastic Linear Programming textbook, [Kall and Mayer, 2010], is another useful literature that summarized different method of constructing model optimization with uncertainty. It is very beneficial in stepping up the model from deterministic model to a stochastic one.

During the development of the deterministic model, a lot of calculus has to be done. [Abel, 2011] provided a very good reference in dealing with time-dependent linear scale equation. Considering the general linear scalar equation,

$$\dot{v} = a(t)v + b(t)$$

$$v = v_h + v + p$$

Homogeneous Solution:

$$\dot{v} = a(t)v$$

$$\int_{v(t_o)}^{v(t)} dv \frac{\dot{v}}{v} = \int_{t_0}^{t} d\tau a(\tau)$$

$$log(v(t)) - log(v(t_0)) = \int_{t_0}^{t} d\tau a(\tau)$$

$$v(t) = v_0 e^{\int_{t_0}^{t} d\tau a(\tau)}$$

Inhomogeneous Solution:

$$\dot{v_p} = \dot{C}e^{f(t)} + C\dot{f}e^{f(t)}$$

$$\dot{v_p} = (\dot{C} + C\dot{f})e^{f(t)}$$

$$\dot{v_p} = a(t)v_p + b(t)$$

where $\dot{f} = a(t)$.

$$\dot{C} = b(t)e^{-f(t)}$$

which is solvable by,

$$C(t) = \int_{t0}^{t} b(\tau)e^{-f(\tau)}d\tau$$

the full solution is

$$v = v_h + v_p = (v_0 + \int_{t0}^{t} b(\tau)e^{-f(\tau)}d\tau)e^{\int_{t_0}^{t} d\tau a(\tau)}$$

This equation was used in the early stage of the optimization model development in developing the early deterministic model.

In regards of model development, there are plenty of wind turbine model development literature. [Petru, 2001] is one of the literature that cover a wild range of turbine behavior into mathematical models. However, it did not cover the model coupling between the fatigue load with power production with financial calculation.

As the optimizer would conduct an sensitivity analysis, literature review in relation to the sensitivity analysis approach are studied. [Mouida and Alaa, 2011] has adopted the One-Factor-At-A-Time (OAT) approach in conducted sensitivity analysis. The OAT is a typical screening design to assess all constant parameter effect on the model result and classify them according to their sensitivity level.

2.5 Financial Model

Financial model and its optimization is not a new topic as well. Track back to 1998 Risø has already started to optimize wind farm in order to reduce cost. [Fuglsang and Thomsen, 1998] has documented some preliminary investigation in wind farm layout optimization for a wind farm with approximate 100 wind turbine in the southern part of Denmark. Numerical optimization and aeroelastic calculations were carried out to find the optimal wind turbine layout design for minimum cost of energy. The optimized solution showed a potential improvement of the annual energy production of 28%. The optimized scheme were also able to reduce cost by 11%.

When new era comes, financial model development shift towards technology advancement and comparison. A financial feasibility and investment attractiveness study is conducted [Mathur et al., 2017], to evaluate the effectiveness of a coupling control between Lidar and proactive individual pitch control. In this paper, a state-of-the-art financial model in determining attractiveness of a new technology implementation is developed. With the assumption of the wind turbine model, its capital cost, operations and maintenance (O&M) and component replacements cost; and the financial assumptions such as Internal Rate of Return (IRR). The net present value (NPV) of cash flow, payback period and equivalent annual annuity (EAA) could be evaluated with or without the implementation of the Lidar technology. The pro-forma cash flow and net present value of the wind turbine is a very valuable evaluation in technology adaptation.

Another literature compares different financial structure for wind turbine project in the United State [Harper et al., 2007]. Where it further divide different financial model into 7 categories, which has different financial characteristic in model development. The 7 categories are Corporate, Strategic Investor Flip, Institutional Investor Flip, Pay-As-You-Go, Cash Leveraged, Cash & PTC Leveraged and Back Leveraged. The idea of all the 7 categories are distinguish with the different tax or financial and stakeholder profile. Some of them are reported to be more beneficial in lowering LCOE but with a high financial constraints and vise versa. However, the financial model developed in this project shall not take into account of the 7 categories as the United State is not part of the target study area, and a more simplified financial model shall be developed. If one is interested in further detail breakdown, it is encouraged to visit the literature for more explanation.

[Obling, 2010] is a literature that investigate the possibility of developing a real options valuation model that improve the valuation of wind farm under development compared to discounted cash flow valuation model, it studies some developing wind farms in Denmark. As a result, a lot of the financial model and parameters are useful for the project model development. The financial time line describing how wind farm are built financially provide significant insight in the financial model development.

Financial Parameters

In order to main the financial model realistic, up-to-date financial parameters have to be utilized, for example the CapEx calculation, where a reasonable EUR/ MW shall be

obtained to make a realistic model. [Fingersh et al., 2006], [Deloitte, 2014], [IRENA, 2012], [Mbistrova, 2017], [IRENA, 2017] and [Stehly et al., 2017] are reviewed. Literature provide the recent trend of the LCOE of wind turbine which is extremely useful in determining the suitable value for the financial model. For example, the value shown in [Stehly et al., 2017] and [IRENA, 2017] are similar for the cost of installment per MW in offshore wind farm category. This provide insights for decision making when formulating the model.
Fig 3 and 4 are figures extracted from IRENA 2017 Renewable Power Generation Cost Report [IRENA, 2017]. They showcased the trend as well as some numerical value for wind farm investment. These parameters are also very useful for financial model development.

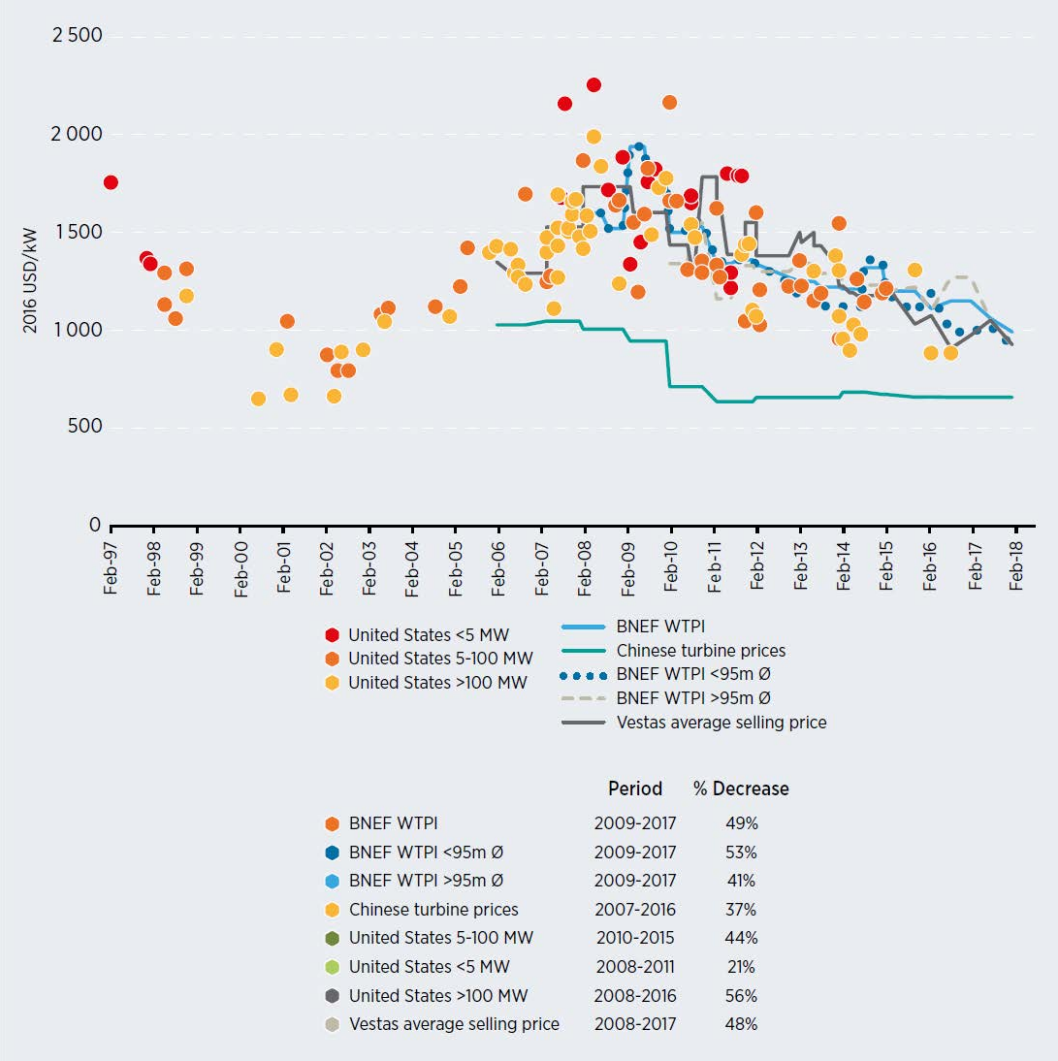

Figure 3: Wind turbine price indices and price trends, 1997-2017

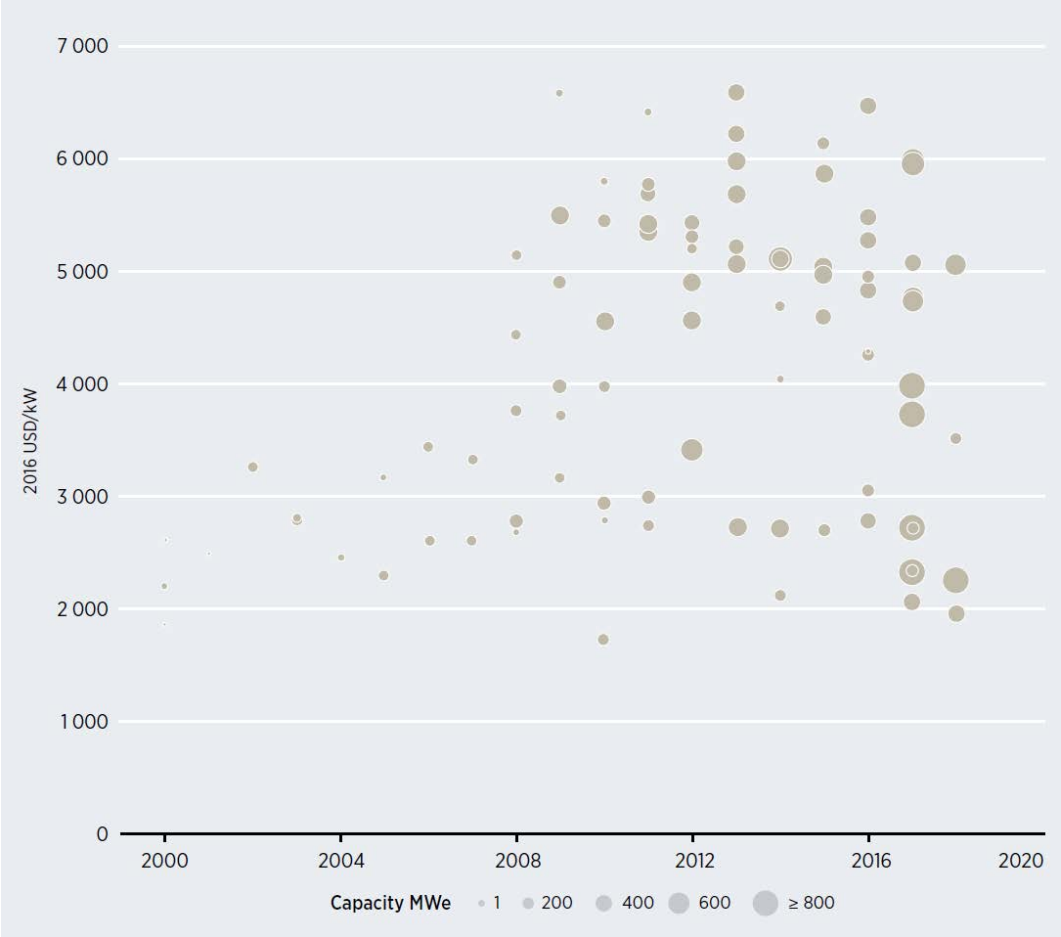

Figure 4: Total investment cost for commissioned and proposed offshore projects, 2000-2018

And finally, [McCrone, 2016], [China, 2017] and [Toke, 2017] discussed the interest rate for the latest green project investment banks have been using. And the electricity price in china as well as Europe.

3 Background information

In this section, all the important background information would be discussed. First, it would cover the assumption of the wind resources for this project. Following with the choice of the wind turbine model used with an introduction in load cases. And end with some financial background for running a wind turbine project.

3.1 Wind Resources

3.1.1 Wind Turbine Class

One of most important standard in wind energy industry is The International Electrotechnical Commission (IEC) standard. The IEC organization aims to promote international co-operation on the electrical and electronic standardization. IEC has outlined a detail standard on wind turbine design under the IEC 61400 instruction manual. Within the manual, the standard has spend an extensive section to describe the difference between wind turbine classes as to further indicate their corresponding environmental condition, in order to ensure an appropriate level of safety and reliability should be taken in the design phase.
Figure 5, has shown the different attributions on the reference wind speed and turbulence intensity corresponding to their wind class.

Wind turbine class		I	II	III	S
V_{ref}	(m/s)	50	42,5	37,5	Values
A	I_{ref} (-)	0,16			specified
B	I_{ref} (-)	0,14			by the
C	I_{ref} (-)	0,12			designer

Figure 5: IEC Standard Wind Class

The mean wind speed of the wind turbine class could be calculated with equation 3.1

$$U_{mean} = 0.2V_{ref} \tag{3.1}$$

Due to the fact that more wind turbine project are moving toward offshore, the wind turbine class for this project is assumed to be IA, wind class that portrait offshore climate. This also means that the mean wind speed and the turbulence intensity would be 10m/s and 0.16 respectively.

3.1.2 Weibull Distribution

The Weibull probability distribution is a statistical calculation of the wind resources, it represents the distribution of wind speed at a given site. The distribution also play a very significant role in the evaluation of the wind energy in the region. Weibull distribution is widely used by researchers involved both in wind speed and wind eregy analysis for many years [Piotr, 2017]. The well accepted distribution function, is a two-parameter function

including the shape and scale parameter, k and A respectively.

The Weibull distribution is utilized as the wind resources model for the project. The wind distribution provided by the Probability Density Function (PDF) would be used to calculate the power production as well as to compute the fatigue load of the turbine.
The Weibull distribution function is represented by the equation 3.2.

$$f(x) = k\frac{x^{k-1}}{A^k}exp(-(\frac{x}{A})^k) \tag{3.2}$$

The relationship between the mean wind speed with the two shape and scale parameters is represented by the equation 3.3

$$U = A\Gamma(1 + \frac{1}{k}) \tag{3.3}$$

in which, x is the 10-minute mean wind speed, U is the annual mean wind speed, A and k are the scale and shape parameter for the Weibull distribution respectively.
In wind industry, the shape parameter, k, usually has a good approximation for the wind speed data and is internationally applied when k = 2 [Piotr, 2017]. The distribution also become a Rayleigh distribution when k = 2.
As mentioned from previous section, the mean wind speed is assumed to be 10m/s under the wind class I. The scale parameter in the Rayleigh distribution could then be determined with equation 3.3 and result with A = 11.28 m/s.
According to the Weibull function, the PDF of the assumed wind condition could then be computed with the shape and scale parameter be set as 2 and 11.28 and formulate the PDF as shown in 3.3

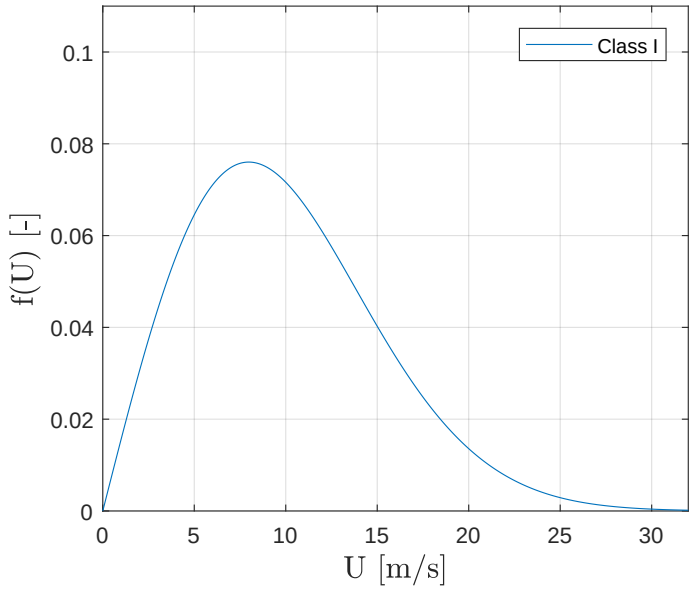

Figure 6: Probability Density Function for the wind class I

3.1.3 Turbulence Intensity

Turbulence intensity is an index that represents the turbulence in flow over the terrain with a specific roughness. Turbulence intensity could be calculated with equation 3.4 and the value should be between 0.05 and 0.2 most of the time.

$$I_u(z) = \frac{\sigma_u}{U(z)} \tag{3.4}$$

in which, σ_u represents the standard deviation of the wind fluctuations and could be calculated according to IEC standard as shown in equation 3.5

$$\sigma = I_{ref}(0.75V_{hub} + b); \quad b = 5.6m/s \tag{3.5}$$

3.2 Wind Turbine

The DTU 10MW Reference Wind Turbine (DTU 10MW RWT) has been chosen to be the wind turbine model to be studied in this research. The DTU 10MW RWT is a turbine designed as part of the Light Rotor project. Not only the turbine is designed for 10MW, a prospective power production for offshore wind turbine, but the turbine is also modeled for Horizontal Axis Wind turbine simulation Code 2nd generation (HAWC2), an aeroelastic code developed also by DTU in dealing with wind turbine calculations. Simulations to compute fatigue loads could be done with the HAWC2 tools.
The attributions of the DTU 10MW RWT are as shown below in table 2.

Table 2: Key parameters of the new turbine design compared to the DTU 10MW RWT

Parameter	DTU 10MW RWT
Wind regime	IEC Class IA
Cut-in wind speed	4 m.s^{-1}
Cut-out wind speed	25 m.s^{-1}
Rated wind speed	11.4 m.s^{-1}
Rotor diameter	178.3 m
Hub diameter	5.6 m
Minimum rotor speed	6.0 rpm
Maximum rotor speed	9.6 rpm
Maximum generator speed	480 rpm
Gearbox ratio	50
Maximum tip speed	90 m.s^{-1}
Blade prebend	3.332 m
Blade mass	41715.7 kg

3.3 Design Load Basis (DLB)

Wind turbines usually stand for 20 years after erected. There would be times when the turbine has to be shut down due to regular maintenance, extreme wind or production optimization, etc. During the design process of the turbine, all of these scenarios are described as the design load cases (DLC) and verified through simulations. The validation of the turbine through this Design Load Basis focus in verifying the structural integrity

of all the components under the varies scenarios.

According to the IEC 61400-3 and the Loads and site conditions for wind turbines by certification body DNV-GL, DLCs are divided into several categories including, power production, power production with the occurrence of fault, start up, normal shutdown, emergency stop, parked (standing still of idling), parked with fault conditions and transport, installation, maintenance and repair. All of the mentioned DLCs are the suggested minimum categories, the turbine structural design shall comply. Because the DLCs are real situations that the turbine would experience when they are constructed at the site, the outcome of the DLCs verification could help the turbine to be well designed in a holistic way. For example, when turbine has conduct an emergency shutdown, the calculation for the DLC 5.1 would be able to summarize if the turbine structural integrity comply with the requirement. Similarly, when the turbine was transported and being repaired, DLCs 8 would be able to summarize those situation. All these design situations are well defined to cover all the expected activityies of the wind turbine. In table 3 below, it shows the general DLCs for turbine verification. To particular wind turbines or their operation environments, for example offshore, the DLCs would changes in numbers and focus.

Table 3: Key DLCs for onshore wind turbine verification

Design Situation	**DLCs**
1) Power Production	1.1, 1.2, 1.3, 1.4, 1.5, 1.6, 1.7
2) Power Production + Occurrence of Fault	2.1, 2.2, 2.3, 2.4, 2.5
3) Start Up	3.1, 3.2, 3.3
4) Normal Shutdown	4.1, 4.2
5) Emergency Stop	5.1
6) Parked (standing still or idling)	6.1, 6.2, 6.3, 6.4, 6.5
7) Parked with Fault Conditions	7.1, 7.2
8) Transport, Installation, Maintenance and Repair	8.1, 8.2, 8.3, 8.4, 8.5, 8.6

In this study, the DLC 1.2 would be focused as it is the case to investigate in fatigue load. Under the design situation number 1, Power Production, it is assumed that the wind turbine has full connection to the grid as well as operating normally without faults. Yaw misalignment would also be taken into account in the DLC 1.2 case, it is usually taken as $\pm$ 10^o so the simulation has to be done in -10^o, 0 and $+10^o$. Although the DNV-GL load cases manual suggested $\pm$ 8^o, $\pm$ 10^o is adopted in this study.

DLC 1.2 is a load case that assess the fatigue load under power production in normal turbulence scenario. The entire operational range of the turbine is simulated with normal turbulence under the IEC wind class suggestion. As mentioned, yaw misalignment is set to be $\pm$ 10^o. Under HAWC2 simulation, six seeds per wind speed and yaw misalignment are used. The seed represents the different turbulence box created in the simulation. The simulation length is set to be 600s, with wind speed from 4m/s to 26m/s in steps of 2m/s. Gust and Fault are not studied in this load case.

After the simulation, the load spectrum of each load sensors on the turbine under each wind speed and seeds are computed. They are all combined to calculate the life-time load spectrum. Detail methodology would be discussed in the section 4.

3.4 Wind Turbine Financial Model

This project optimizes the financial model with different turbine operations under the constraints of the turbine structural integrity and the uncertainty factors such as the fluctuation of electricity price. A financial model of the wind turbine is developed in order to analyze the feasibility and attractiveness of the optimized operation. Furthermore, a pro-forma cashflow based economic tool is modeled for comparison and detail financial breakdown.

In this section, the economic side of the wind farm project life cycle will be discussed in detail. The discussion will act as a foundation for the financial model.

3.4.1 Project Life Cycle

The project life cycle provides important milestones throughout a wind farm project, which indicate the amount of time and financial support developer has to put into the project. These processes would influence on the amount of money developer have to investigate into the project or the amount of tax or interest they have to pay. All this numbers would influence the attractiveness of the project, for example, if the construction process is delayed, causing the turbine only to start operate one year later than designed. It is very likely that the developer has to pay extra interest for the debt and cash flow would be delayed as well. By know the activities the project has to go through, a more accurate financial model can be formulated to reflect each projects point of interest and their optimization focus.
Project would normally divided into three phases, Pre-development, Development and Operation Phase. Each of these phase represent the certain type of work or process to be conducted before the next phase proceed under a certain time frame as shown in figure 7.

Tender process, Government subsidies (if possible) and land lease contract are all considered as Pre-development phase. This process is usually hard to estimate in terms of time cost, since most of the activities are legal related, which could take up to 10 years. Although it is hard to estimate the time for this process, the amount of money developer has to spend in this phase are minimal compare to the construction stage. As a result, the financial cost for this process only consist a small percentage of the Capital Expenditure (CapEx) for the whole project.

As for the Development phase, it includes feasibility studies, Environmental Impact Study, complaints & compensation and construction. This stage of the project involve all the technical and social aspect of the project and consume most of the CapEx. This stage usually take approximate 3 years depending on the varies factors, for example, the site location from the manufacturing plants, logistic difficulties, complexity of the terrain, etc.

Operational phase represents the stage where turbines are all constructed and commissioned for electricity generation. Revenue of the project starts to generate from this stage based upon the electricity price or under different agreements with governments, for example, Feed-in Tariffs (FIT), Feed-in Premiums (FIP), Auction System, etc. Even though most of the revenue is generated in this stage, the revenue has to cover the Operation & Maintenance (O&M) cost and the debt service throughout the project. This period usually last approximately 20-25 years, and the payback period of the project is usually 10 years.

During the Pre-development and Development Phase, there is no revenue from the project, as the turbines are not in operation. Most of the CapEx are spent during the construction stage, of which is the last stage in the development phase before the Operation Phase. The financial model, thus, is simplified by assuming that all the investment are put in year zero when the turbines are constructed and ready to produce electricity.
On the other hand, revenues starts to generate during the Operational phase and are calculated according to the electricity price during the 20 years. In the simplified financial model, the electricity price is set to be a constant value based on the Feed-in Tariffs concept. Furthermore, the electricity price is later considered as an uncertainty to demonstrate the project operate under more competitive auction system. Optimizing the operation under different economic systems is one of the goals in this project.

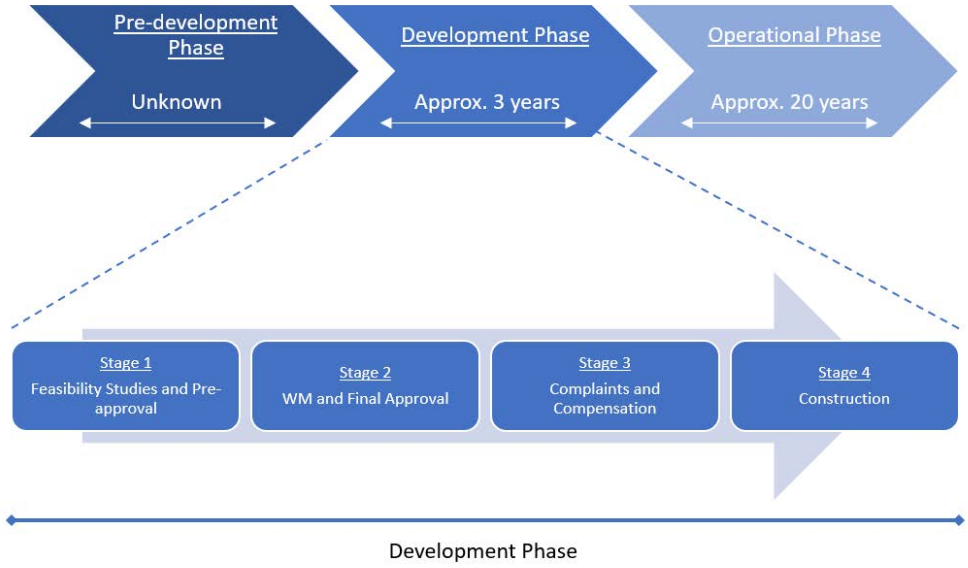

Figure 7: Project Life Cycle

3.4.2 Financial Model

The flow chart of the simplified financial model is shown below in figure 8, the purpose of this financial model is to integrate it as a function in the optimization process.

The first step of the financial model is to obtain a ballpark value of the CapEx at year zero. This would be in the form of debt in the project balance sheet. This value represents all the cost for Pre-development and Development phases as mentioned in the previous section. The calculation of the revenue would be based on the turbine power output capacity and the wind resources at the development site. As mentioned in the wind resources and operation mode section, the Rayleigh Distribution , representing the wind distribution at the site, combines with the 10MW power curve of the turbine to compute the AEP of the turbine. The energy is then sold based on the assumed electricity price to generate revenues for the project.
After calculating the annual revenue, cash after expenses can be computed by deducting the Operating Expenses (OpEx). Furthermore, depending on the debt service, the cash after debt would varies based on the interest rate. The net cash that generated after all the OpEx and debt service could spend on paying back the debt or keep in the form of cash depending on the debt payback strategies. For example, interests induced by debt could be minimized by spending all the available cash after debt in paying back the debt. On the other hand, leaving a portion of the net cash could be beneficial based on overall company financial status; however, extra interests shall be expected, which would affect the ultimate project payback period.

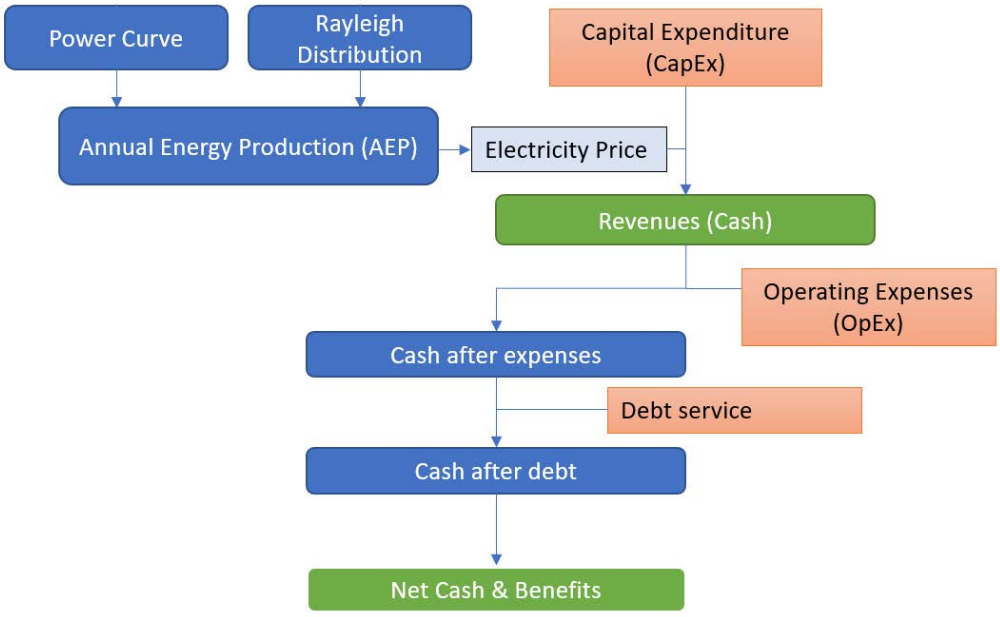

Figure 8: Financial Model Flowchart

3.4.3 Financial Values and Trend

This section would define the meaning of each financial input, CapEx, OpEx, electricity price and debt service, their current market values and trends. These values would be adopted for the financial model.
Capital Expenditure, CapEx, as mentioned in previous section consist of all the cost

induced during the Pre-development and Development phases.
The three major component cost categories and many subcategories are caused from wind turbine (e.g., wind turbine components), balance of system (e.g., development, electrical infrastructure, assembly, and installation), and financial costs (e.g., insurance and construction financing). The majority of the land-based project CapEx (67%) is in the turbine itself, whereas the turbine makes up 33% of the fixed-bottom offshore and 24% of the floating offshore reference project CapEx [McCrone, 2016]. Comparing to the cost of the turbine itself and the construction, paper works including feasibility studies and environmental impact studies only take up small amount of the total project cost.

With the increasing competitions within the industry, a lot of research and development have been conducted in minimizing the cost of the turbine and installation. As a result, turbine cost has been driven down tremendously over the decade. In fact, recent project developments in Denmark and Mexico could sustain their financial model without receiving subsidies from the government.

Figure 9 below[1] shows the trend of the CapEx of wind turbine from 2010 to 2017 according to IRENA report in 2017. It is assumed that the turbine used in this project would be offshore, and a value of EUR 2441/ kW is used for this financial model. The CapEx has also been assumed as a one time payment at the beginning of the operation period.

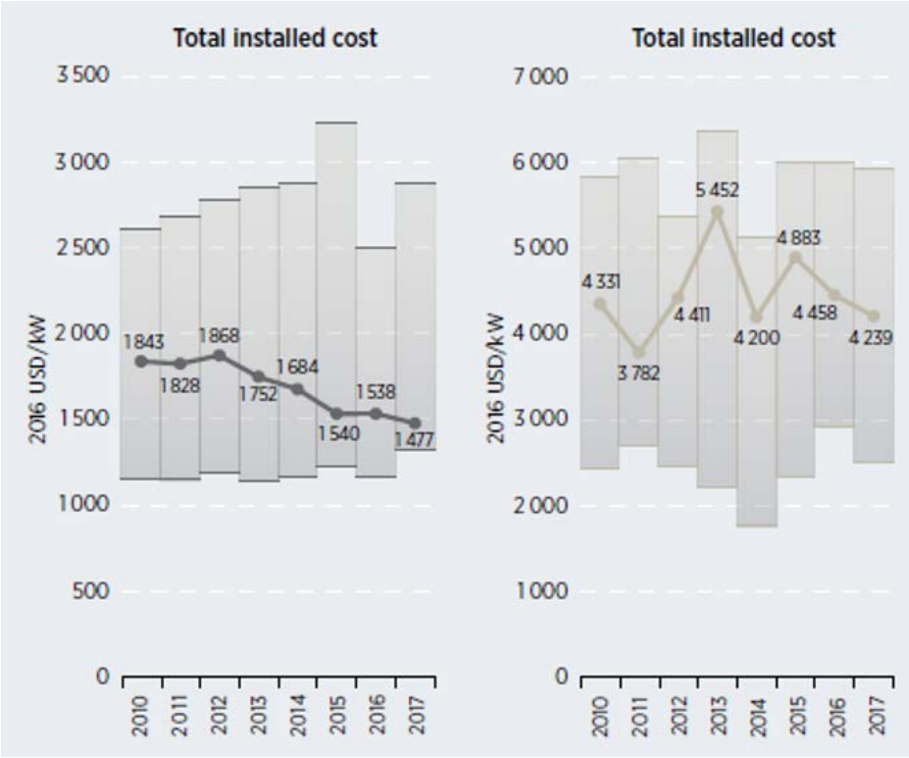

Figure 9: CapEx Trend for onshore (left) and offshore (right) wind turbine

As for the Operating Expenses (OpEx), it mainly consist of the cost of regular mainte-

[1]Figure reference from IRENA 2017 [IRENA, 2017]

nance, spare components, insurance, etc. Similar to CapEx, the OpEx is also driving down by researches and new technologies, for example, the implementation of drone inspection to replace heavy labor cost for offshore wind farm. The OpEx is calculated annually for clear yearly pro-forma statement. The value of EUR 0.0146/ kWh is used for the financial model according to Goldwind project reference.

For the electricity price, this is a value that would varies in different countries and agreement with the government. Some of the project would be able to obtain subsidies but some of them could receive no guarantee price and have to operate under the fluctuation of electricity price and auction everyday. In this project, the electricity price from Denmark and China are used, with value EUR 57.5 and 73.7 respectively. The two values are collected from Nordpool and Chinese government document in 2017 [China, 2017]. Similar to the cost of the wind turbine, the electricity price for wind turbine has also dropped a lot throughout the decade, and some projects no longer require the subsidies from the government in order to be profitable. It shows that the industry is becoming financially robust and stable.

For debt service, interest rate for the debt, it is a value that also varies according to individual banks and country system. Available data could be found in Germany. "For instance, onshore wind developers in 2015-2016 have been enjoying an all-in cost of debt of just 2 percent for new projects, down from 5 percent in 2010" [McCrone, 2016]. In this financial model, a one-percent for the debt is used for realistic financial model, of which results could be found in section 6. This financial model would then be used as a function that would be able to output payback periods, revenues, incurred interest, etc. for the optimization model to iterate the optimal operating strategies. The fluctuation of electricity price is one of the uncertainties the simulator wish to optimize.

4 Methodology

In this study, a fatigue load and operation mode analysis would be examined and determined as the first part of the project. The second part of the project would be to produce the optimized operation for the wind turbine lifetime under frontloaded modes and evaluate the scheme with the state-of-the-art loan principle, cost of energy and electricity price. Different uncertainties and assumptions would also be taken account into the evaluation.

4.1 Fatigue Load and Operation mode Analysis

Number of simulations would be expected under optimizing and determining the frontloaded operation modes and the fatigue loading. Under these scope of work, especially for the fatigue load and controller tunning, HAWC2 and matlab would be the major software be used under this project.

Fatigue loading is contributed by cyclic loading on the structural components, for example, turbine blades, tower, generator, etc. However, the cyclic loading in real-life are not all constant magnitude and often hard to determine the loading cycle due to the fluctuation of wind. Fatigue calculation thus utilizes Rainflow Counting Algorithm (RFC) to determine the number of cycles and the maxima and minima from the time series analysis of the stress exerted to the components. A demonstration of the RFC is shown in figure 10 [2].

As shown from the figure, on the upper left, it shows a normal stress time series on a component, taking the blade stress as an example here. The time series is the transform into maxima and minima in upper right figure. The sequence of the maxima and minima are then converted into a fatigue load spectrum in the lower left figure. The spectrum could then be transformed into a cumulative stress cycle plot as shown in the lower right figure. The whole process is calculated with the RFC algorithm to count the number of cycles per each load ranges. The fatigue load are then being calculated, and could be checked against the S-N curve of the material design if possible. However, without the S-N curve of the turbine materials, this project would check the fatigue loads against the baseline operation, which is designed for full life-time.

The aforementioned S-N curve provide sufficient insight in determining the fatigue load, and it could be computed with the following equation.

$$R_{eq} = (\frac{\sum n_i R_i^m}{n_{eq}})^{1/m}$$

where R_{eq} is the equivalent load; n_{eq} is the equivalent cycle, normally equivalent load is calculated in the form of 10 mins (1Hz); m is the slope of the S-N curve, which governs the type of material used for the components.

[2] Figure reference from [Sanchez et al., 2017]

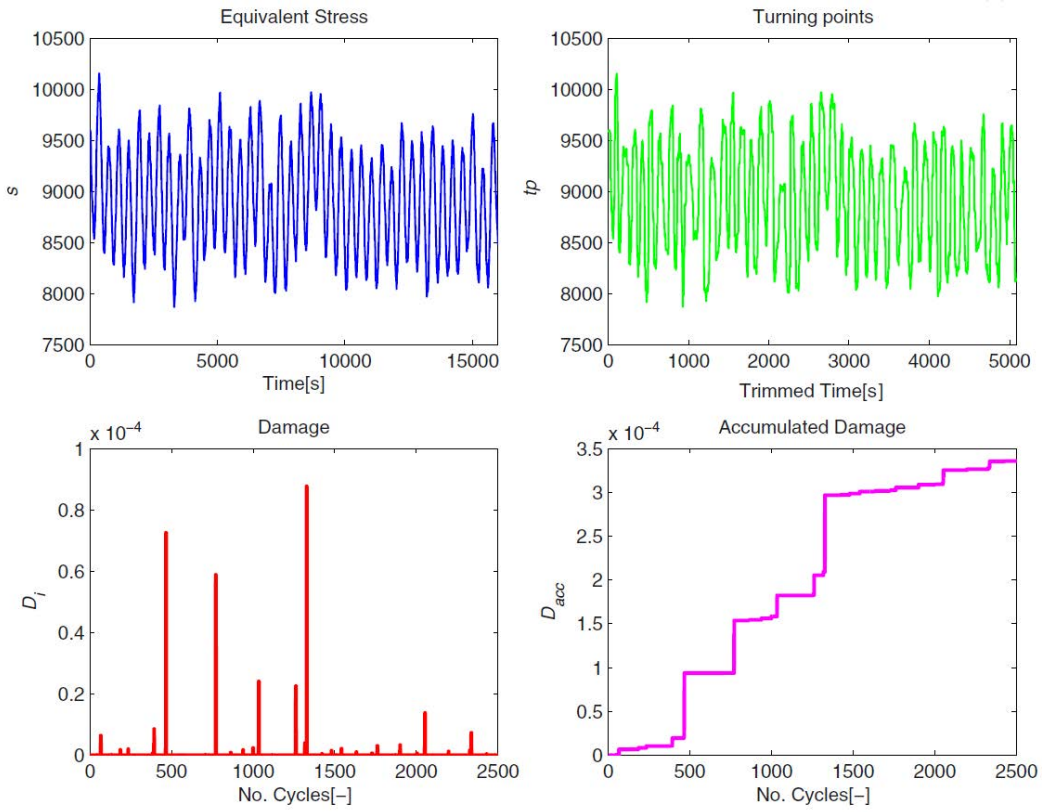

Figure 10: Rainflow Counting Algorithm

In order to calculate the lifetime equivalent load, the following equation could be used.

$$R_{eq,L} = [\frac{1}{n_{eq,L}} \int R_{eq}^{m} n_{eq} P(V) n_T dV]^{1/m}$$

where $R_{eq,L}$ is the life-time equivalent load; $n_{eq,L}$ is the life-time equivalent cycle, 1e7; P(V) is the Rayleigh Distribution; and n_T is the total life time, 20 years.
A more detailed fatigue calculation derivation is demonstrated in the below section.

4.1.1 Lifetime Equivalent Fatigue Load Calculation

In fatigue load analysis, the objective is to ensure the lifetime of the wind turbine components which are subjected to the corresponding lifetime load. The lifetime load represents the profile of loads that would exerted to the turbine over its lifetime under a specific wind resource location.

Wöhler Curves, S-N Curve

In this section, the S-N curve and the theory behind fatigue load would be explained, their relationship is really important in understanding the concept of lifetime equivalent fatigue load for wind turbine.

S-N curve of typical medium strength steel as shown in figure 11 below, add reference boyer1985 , would be used as an example in explaining the relationship.

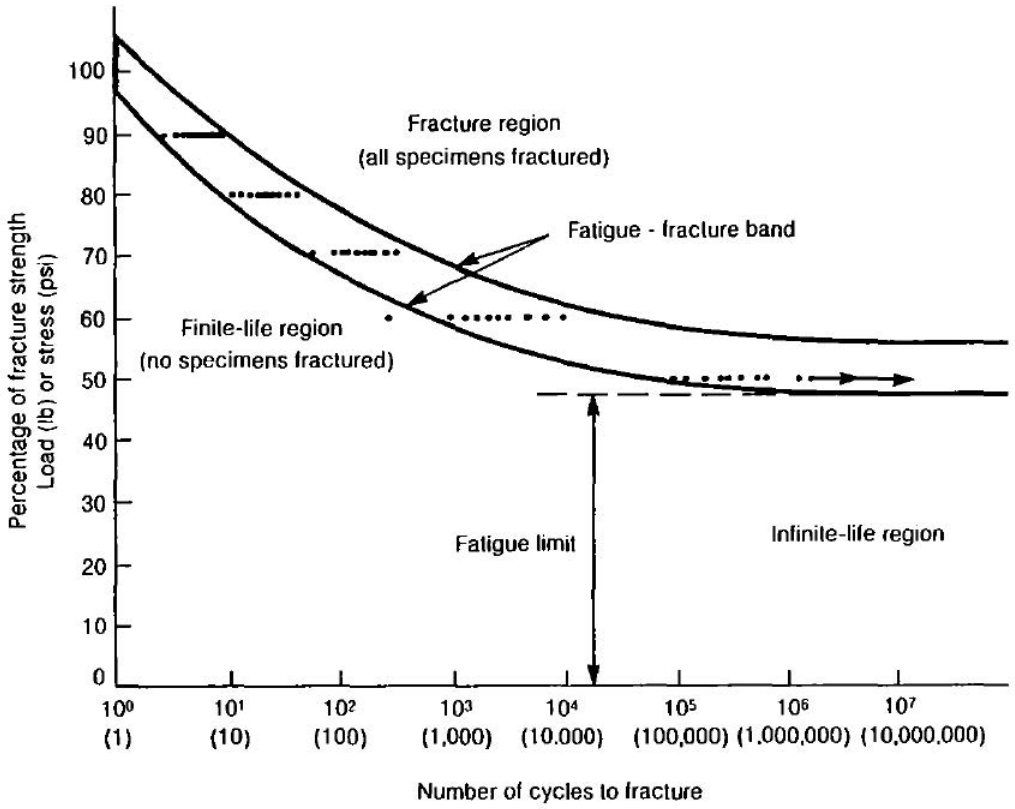

Figure 11: S-N curve of typical medium strength steel

S-N curve are all based on testing results. In the figure, the y-axis, represented by percentage, addresses the percentage of the fracture strength or ultimate strength, that the material can stand before breaking. The x-axis represents the number of same magnitude cycles of of load is applied to fracture. From the figure, when it is 100 percent, it illustrate that the material, steel, would break under this magnitude of single load. Even if the identical steel pieces are tested, they would have small different in their ultimate strength and it is addressed by the different test point shown on the y-axis within the two fatigue-fracture band curves.
When the testing loading is reduced by 10%, to 90% of the ultimate strength, obviously it would take numbers of cyclic loading to the steel piece before fracture happens, and all the testing data would be labeled in the S-N curve/ However the order of magnitude of the earliest and latest fracture cycles are not the same, but they are more than two to one. It is because the number of cycles are in logarithmic axis. As a result, it would be safe to use the earliest fracture point to indicate the fatigue life of the material. As it could be observed, this discrepancy in fracture cycle continue to expand as a lower load is applied to the material and it formed the two curve shown in the figure. Not only the number of cycle to fracture increases as the load reduces, the variance of the fracture cycles under the same load also increases. However, it should be reminded that the relationship between

the load and the number of cycles to fracture is never a linear relationship. According to a Siemens Experimenter, JohnHiatt, it is claimed that by doubling the number of cycles under the same amplitude of loads, the damage would be doubled. Meanwhile, when the amplitude is doubled, the damage instead is 20 times more. This another example showing that the relationship is not linear.

Another important information about S-N curve is the three regions demonstrated in figure 11. Every area below the first fatigue-fracture band curve is called the Finite-life region, which represent the material are safe to operate under such lifetime or magnitude of loads. There is also an Infinite-life region below the first fatigue-fracture band curve, it is called infinite-life because the number of cycle goes into millions and would take a very long time for testing. Some materials would have a flattened out S-N curve as shown below 50% of its ultimate strength, but some would not.
The second region is the area between the two fatigue-fracture band curve. The last region is the area beyond the second fatigue-fracture band curve and it is called the Fracture region. These two region are very similar as any operation points within this area would yield fracture or possible fracture. As a result, the material should not operate in these two regions.

Rate of Cyclic Load Application

The above conclusion is assumed that the rate of the load applied to the material does not contribute to the fracture, as such the rate does not affect the S-N curve. However, if the frequency of the cyclic load is very close to the structure natural frequency, the rate of the load application would undoubtedly influence its failing cycles. This effect, however would not be discussed in this study due to its scopes.

Miner Rules

Miner's Rule is a method to calculate damages induced by cyclic loading, in another word, it calculate the damage of fatigue loads. By using the material data, the S-N curve, Miner's Rule is a linear damage accumulation mathematical model that assess if the damage is fatal.
In Miner's by definition is the fraction of the accumulated damage over the total damage allowable before failure. As a result when the damage is equal to 1, failure would occur. Equation 4.3 demonstrated the accumulative damage done under a specific load.

$$D_i = n_i d_i = \frac{n_i}{N_i} \tag{4.1}$$

where n_i represents the number of exerted cycle of loads; and N_i represents the number of cycle to fail.
With the S-N curve shown above in figure 12, the following mathematical relationship could be formulated.

$$logS_o - \frac{1}{m} logN_i = logS_i \tag{4.2}$$

$$N_i = (\frac{S_o}{S_i})^m \tag{4.3}$$

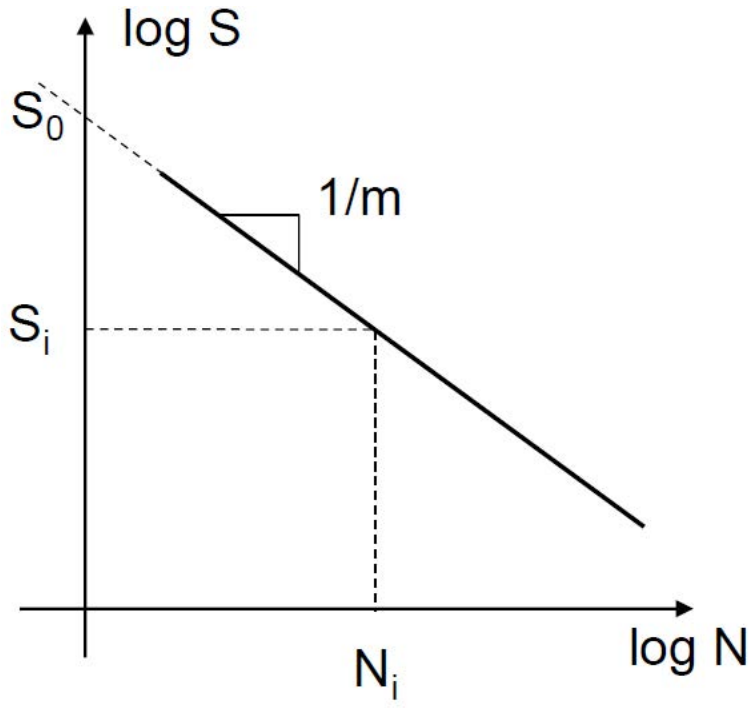

Figure 12: S-N curve relation

$$D_i = \frac{n_i}{N_i} = \frac{n_i S_i^m}{S_o^m} \tag{4.4}$$

$$D_{total} = \sum D_i = \frac{1}{S_o^m} \sum n_i S_i^m \tag{4.5}$$

where S_o represents the ultimate strength of the material; S_i represents the fatigue load; and m is the slope of the S-N curve governs by the type of materials. Typically steel and composite material used in wind turbine manufacturing have values of 4 and 12 respectively.

Under operation, wind turbine will undoubtedly receive loads with varies amplitudes. The exact number of cycles and the amplitude would be determined by the rainflow counting algorithm. The accumulative damage under that load profile would be determined by the summation of all the cyclic loads according to equation 4.5.

As for the method to calculate the equivalent load, the equation 4.4, could be modified into equation 4.6 as shown below.

$$D_{total} = \frac{n_{eq} S_{eq}^m}{S_o^m} \tag{4.6}$$

By putting R into S,

$$R_{eq} = (\frac{\sum n_i R_i^m}{n_{eq}})^{1/m} \tag{4.7}$$

where R_{eq} represents the equivalent loads and n_eq represents the equivalent cycles. In this case n_{eq} shall be 10^7 for wind turbine lifetime; m is the slope of the S-N curve; $\sum n_i R_i$ is

the sum of all multiple of the loads and their number of cycle.
Furthermore, when doing the lifetime equivalent fatigue load for wind turbine, the Rayleigh distribution of the wind profile should also be included in the calculation in order to formulate equation 4.8 to calculate the lifetime equivalent fatigue load.

$$R_{eq.L} = [\frac{1}{n_{eq.L}} \int R_{eq}^{m} n_{eq} P(V) n_T dV]^{1/m} \tag{4.8}$$

4.2 Simulation Set-up

This this thesis, there are no physical experiment to be conducted. However, most of the calculation would be done within Matlab, HAWC2 simulation. The thesis would adopt the high fidelity simulator HAWC2 developed by Technical University of Denamrk (DTU).

4.3 HAWC2

In HAWC2, the simulation would be run within the cluster setup in Riso. With the cluster set up, Design Load Case (DLC) 1.2 would be focused in this thesis.
DLC 1.2 is load cases introduced from the International Electrotechnical Commission (IEC). The DLC 1.2 is intended to simulate the power production of wind turbine without faults. Its simulation would be conducted under the entire operation range in wind speed with the turbulence intensity suggested by the IEC wind turbine class. Furthermore, Yaw misalignment is taken into account in the simulation, where +/- 10 deg should be considered in the calculation. Six number of turbulence seeds are also required per wind speed in the simulation.

4.4 Matlab

With the time series simulation results obtained from HAWC2, Matlab are used to process the RFC and the fatigue load calculation. Since RFC is not an implicit algorithm in HAWC2, the time series results have to be post-process by RFC algorithm, a well cited algorithm and tool that was developed by Niesłony [Niesłony, 2009]. Matlab would be used under the set up of operation mode, the change in wind turbine controller and aeroelastic simulation in the wind turbine. In addition, with all the findings from the fatigue calculation, a optimizer or simulator is developed for the interactive wind turbine operation optimization.

5 Operation Modes

Different operation modes would be designed for the optimization in this study. The difference and detail configurations of the wind turbine operation modes would be discussed in this section.
The purpose of naming the three schemes is to describe each operation mode clearly. The three designed scheme are up-rated and de-rated modes as well as the normal unchanged mode. These three operation modes would be used as tools to optimize the wind farm life-time operation scheme in order to reduce the interest payment. On the other hand, the optimization process would take into account of the design constraint such as the lifetime equivalent fatigue load, turbine financial model, power generation, etc.
The DTU 10MW RWT is designed with its own operation strategy and designed power curve. During the course of design discussion, a brief idea of adjusting the power curve by keeping the same level of power output but with an earlier rated wind speed had been discussed. This method focus on keeping the same rated power but squeeze power production with an earlier rated wind speed. However, this method is considered unsuitable in this project as pushing rated power in an earlier wind speed, the power curve in region one, when the power output is building up to rated power, and the optimal tip speed ratio will be changed. In this way, the turbine will have to be redesigned in order to operate at most efficiency. The procedure of doing so would have to adjust the tip speed ratio of the turbine, of which require new iteration in the rotor design. Although this method is one of the most straight forward way, in order to avoid redesigning the rotor and to make use of the available resources this approach is not adopted.

Instead, the strategy that is adopted in manipulating the operation mode of the turbine is to keep its tip speed ratio and optimal lambda curve in region one of the power curve by changing the output from pitch controller. With different output of the pitch controller to the blade, the turbine could generate more torque under the same rotation per minute and different level of power output.

Total of three schemes are set up for the project, including baseline, proposed 9MW and proposed 11MW schemes, they represent the turbine that run at rated 10MW, 9MW and 11MW respectively.

5.1 Baseline Scheme

The baseline case is the original designed DTU 10MW RWT normal operation mode. As shown in the figure 13, the baseline scheme has the rated wind speed as 11.4m/s and 10MW power output.

5.2 Propose Scheme

The proposing strategy has two schemes, including a proposed 9MW and proposed 11MW scheme. The two schemes have different operation setting to control the wind turbine.

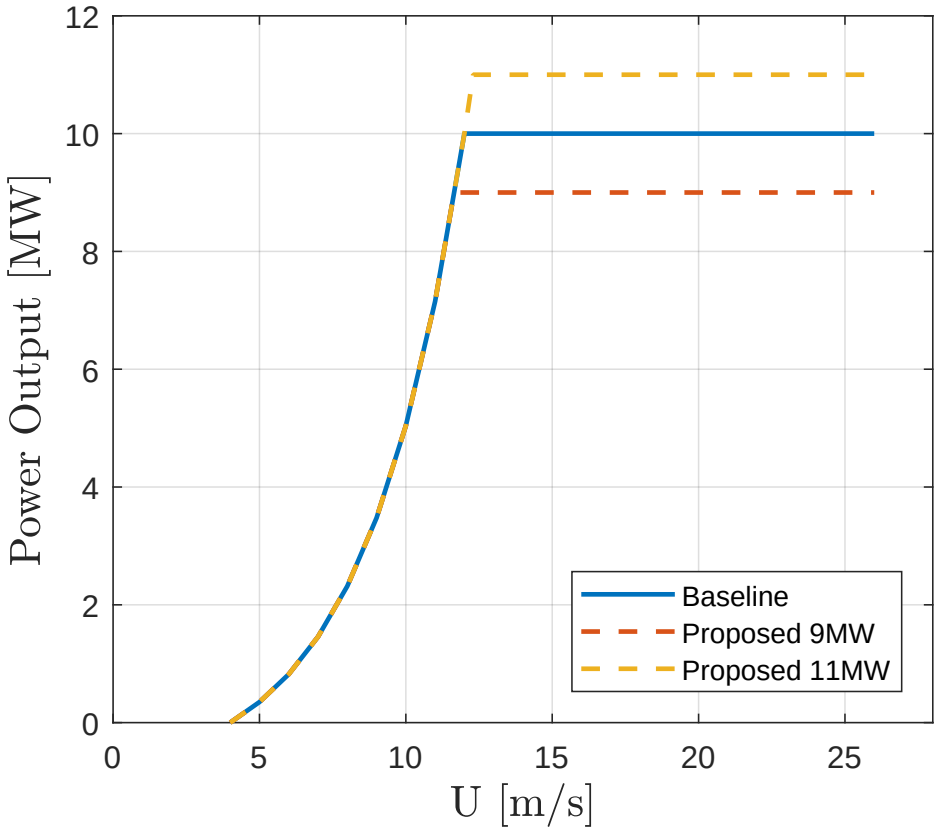

Figure 13: Baseline and Proposed Scheme

For the proposed 9MW scheme, the turbine would operate as demonstrated in red dotted line in figure 13. The turbine will operate exactly the same as baseline before rated power is achieved. As a result, the rated wind speed would not be the same as baseline and would be achieved earlier. In order to achieve a new rated power, the pitch controller would have to be initiated earlier when the new rated wind speed is met. This also implies that a new gain schedule is required.
As for the proposed 11MW scheme, the turbine power curve is shown in figure 13 in yellow dotted line. Similar to the proposed 9MW, the turbine operates same as the baseline before rated power. And instead, the power generation continues until it reaches 11MW and stay constant thereafter. As a result, the rated wind speed for proposed 11MW scheme would higher than the baseline one. And a new gain schedule would be required for the pitch controller.

5.3 Operation Mode Validation

As mentioned in section 5, two new operation modes, the Proposed 9MW and 11MW, are being set up for this project. The behavior of the turbine under the two modes are studied in this section in order to validate if their operation align with the design specification.

5.3.1 Rated Power

Since the simulations are done by HAWC2, the wind turbine model file that used as the input for HAWC2 is adjusted by specifying the desire rated power, such that it would be 9MW, 10MW and 11MW for proposed 9MW, baseline and proposed 11MW schemes respectively.

The first evaluation step to check the schemes is to look from their corresponding power output before and after rated wind speed. As the rated wind speed is 11.4m/s, 10 minutes simulation result with mean wind speed 6m/s and 14 m/s are picked to show the power generation curve.

As shown in figure 14, it shows three different simulations results with turbine specified for rated 9MW, 10MW and 11MW under the same turbulence model. According to the simulation results, all three cases have the same mean power output, $1.7\text{x}10^6$ W with $7\text{x}10^5$ W standard deviation. The fluctuation of the power output is a direct contribution due to the introduction of turbulence model in the HAWC2 simulation and the design of the turbine controller. In this comparison, all three cases have the same turbulence model and turbine controller; as a result, the simulation results shows same results.

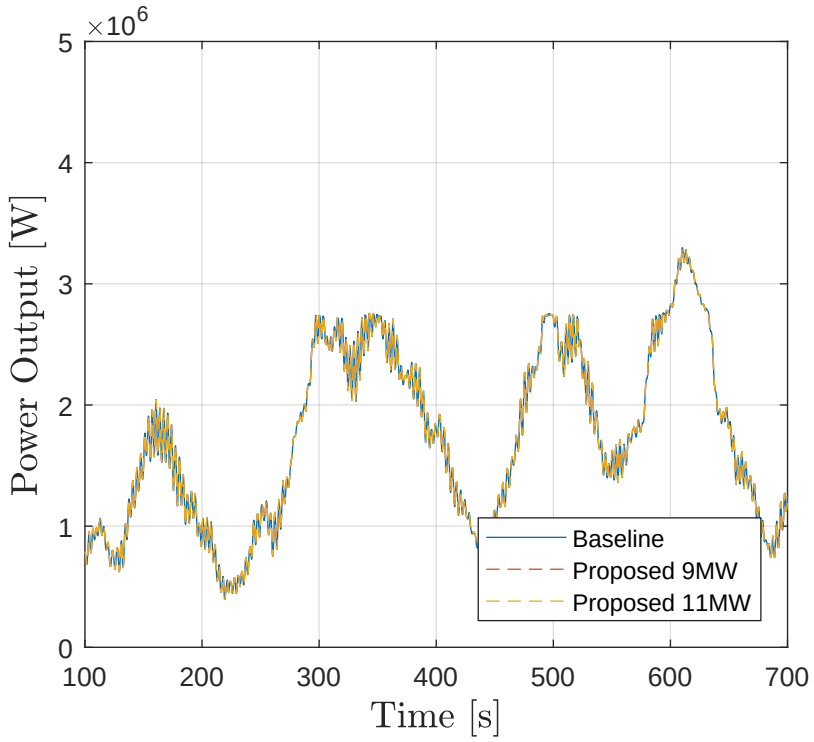

Figure 14: Power difference under 3 different schemes at 6m/s wind speed

In figure 15, simulation results are shown with the same simulation conditions as mentioned in previous paragraph except being at 14m/s, after rated wind speed. As expected, the 10 minutes simulations show that the baseline scheme produce 10MW power meanwhile the proposed 9MW and 11MW schemes produce 9MW and 11MW after reaching

rated wind speed. Since the controller strategy switch from torque to pitch control after hitting rated power, it could be observed that slight difference is shown in the time series of the power production. From the simulation, the standard deviation of the three simulations are very similar, $1.4x10^5 \pm 10\%$.

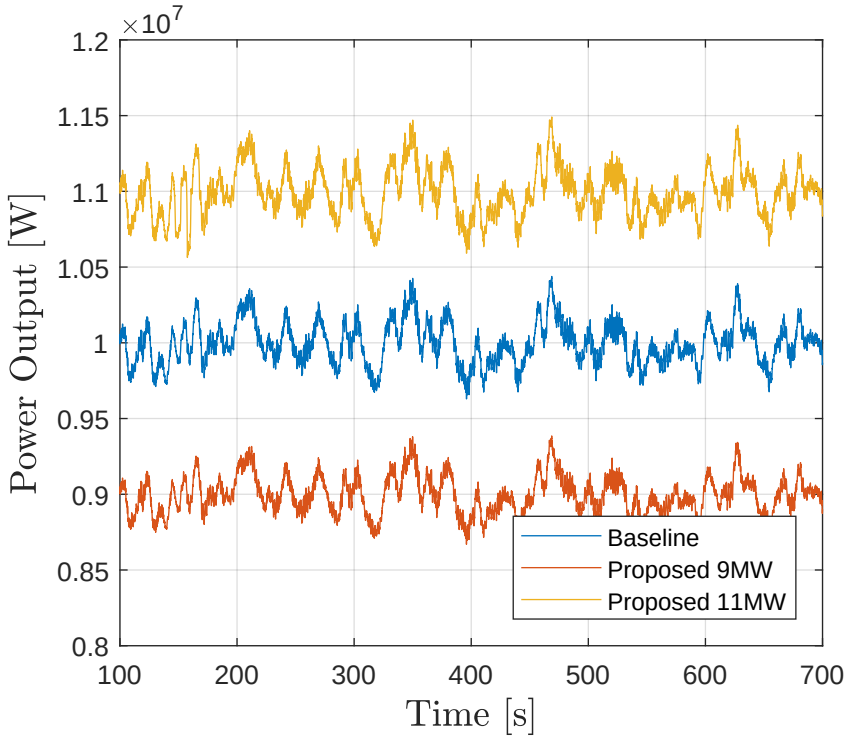

Figure 15: Power difference under 3 different schemes at 14m/s wind speed

Wind Turbine Steps Response

Although the previous section confirmed that the two proposed schemes operate according to design before rated wind speed, where the power curve is the same for all three schemes before rated for the optimal tip speed ratio, and after rated wind speed, of which pitch control kicks in to obtain the designated power output, the transition when pitch controller become active could not be conclude clearly with only 10 minutes mean wind speed simulation. As a result, all three turbine model are simulated again under step response in order to validate an appropriate transition is achieved.

Step response simulation starts from 4m/s with an increment of wind speed of 1m/s per step per 40 seconds until 26m/s. And the simulation last for 1000 second. The purpose of the step response is the observe the reaction of the turbine, mainly contributed by the controller under the influence of wind steps, of which the transition of switching controller would be able to observe in detail. The 40 seconds step time is selected due to a general observation that the controller would be able to settle in a steady state within the specified time without influencing the next step response. This time step is designed such that the simulation time of the step response could be optimize without sacrificing the

simulation accuracy.

In figure 16, it shows the step response of the baseline, proposed 9MW and 11MW simulations. The figure shows wind speed from 5m/s to 19m/s between 100s to 700s. It could be observed that, for baseline scheme, wind speed hit 11m/s at 350s, and when wind speed advance with the step at approximate 380s, power fluctuate and settle at its rated power, 10MW. Further wind steps are quickly settle to its steady state, 10MW, thereafter.
As for proposed 9MW and 11MW schemes, it could also be observed that the pitch controller kicks in earlier and later than the baseline respectively in order to keep its specified rated power.

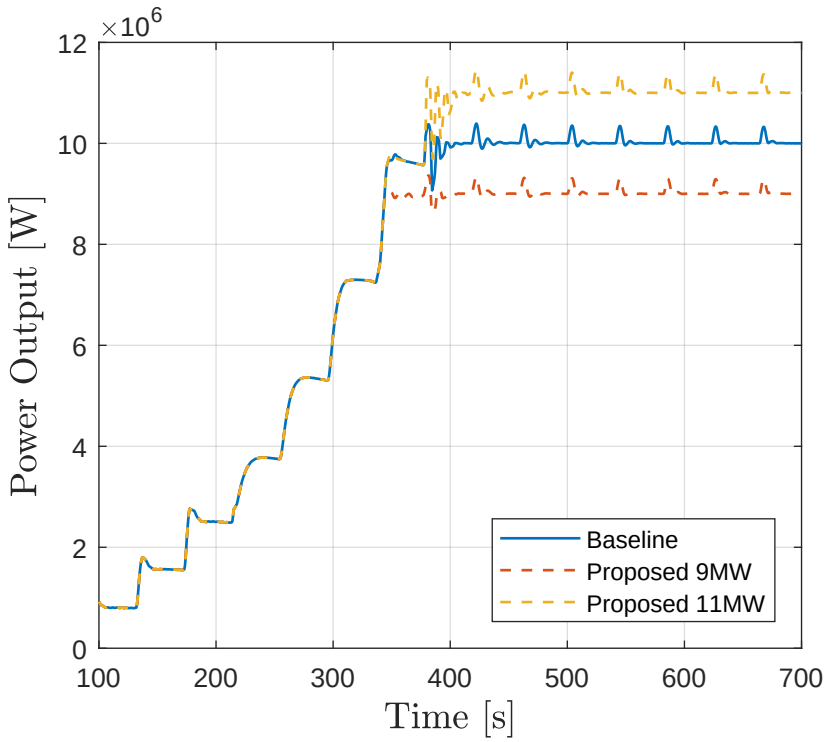

Figure 16: Power output of three different schemes in step response

As shown in the figure 17 and 18 below, the pitch controller pitch the blade differently in order to adjust to the rated power. In these simulation the maximum rotation per minute is kept constant, which means that in order to adjust the rated power, the generator torque would be different in each of the scheme, of which are directly affected by the pitching of the blade. It could be observed that generator torque also decreased and increased in proposed 9MW and 11MW respectively.
In this section, it is important to mention that the generator is assumed to works normally even with the increase in torque. Such that the turbine would work fine under 11MW operation mode.

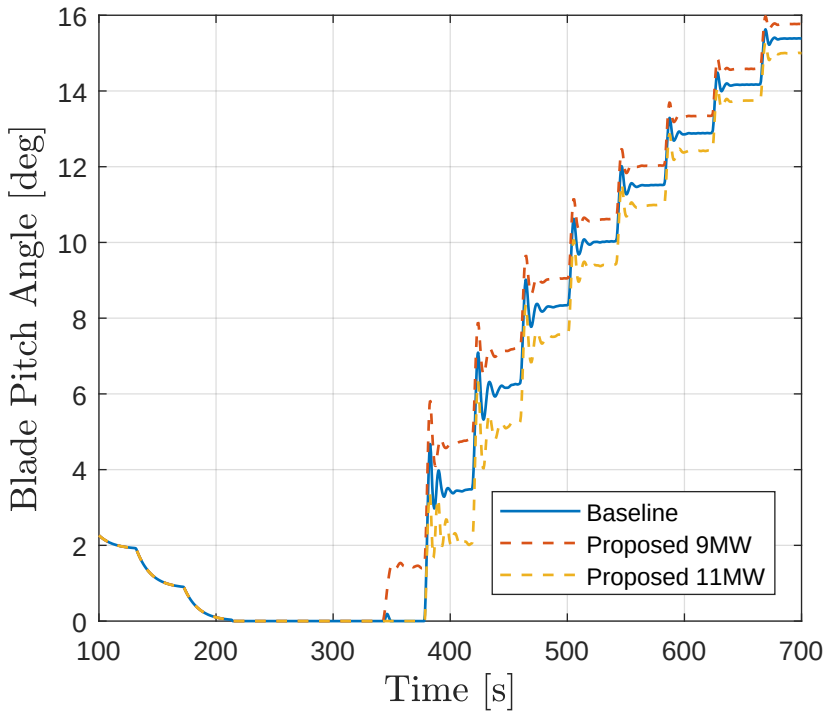

Figure 17: Blade pitch of three different schemes in step response

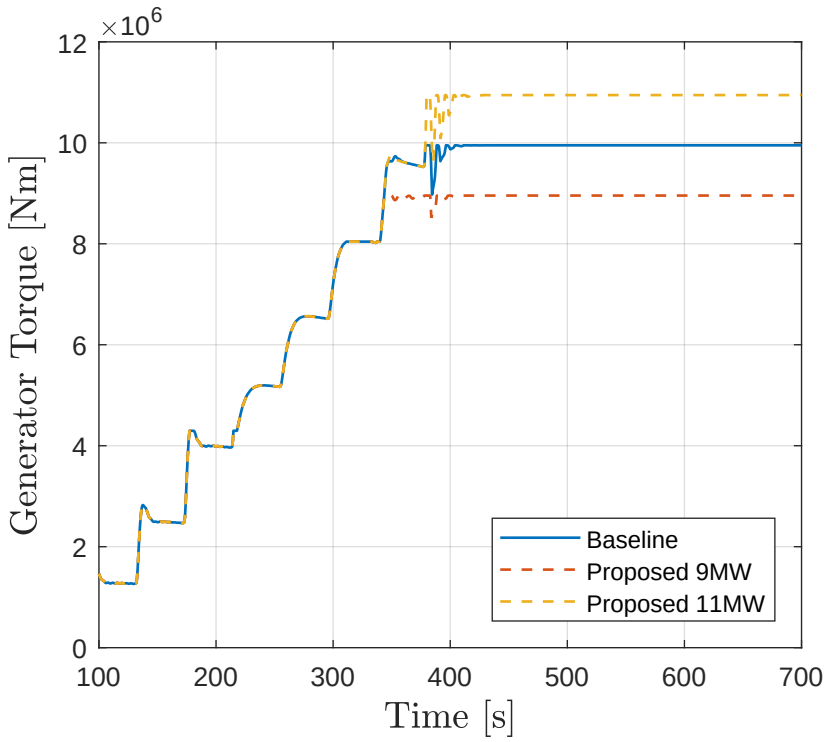

Figure 18: Generator torque of three different schemes in step response

6 Fatigue Calculation Results

6.1 Fatigue Load Summary

The fatigue load calculation results are summarized for all the operation modes after the calculation from matlab scripts as described from the HAWC2 results. Tables below shows the life-time equivalent fatigue load for all the schemes in 4 significant figures. The percentage different in fatigue loads for between the up-rated and de-rated with the baseline operation mode would be treated as a weighting factor for the optimization.

Channels	**Baseline** [kNm]	**Proposed 9MW** [kNm]	**Diff.** [%]
MxTB	195200	188900	−3.25
MyTB	40930	39180	−4.28
MxTT	16970	16340	−3.77
MyTT	9888	8866	−10.34
MzTT	12890	12690	−1.60
MxMB	14350	14610	+1.80
MyMB	15730	14890	−5.34
MxBR	11500	10780	−6.20
MyBR	22630	22570	−0.29
MzBR	312	290	−7.00

Table 4: Life-time equivalent loads for different scheme

Channels	**Baseline** [kNm]	**Proposed 11MW** [kNm]	**Diff.** [%]
MxTB	195200	212610	+8.87
MyTB	40930	42750	+4.43
MxTT	16970	17700	+4.28
MyTT	9888	10890	+10.11
MzTT	12890	12940	+0.36
MxMB	14350	13980	−2.60
MyMB	15730	15590	−0.87
MxBR	11500	11570	0.64
MyBR	22630	22610	−0.09
MzBR	312	351	+12.59

Table 5: Life-time equivalent loads for different scheme

6.2 Fatigue Load Analysis

Similar to the validation of the wind turbine model from section 5.3, simulation results would be compared for all three cases at before and after rated wind speed. And results of wind speed 6m/s and 14m/s will be compared.

Channels and Coordinate System

As shown in table 4 and 5, there are total of 10 channels of load on different components and directions. Each of the component has their own coordinate system defined in the simulator, of which is shown in figure 19.

For the first channel, MxTB, it represents the moment along x-axis at the tower base, which could also be described as the fore-aft moment at the tower base. Meanwhile, the value of MxTB is positive in all simulations represents that the tower base along x-axis is exerted with counter-clockwise moment due to the wind loads to the tower. Similarly, for MyTB that represents the moment along y-axis at the tower base.

Similarly, MxTT, MyTT, MzTT, MxMB and MyMB represents the moments act along their corresponding axis at tower top and the main bearing, of which the coordinate system could refer to figure 19.

For the turbine blades, moments are described as MxBR, MyBR and MzBR. They represents the flapwise, edgewise and torsional moments.

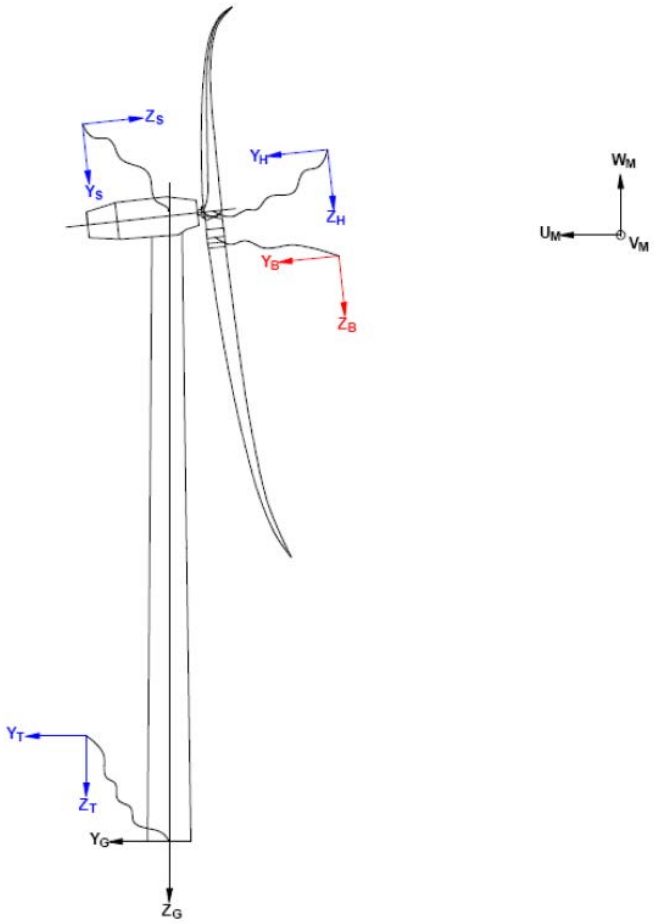

Figure 19: Coordinate system in HAWC2 simulator (reference from HAWC2 user's manual)

6.2.1 Results

Before Rated Wind Speed

For simulation that were conducted before rated wind speed. The moment loads were not expected to have big differences among the three schemes since they should have been operated under the same control strategy. As shown from table 4 and 5, the side-side moment at the tower top (MyTT) and blade root torsional moments (MzBR) have the largest impacts under the three schemes, their results at 6m/s are shown in figure 20 and 21. It is observed that three schemes moments align with each others, which affirms that no extra or less loads were exerted to the structure before rated wind speed.

It should be reminded that all results shown are under the influence of the same turbulence model and only part of the results are shown here in the figures for demonstration purpose.

After Rated Wind Speed

Simulation results of 14m/s are shown below from figure 22 to 31. Figure 22, 23, 25, 29 and 31 shows significant difference in loads for the three schemes. If we compare the observation with the fatigue load summary shown in table 4 and 5, it can be observed that all the above mentioned channels have more than 4% difference between the proposed 9MW and 11MW operation scheme than the baseline. As a result, these channels are considered more influential in determining the impact to life-time fatigue limit when frontloading the wind turbine.

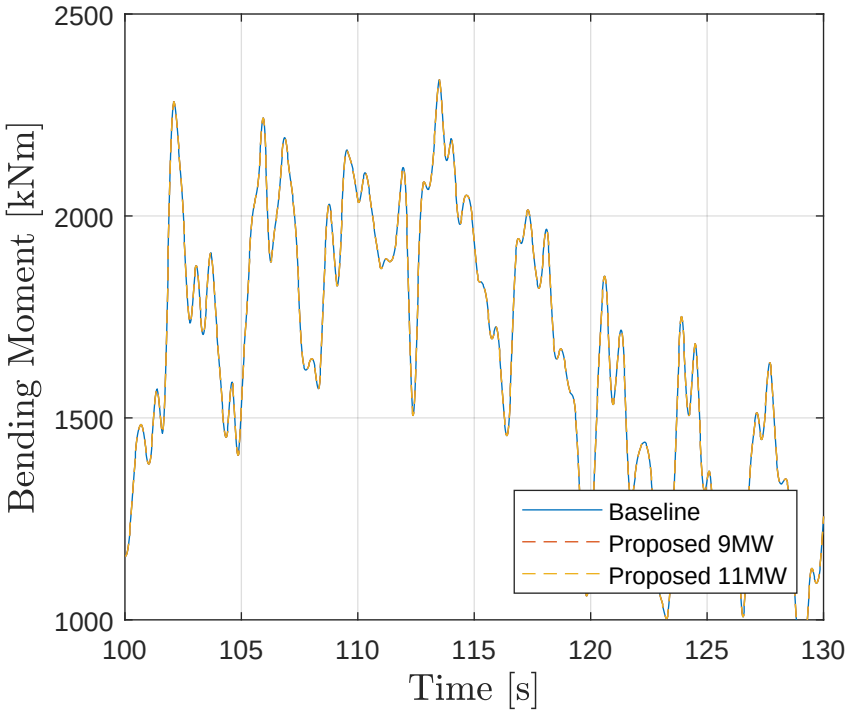

Figure 20: MyTT time series at 6m/s

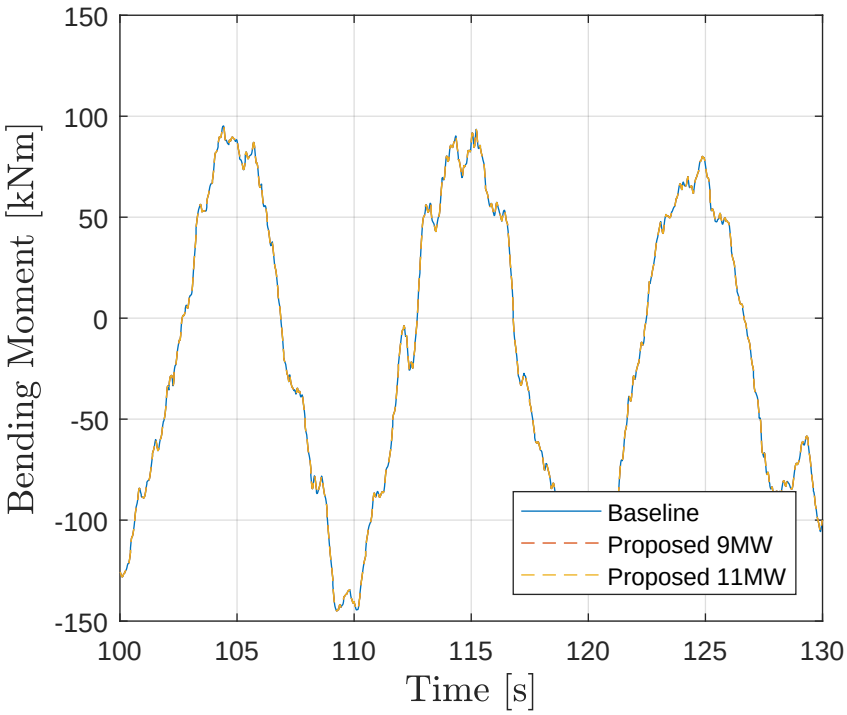

Figure 21: MzBR time series at 6m/s

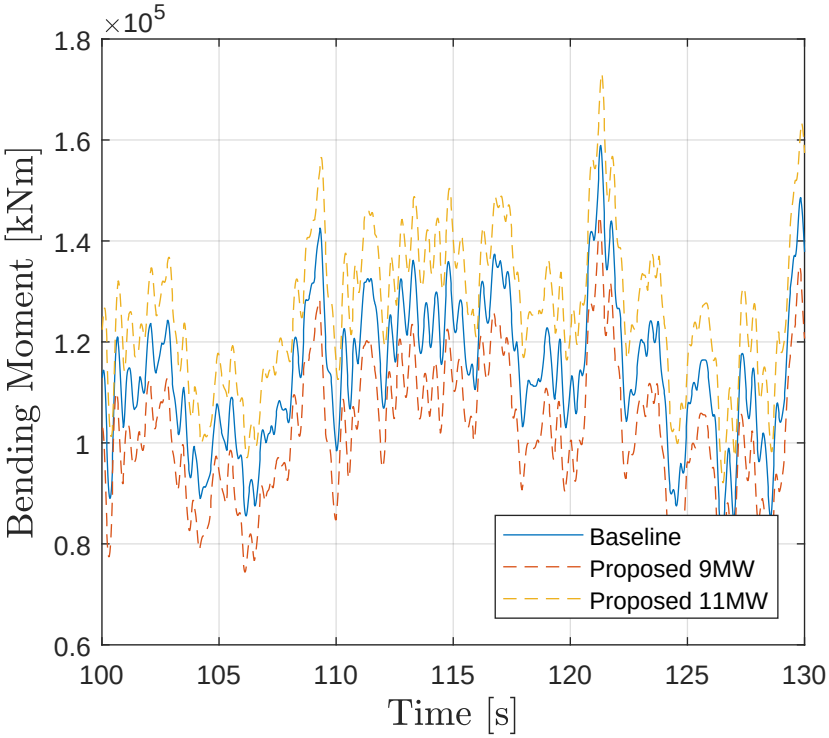

Figure 22: MxTB time series at 14m/s

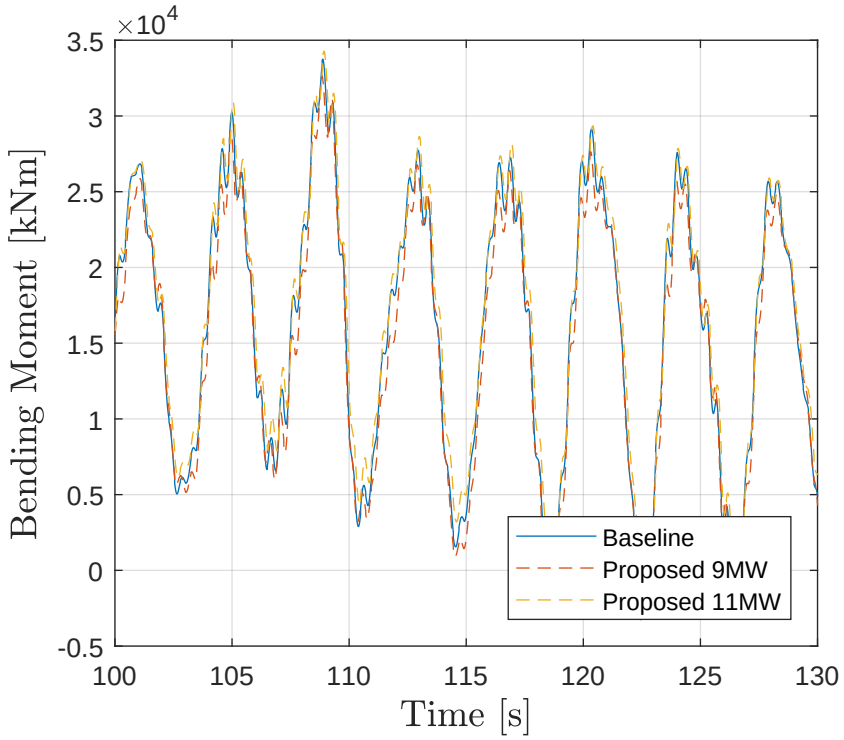

Figure 23: MyTB time series at 14m/s

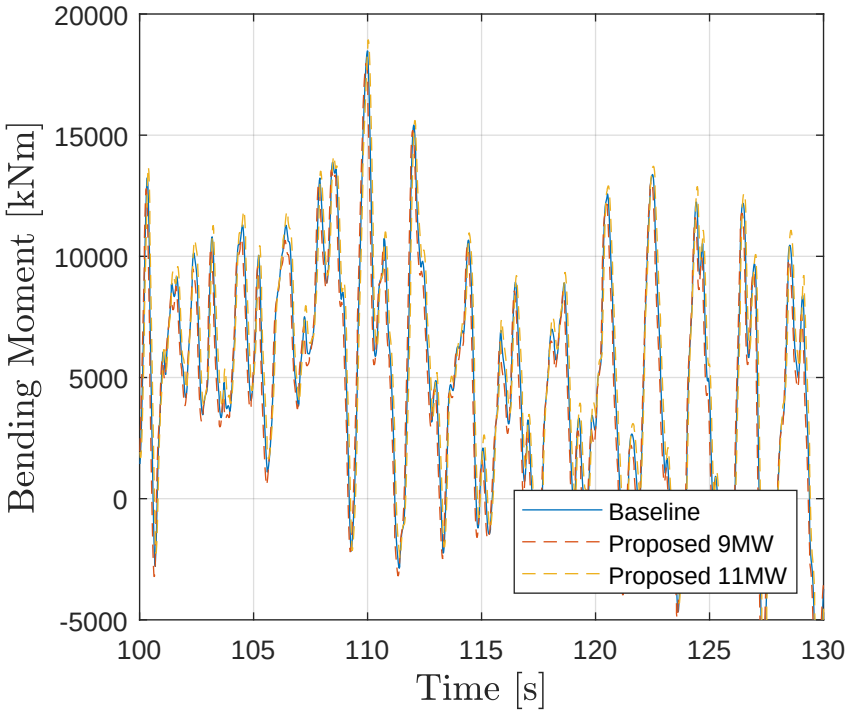

Figure 24: MxTT time series at 14m/s

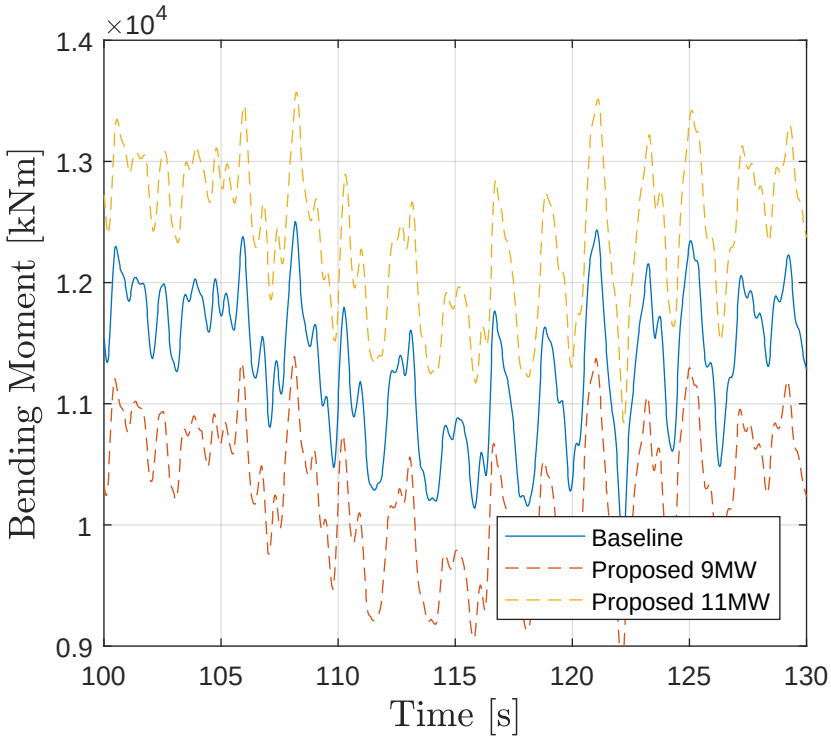

Figure 25: MyTT time series at 14m/s

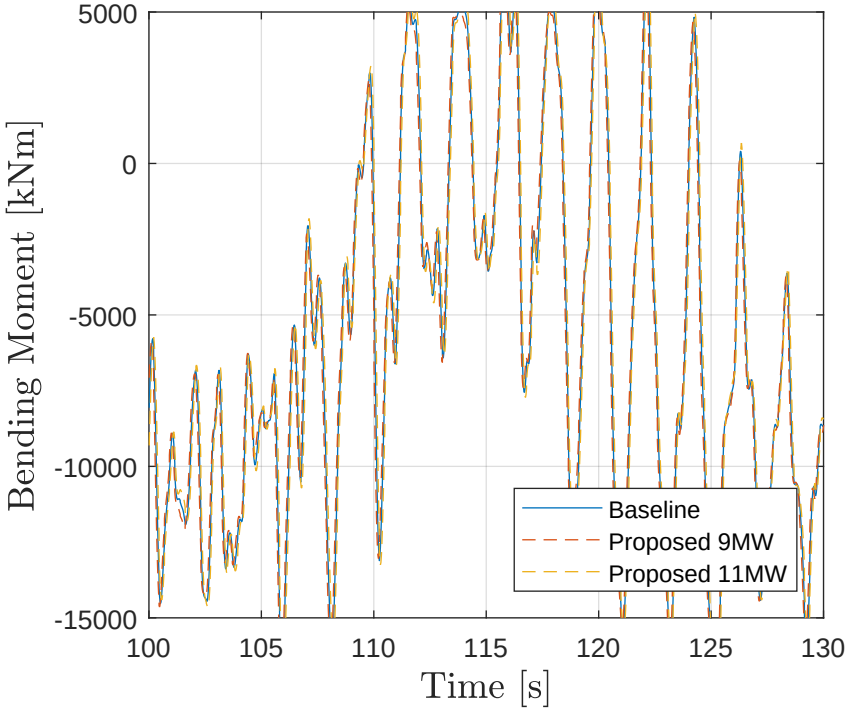

Figure 26: MzTT time series at 14m/s

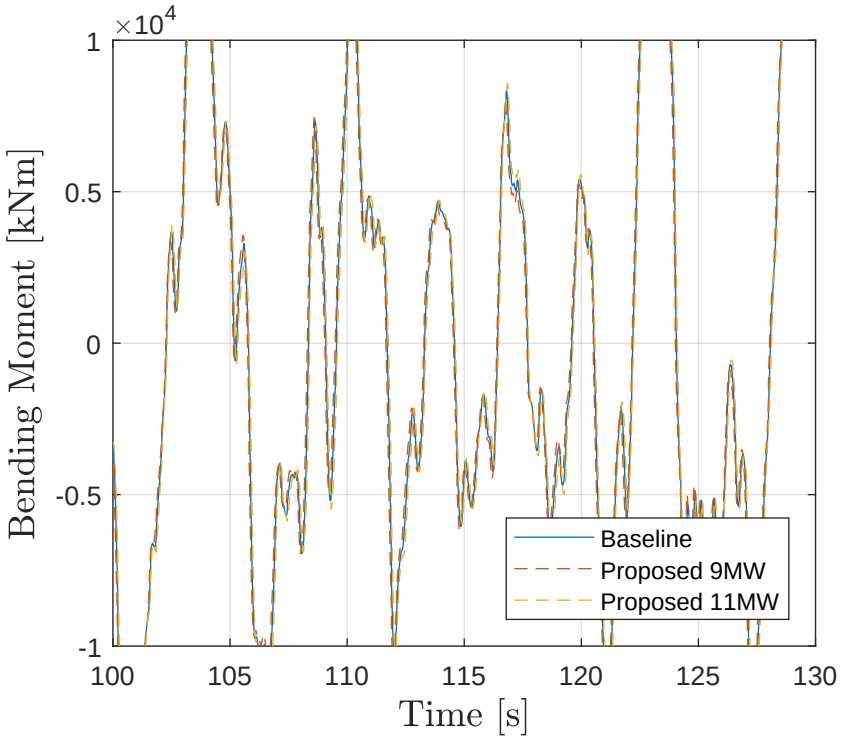

Figure 27: MxMB time series at 14m/s

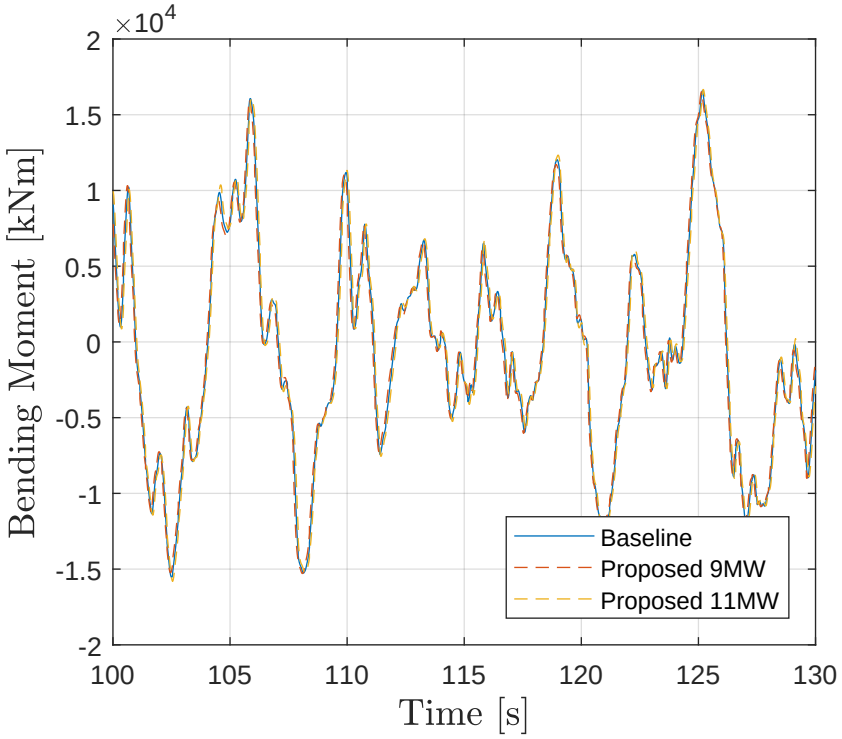

Figure 28: MyMB time series at 14m/s

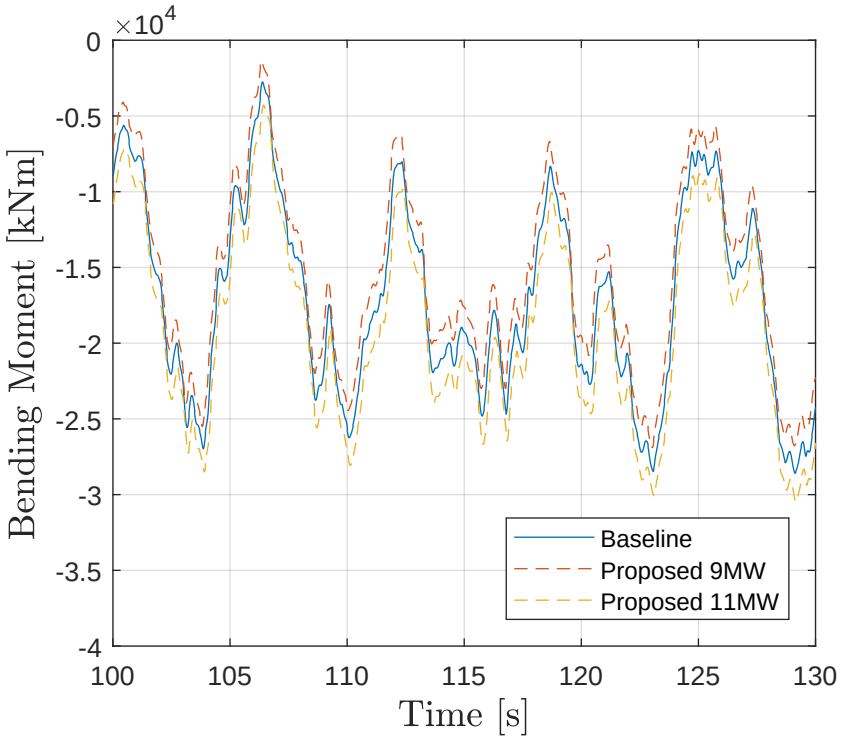

Figure 29: MxBR time series at 14m/s

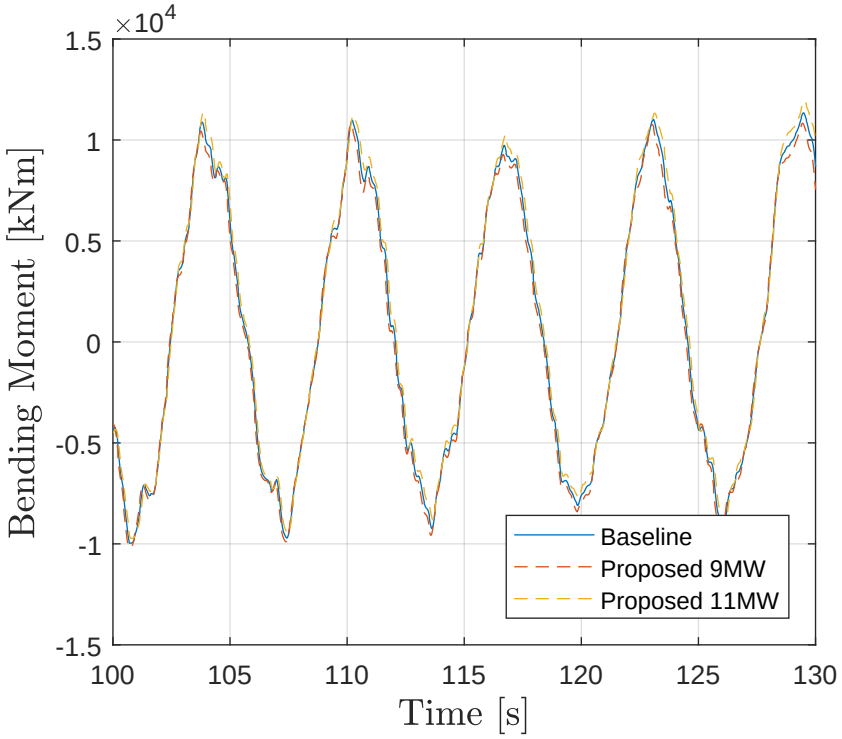

Figure 30: MyBR time series at 14m/s

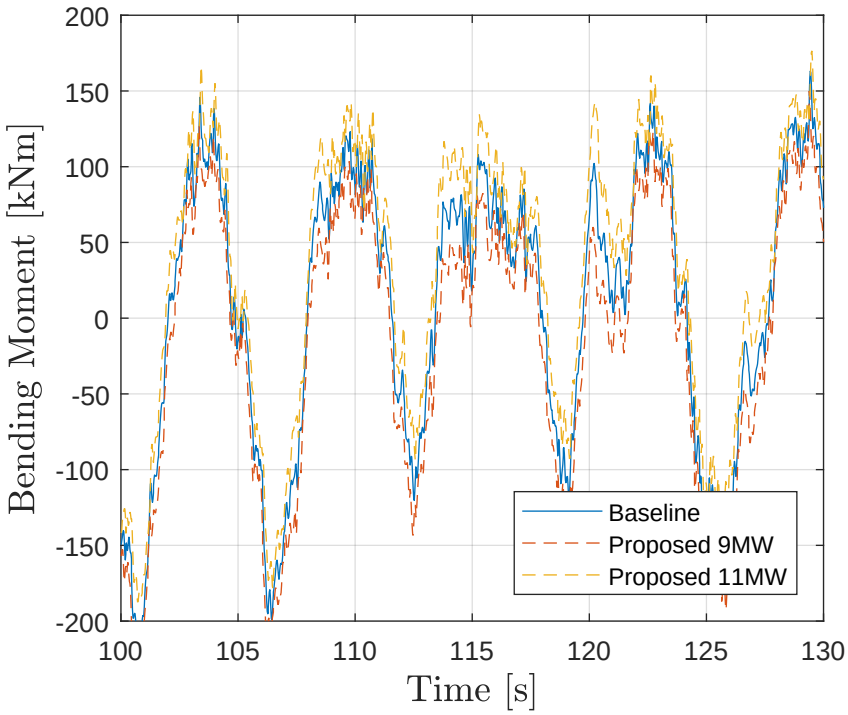

Figure 31: MzBR time series at 14m/s

Since there are multiple percentage difference in each of the channels of the turbine load sensors, the project has assumed that the up-rated and de-rated weighting factor would be ±10%. It is understood that the different components of the turbine would behave differently. In order to spend more focus on the optimizer development, the assumption is made.

6.3 Extreme Load

As mentioned in the background information section where different DLCs were discussed, there are several DLCs have to be done when certifying a wind turbine. The simulations that were conducted for fatigue load analysis in this project could also be used for extreme load calculation, DLC 1.1. The maximum and minimum loads of the simulations for the three operation modes have been plotted for reference in the appendix B from figure 56 to 65. These values were not treated in this project since it was not part of the scopes. However, they could give a brief idea on how the extreme load distribution across the three operation modes. One could see that the maximum load of MyTT in 11MW opeartion mode is, in fact, slightly higher than the 10MW operation, which shows similar behavior in fatigue load analysis.
One should remember that in full scale analysis, all DLCs has to be simulated in order to certify the turbine into action.

7 Optimization Model

With the up-rated operation modes obtained from the previous part. Energy production optimization of the wind turbine would be focused in this section. An optimization of the fatigue load and the operation scheme that yield the most revenue without sacrificing turbine integrity would be determined and evaluated in this section.

With the fatigue load and operation mode are formulated and computed, the rate of the fatigue load in each of the operation could be determined and they would be assigned with a weighted factor. By making few financial assumption such as the revenues, operating expenses, debt service, etc. a comprehensive model between the interaction of fatigue load, operation and their financial benefit would be derived. A simulator could be developed for the mode and determine the optimal solution under different derived situation.

Furthermore, the optimization process is presented and the mathematical model that describes its dynamic are also developed. The modeling process would be discussed first, follow with the deterministic and stochastic simulation using differential equations. Some of the model development are demonstrated with the Matlab scripts as well.

7.1 The Debt Calculation Process

The debt calculation process is illustrated schematically in figure 32. It consists three modules that represents the normal wind turbine operation process including, the wind farm operation, the company and the bank.
It is assumed that the company has to payback all the CapEx debt as well as the incurred interests borrowed from the bank within the wind farm life-time. The sources of income from the company is the power generation from the turbine, which could varies based on the specified strategic operation scheme. The operation scheme could be strategic based on the turbine structural integrity, weather uncertainty or fluctuation of the electricity price point of view. Assuming that the company would be paying off the debt with the revenue generated, the debt calculation could be summarized as a continuous model to identify the remaining debt the company have to pay back. And it shed light on the logic and process in developing the debt model, such that it could be optimized to payback the debt earliest.

In modeling the debt calculation, a block diagram of the debt calculation process is developed and illustrated in figure 33, where it summarized the calcuation into two major system models, the wind turbine model and the financial model.
The wind turbine model, focus on identifying operation limits and conditions of the model, which receives three separate inputs, t_1, t_2 and t_3. The model then compute the power production (P), accumulated life-time equivalent fatigue loads ($F_{eq,L,accumulate}$) and the total life-time of the project according the the distribution of the three t. The three inputs, t_1, t_2 and t_3, correspond to the time spent on either of the three operation scheme developed in previous section, 11MW, 10MW and 9MW, respectively. These three input is the variable that would like to be optimized such that an optimal operation scheme

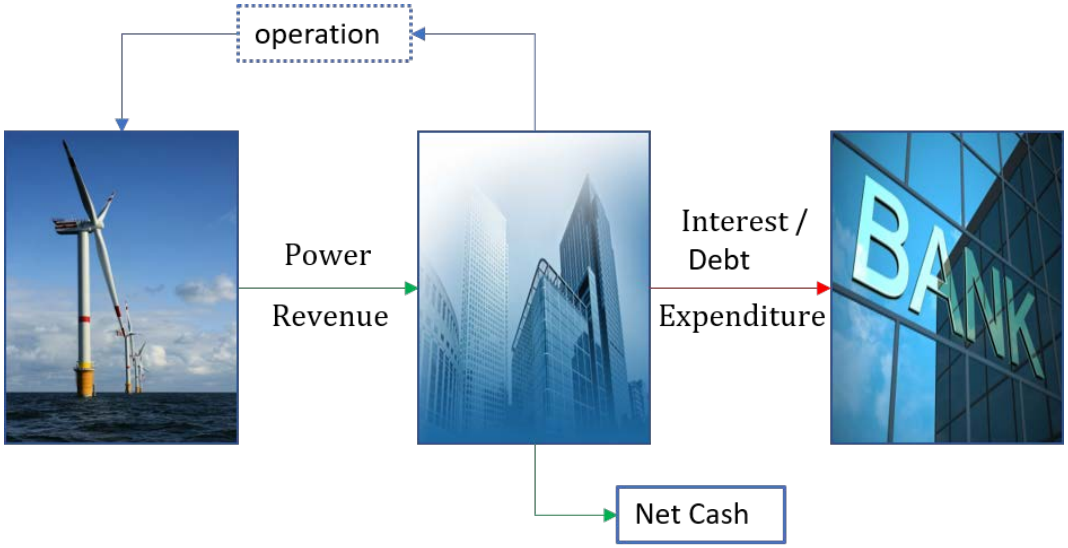

Figure 32: Schematic diagram of the System Model

could be formulated under the full model. Below is an example of how the t represent the turbine operation. t represents the time line of turbine lifetime and t_1, t_2 and t_3 represents the time spent of three different operation stages. From t=0 to t=t_1, the turbine will be operating in 11MW, while from t= t_1 to t=t_1+t_2, it would be operating in 10MW. And lastly, from t= t_1+t_2 to t= t_1+t_2+t_3 the turbine will be operating in 9MW. The optimization process would output the optimal t for each mode under the turbine structural limit. If the turbine is to be operated normally without any frontloading, the t_1 and t_3 would be zero and t_2 would be equivalent to 20 years. During the model development, the wind turbine model block acts more like a constraint logic block that provide the framework for the financial optimization.
The financial model instead is the most important model to develop, such that it calculate the debt under the framework provided from the wind turbine model. The financial model aims to compute all the financial values, such as the total paid interests, total profits and the debt at any time during the operation, for optimization purposes.

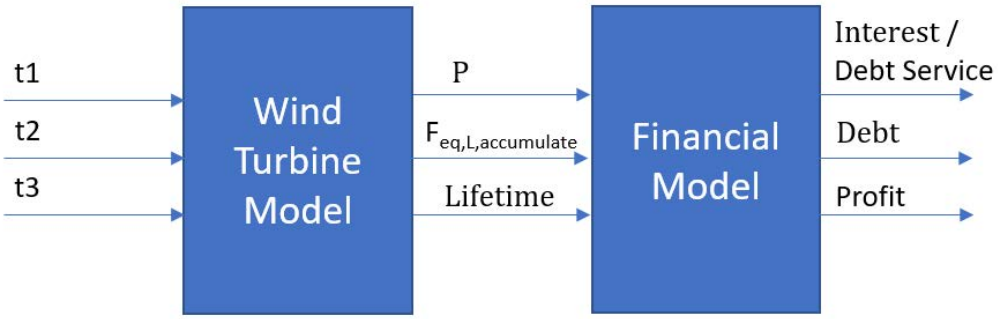

Figure 33: Block Diagram of the System Model

7.2 Continuous Debt Calculation Modeling

This section would continue to discuss and demonstrate how the debt calculation model is developed.

7.2.1 Interest Rate and Future Value

Before going into the model development, the interest rate for the debt is computed first. As a continuous model is to be developed for the debt calculation, the interest rate should not be compounded annually, with the annual interest rate 2% as mentioned from section 3. A more accurate approach would be to compound the interest rate daily. In order to do so, the interest rate has to be maneuvered.

$$D_0(1 + \frac{i_{daily}}{100})^{365} = D_0(1 + \frac{i_{annual}}{100})$$

where D_0 is the initial debt and is set to be EUR 24.4 million for the 10MW wind turbine in this project.

$$i_{daily} = [(1 + \frac{i_{annual}}{100})^{\frac{1}{365}} - 1] \cdot 100$$

From this equation, the daily interest rate is computed to be 0.0054%. This value is fair small, but if computed compound for 365 days, the result would be the same as the annual 2% interest rate. All the interest rate used in the model development below would be using the daily interest rate and shown as i.

Continuous Compounding VS Compounding with Finite Period

This section would discuss the impact of different interest rate and its corresponding compounding method to the financial calculation accuracy. When calculating interest, the calculated interest based on finite number of period, such as annually, monthly or daily, is different to the result calculated with continuous compounding method, of which has an assumption in constant compounding over infinite number of periods. Most of the interest calculated from banks are continuously compounded. As a result, in order to realize the financial calculation, the compounding method that has the closest value to continuous compounding is chosen.
Continuous compounding and compounding with finite period have different calculation method, but not complicated. Equations to calculate the future value for the two methods are listed below in equation 7.1 and 7.2.
For compounding with finite period,

$$FV = PV[1 + (\frac{i}{n})]^{nt} \tag{7.1}$$

where FV is the future value; PV is the present value of the investment/debt; i is the interest rate; n is the number of compounding periods; t is the number of years.

For continuous compounding,

$$FV = PVe^{it} \tag{7.2}$$

As an example, assuming that EUR 10000 was the CapEx of the turbine, with 10% interest over the year. Below calculation are computed to show the ending value of the debt when the interest is compounded annually, semiannually, quarterly, monthly, daily and continuously.

Compounding	Equation	FV	Value Difference	% Difference
Annually	$10000 \cdot (1 + \frac{10\%}{1})^{1 \cdot 1}$	11000.00	51.71	0.47%
Semiannually	$10000 \cdot (1 + \frac{10\%}{2})^{2 \cdot 1}$	11025.00	26.71	0.24%
Quarterly	$10000 \cdot (1 + \frac{10\%}{4})^{4 \cdot 1}$	11038.12	13.59	0.12%
Monthly	$10000 \cdot (1 + \frac{10\%}{12})^{12 \cdot 1}$	11047.13	4.58	0.041%
Daily	$10000 \cdot (1 + \frac{10\%}{365})^{365 \cdot 1}$	11051.56	0.15	0.0014%
Continuous	$10000 \cdot e^{10\% \cdot 1}$	11051.70	0	0%

Table 6: Summary of Different Compounding Method (EUR)

If we choose to use compounding annually, there is quite a difference in the future value, and it is not a good methodology to adopt when we want to calculate continuously for the debt.
With daily compounding, the future value is extremely close to the continuous compounding, with only EUR 0.15 difference. As a result, the daily compounding method is suitable to calculate interest for the debt in this project.

Calculation Method for Returns the periodic payment for an Annuity (PMT)

For the future value of periodic payment, the governing equation is described in 7.3. If one is interested in the derivation of the equation, one could find it from financial handbook.

$$FV = pmt \cdot (1 + i) \cdot \frac{(1 + i)^n - 1}{i} \tag{7.3}$$

where pmt is the periodic investment/payment; i is the interest rate corresponding to the compounding period; n is the number of period. The derivation of the equation is shown in appendix C.

7.2.2 Objective Function

In order to do optimization, and objective function have to be developed. A debt function in time has been developed to calculate the final debt when the project is over at 20 years. By assuming that the state, $x = \begin{bmatrix} t_1 \\ t_2 \\ t_3 \end{bmatrix}$, and $D_{20years}$ be the Debt at the end of the project. $D_{20years}$ would be positive before the loan is aid. When the loan and interest are all

paid off and project is start to generate cash for the company, the $D_{20years}$ would become negative. The objective function is shown below.

$$D_{20years}(x) = \underbrace{D(t_2)(1+i)^{t3\cdot 365}}_{compound\ interest} - \underbrace{P_3(E-OpEx)(1+i)\frac{(1+i)^{t_3\cdot 365}-1}{i}}_{future\ value} \tag{7.4}$$

$$D(t_2) = D(t_1)(1+i)^{t3\cdot 365} - P_2(E-OpEx)(1+i)\frac{(1+i)^{t_2\cdot 365}-1}{i} \tag{7.5}$$

$$D(t_1) = D_0(1+i)^{t1\cdot 365} - P_1(E-OpEx)(1+i)\frac{(1+i)^{t_1\cdot 365}-1}{i} \tag{7.6}$$

for the $t_{payback} \geq 20$

where $t_{payback}$ is the payback time when the debt is zero; i is the daily compound interest; P_i is the power production by the three different operation mode, i = 1,2,3 and represent 11MW, 10MW and 9MW respectively, E is the electricity price and OpEx is the operating expenses, where these three parameters would be explained in the later section.

In the objective function, $D(t_1)$ and $D(t_2)$, in equation 7.5 and 7.6, represents the remaining debt at t_1, when 11MW operation mode finishes and the remaining debt at $t_1 + t_2$, when 10MW operation mode finishes. And the value of $D(t_1)$ and $D(t_2)$ would change according to t_1 and t_2. In the three equation 7.4, 7.5 and 7.6, the t_1, t_2 and t_3 are kept in the from of years for better comprehension.

The objective function utilize the method in calculating compound interest for the debt accumulation and future value of constant revenue as shown in equation 7.4 to calculate the final remaining debt $D_{20years}(x)$.

It should be noticed that the equation 7.4, 7.5 and 7.6 are only valid when debt cannot be paid back within the 20 years time, $t_{payback} \geq 20$. Since the three equations took account of the compound interest rate from the debt, If debt is paid off within the 20 years time, the objective function would have another expression to represent the the revenue generation without affected by the interest rate as shown below.

When $t_{payback} \leq t_1$, which means that the payback period happens during t_1, the 11MW operation. Equation 7.6 is still valid for $t_1 \leq t_{payback}$. For example, when $t_{payback} \leq t_1$

$$D(t_1) = D(t_{payback}) - P_1(E-OpEx)((t_1 - t_{payback})\cdot 365) \tag{7.7}$$

where $D(t_{payback}) = 0$ And then equation 7.5 and 7.4 would become

$$D(t_2) = D(t_1) - P_2(E-OpEx)(t_2\cdot 365) \tag{7.8}$$

$$D_{20years}(x) = D(t_2) - P_3(E-OpEx)(t_3\cdot 365) \tag{7.9}$$

7.2.3 Payback Time

Since the objective function depends on the payback time, the payback time has to be computed first. Payback time represents when the debt and interests are all paid by the revenue generated by power production. As such, it is when $D_{20years}(x)$, $D(t_2)$ and $D(t_1)$ equals to zero. Elaborating from previous section, when the payback time occurs during t_1,

$$\begin{aligned} D(t_{payback}) &= 0 \\ D_0(1+i)^{t_{payback}\cdot 365} &= P_1(E-OpEx)(1+i)\frac{(1+i)^{t_{payback}\cdot 365}-1}{i} \\ \frac{D_0}{P_1(E-OpEx)}(\frac{i}{1+i}) &= 1-\frac{1}{(1+i)^{t_{payback}\cdot 365}} \\ (1+i)^{t_{payback}\cdot 365} &= \frac{1}{1-\frac{D_0}{P_1(E-OpEx)}(\frac{i}{1+i})} \end{aligned}$$

$$t_{payback} = \frac{ln[\frac{1}{1-\frac{D_0}{P_1(E-OpEx)}(\frac{i}{1+i})}]}{ln(1+i)\cdot 365} \tag{7.10}$$

With the $t_{payback}$ computed, the objective function would be able to calculate the debt at 20 years.

Example Demonstration

The logic in Matlab is demonstrated in the logic chart shown below in figure 34. This logic is used to calculate the remaining debt of each period (t_1, t_2 and t_3).
The code would first check if the previous period is in debt, in the "Debt at the beginning of the period" block. If there are no more debt to be paid at the beginning of the period, the code would regard the period as an pure profit period, calculating all the energy production according to the electricity price. However, if the period is initially in debt, which means the code would follow the red arrow to check the "end of period debt value calculation". In this process, the code would investigate if the debt could be paid at the end of the period by calculating the future value of the debt as well as the continuous revenue generation from the energy production. If that period is still in debt at the end, the code would then follow the red arrow in the chart and calculate the remaining debt at the end of the period. This value would then be used in checking if the previous period was in debt for the next period iteration. However, if debt was being paid back within a period, the code would calculate the when exactly did the payback time happens. Furthermore, the amount of profit not affected by the interest rate would be calculated as the remaining debt (negative = profit) at the end of the period.
A section of the Matlab script is demonstrated in appendix E to show the example gone through in section 7.2.2 and 7.2.3.

Referring to the figure 72, there are three condition in calculating the Debt, it is named `Debt_remaining_t1` in the matlab script. When payback time does not happen during t_1, as a result, an equivalent calculation is made from line 26-30 based on equation 7.6.

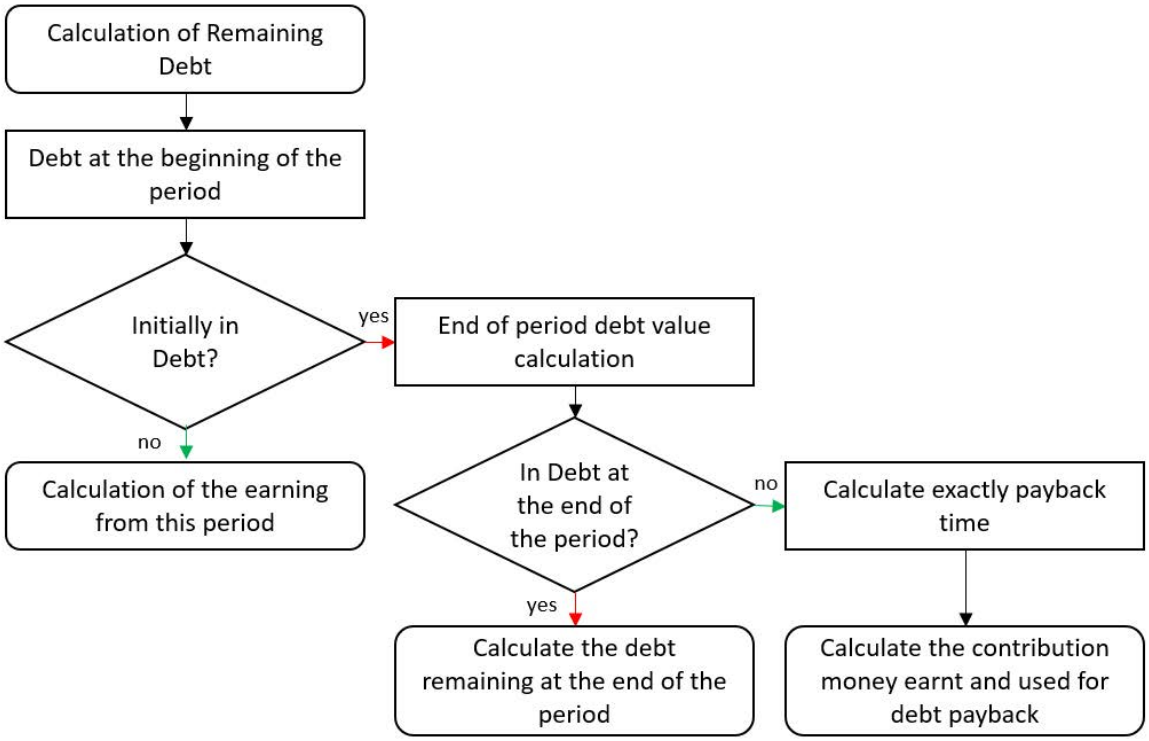

Figure 34: Matlab logic for demonstration

Alternatively, when payback time occurs during t_1, the model compute the $t_{payback}$ and compute the remaining debt as shown from line 32-41. Lastly, if the $t_payback$ occurs before t_1, or no debts have to paid at the beginning of the operation, line 43-46 would calculate the revenue generation according to t_1.
This example showcased the general logic that applied to the whole objective function and t_2 as well as t_3 are constructed in the same way. The result has compared with the pro-forma balance sheet calculation with excel and obtained the same numbers.

7.2.4 Revenue

As mentioned in equation 7.4, 7.5 and 7.6, the power production depends on t_1, t_2 and t_3 as well.
First of all, the P [kWh] of each operation modes are calculated based on Rayleigh distribution.

$$P \begin{bmatrix} 11MW \\ 10MW \\ 9MW \end{bmatrix} = \begin{bmatrix} 1.442e5 \\ 1.358e5 \\ 1.268e5 \end{bmatrix}$$

The power production shown above, are the results of dividing the AEP by 365, which means they are the value for daily power production. They are divided to suit the calculation requirement in the objective function. It is also assumed that the daily power production is linear. Although the daily production is unlikely to be linear, and would affect on the debt calculation, this assumption is based on the point of view to construct a more systematical financial model. If the power production shall be another factor that

would affect the debt calculation, a time dependent function of the power production could be form to realize the phenomenon.

Secondly, the electricity price, E(t), which could varies according to time, is assumed to be constant at a Chinese market price, EUR 0.0737/kWh.

$$E(t) = E_o = 0.07371$$

7.2.5 OpEx

As for OpEx, the market OpEx value has been chosen, EUR 0.0146/kWh. With the assumption that the OpEx is a constant throughout the project life-time.

$$OpEx(t) = OpEx_o = 0.0146$$

7.2.6 Discretized Model

This section addresses the discretization of the model if it has to be used. The debt calculation may be modeled using the financial balance in each t, where t here is discretized time. Assuming the parameters are the same as previous section, the financial balance takes the form

$$Debt_{new} = Debt_{old} - Payback$$

Consider the time interval, [t, t+Δt], with Δt sufficiently small such that all the values are considered constant during the interval.

Assuming here D(t) [EUR] to be the Debt, P(t) [kWh/s] to be the revenue, E(t)-OpEx(t) [EUR/kWh] to be profit per power and $\alpha(t)$ to be the interest rate for the time interval.

$$Debt_{new} = D(t + \Delta t)$$

$$Debt_{old} = D(t)$$

$$Payback = P(t)[E(t) - OpEx(t)]\Delta t - D(t)\alpha(t)\Delta t$$

$$D(t + \Delta t) = D(t) - (\underbrace{P(t)[E(t) - OpEx(t)]\Delta t - D(t)\alpha(t)\Delta t}_{Payback})$$

$$\frac{D(t + \Delta t) - D(t)}{\Delta t} = \alpha(t)D(t) - P(t)[E(t) - OpEx(t)]$$

$$D'(t) = \alpha(t)D(t) - P(t)[E(t) - OpEx(t)] \tag{7.11}$$

And a first order linear differential equation is obtained in equation 7.11. The discretized model was not utilized in the model development but is still shown in this section to provide further information for readers to distinguish the disretized form of the model.

7.2.7 Constraints

In this optimization process, constraints have to be constructed such that the model would represent our wind turbine system. The constraints in this system are the life-time equivalent fatigue load or the total life-time of the turbine. The two constraints will be transformed into linear equality and inequality constraints.

First, the 10MW operation life-time equivalent fatigue load is set as the fatigue limit such that the turbine would be assumed to break if exceeding the limit.
With the calculation results from previous section on the difference in fatigue loads, the fatigue load is assumed to be used up 10% more and less for the 11MW and 9MW operation.
For a 20 years life-time turbine, the correlation between the operation period, (t_1, t_2 and t_3), and the fatigue load limit could be represented below.

$$F_{eq,L} \geq 0$$

$$20 - 1.1 \cdot t_1 - t_2 - 0.9t_3 \geq 0$$

$$1.1 \cdot t_1 + t_2 + 0.9t_3 \leq 20$$

$$\underbrace{\begin{bmatrix} 1.1 & 1 & 0.9 \end{bmatrix}}_{A} \cdot \underbrace{\begin{bmatrix} t_1 \\ t_2 \\ t_3 \end{bmatrix}}_{x} \leq \underbrace{20}_{b} \tag{7.12}$$

The fatigue load limits has formed the first linear inequality constraints. The linear equality constraints could be formed with the total life-time of the turbine, which is,

$$t_1 + t_2 + t_3 = 20$$

$$\underbrace{\begin{bmatrix} 1 & 1 & 1 \end{bmatrix}}_{A_eq} \cdot \underbrace{\begin{bmatrix} t_1 \\ t_2 \\ t_3 \end{bmatrix}}_{x} = \underbrace{20}_{b_eq} \tag{7.13}$$

With constraint 7.13, one could realize that, in fact, the state could be reduced from $x = \begin{bmatrix} t_1 \\ t_2 \\ t_3 \end{bmatrix}$ to $x = \begin{bmatrix} t_1 \\ t_2 \end{bmatrix}$ since t_3 could be calculated implicitly. This concern was recognized during the model development process, and the reason it was not simplified was that the author believes if the state is defined as it is right now, it would be less confusing and easier for readers to realize the different operation schedules.

7.3 Optimization Process

In the optimization process, **fmincon** function is used in determining the optimal state, x, from the objective function. A section of the **fmincon** function and script is demonstrated in the appendix E. In line 55 and 56 of the script in figure 73, it demonstrated the fatigue life time constraint construction. In line 57 and 58 it developed the 20 years time-life equality constraint.

7.4 Deterministic Model Results

Knowing that all the parameters in this model, it is regarded as a deterministic model. From the optimization process, the optimal state results is computed and shown below,

$$x = \begin{bmatrix} 5.7 \\ 8.5 \\ 5.7 \end{bmatrix}$$

The optimal results is then compared with the baseline operation that operate only with 10MW mode for 20 years, such that

$$x = \begin{bmatrix} 0 \\ 20 \\ 0 \end{bmatrix}$$

Result is shown in figure 35, where blue line and red dotted line denotes the optimal and baseline operation. The net revenue in the upper left plot shows the total profit of the turbine throughout 20 years. At the beginning, the net revenue is negative as the project finance is in debt, and it could be observed that the optimal operation succeed in pushing the payback time from 9.1 to 8.7. And by operating in optimal operation, the project gain 0.2% more profit than baseline and equivalent to EUR 70,000 for one 10MW turbine. In terms of the debt service, as shown in the lower left plot, the optimal operation reduce 5.8% interest incurred that the project have to pay back than baseline and equivalent to EUR 133,000 for one 10MW turbine. Although the incurred interest has been reduced tremendously, the total profit is smaller than such a value due to the fact that a lower operation mode has to be used to compensate the frontloading turbine for the first 5.7 years in the optimal scheme.
For the lower right corner plot, it shows the normalized fatigue usage of the turbine. When the value become zero, it represents the fatigue usage has reach the 10MW reference fatigue level, which is defined to be the turbine limit in this project. As shown in the plot, the optimal operation used up more fatigue at the beginning than the baseline operation and both of them end up at 0 nominal fatigue in year 20.
The last plot, upper right corner, is a surf plot showing the net revenue obtained at year 20 under different operation. The x and y axis represent the t_2 and t_1, where t_3 could be computed with given t_2 and t_1 value. The color shows different level of net revenue of a specific operation. The blue dot in the figure shows shows the optimal operation result, where red dot demonstrate the baseline result. As mentioned previously, the order of magnitude is small for the net revenue difference between the two operations, as a result no obvious observation could be seen in the plot. However, this plot could act as a map for quick check and easy comprehension.

7.5 Results Discussion

In the following section, the simulation results and their corresponding meaning toward the project would be elaborated and discussed. Explanations and examples would be demonstrated both analytically and theoretically.
These explanation would be discussed on top of two examples that would be listed below.

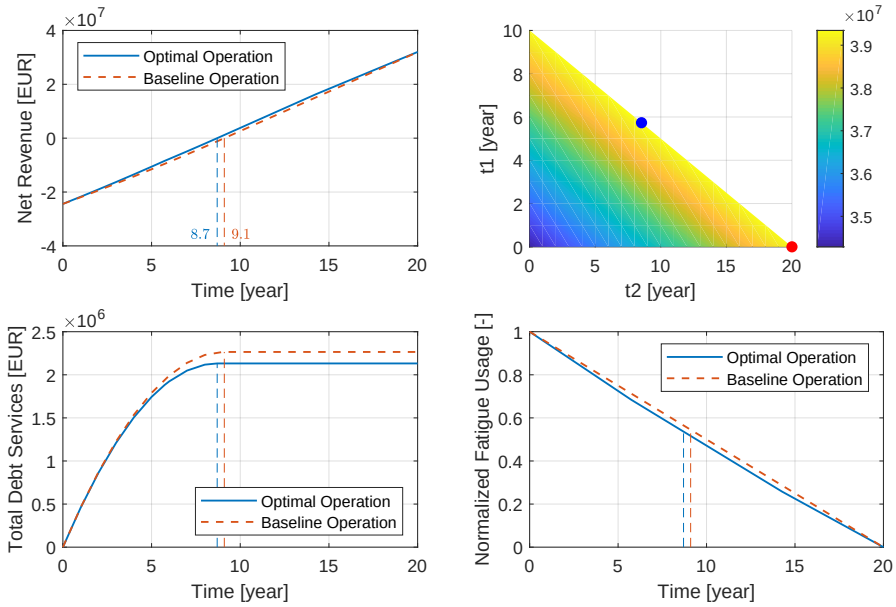

Figure 35: Optimal and Baseline result comparison

The first example is the comparison between baseline case, where the turbine operate normally under 10MW for 20 years, with the optimal case, of which is the optimized operation calculated with uprating and derating operations added within the 20 years operation schedule. The result of this example was briefly described in previous section. However, detail explanations in turbine operation and finance are discussed in order to distinguish the optimization process.
Similarly, another example would be discussed between the optimal operation with the 10 years frontloaded case, which is a operation schedule that would operate frontloaded for the first 10 years.
These example would enable readers to understand the logic and process the optimizer has adopted and clarify what parameters were optimized with reasons.

7.5.1 Comparison between Baseline and Optimal Schedule

The first example, we have here is the comparison between Baseline and Optimal scheme. For simplicity, the two schemes would be represented with their state, optimizing parameters, x_b and x_{opt} respectively.

$$x_b = \begin{bmatrix} 0 \\ 20 \\ 0 \end{bmatrix}$$

$$x_{opt} = \begin{bmatrix} 5.7 \\ 8.5 \\ 5.7 \end{bmatrix}$$

where we have x_{opt} optimal scheme operating at up-rated mode, 11MW, for the first 5.7 years, following with 8.5 years of the normal operation mode while sustaining turbine life-time with the down-rated, 9MW, operation for the last 5.7 years. And x_b, normal 10

MW operation turbine for 20 years.
Their payback period are 8.7 and 9.1 years respectively for optimal and baseline operation.

Operation

The two different operation schedules can also be observed from figure 36. Figure 36 describes how the revenue are being used yearly. The figure separate the the usage of revenue in to three categories, namely debt service (interest), debt and profit, where darker and lighter color represents optimal and baseline schedule. The height of each bar represent the revenue of each year according to their operation schedule.

As it could be observed that the first 5 years of the optimal scheme, the yearly revenue maintained at EUR 3,100,000 level as shown in darker color in figure 36. However, there is a slight decrease in revenue in the 6th year with a value of EUR 3,060,000. It is because in the 6th year, the operation is a combination of up-rated (11MW) and normal (10MW) operation. As a result, the value in the 6th year is slight lower than the previous 5 years but higher than the 7th year, EUR 2,930,000, which is the normal (10MW) operation. And it operates with the same level until the 14th year, when the operation is further tuned down to the de-rated (9MW) operation for the rest of its 20 years operation with yearly EUR 2,734,000 revenue.
On the other hand, the baseline scheme operated only through the normal (10MW) operation mode for 20 years. And thus, it maintained on EUR 2,930,000 level yearly.
As a result, the trend in figure 36 agrees and helps to visualize the financial indication of the two states, x_{opt} and x_b.

Furthermore, the operation scheme of the two state could also be validated from the normalized fatigue usage in the bottom right of figure 35. It can be observed that the up-rated (11MW) operation, which consumes 10% more of the fatigue than the normal (10MW) operation, consume the fatigue usage more aggressively for the for the first 5.7 years. It stays parallel with the normal operation until the 14th year when the de-rated operation kicks in and reach zero at year 20, same as the baseline scheme.

Debt and Debt Service

In terms of debt and debt service between the optimal and baseline schemes, the red and blue color which represent the debt service and debt as shown in figure 36 are studied. It could clearly be seen that for the first year, the debt service is exaclty the same since the initial debt is the same for the two schemes. However, as more revenue is generated for the optimal scheme, debt is also paid back in a faster pace as shown in figure 37.
In figure 37, it can be seen that the initial debt is the same for both operation schemes. However, the debt is paid off more in the first year for optimal scheme.
Subsequently, less debt service is generated for the optimal scheme every year afterward. And debt is paid off in 8.7 and 9.1 years for the optimal and baseline scheme.
This also validate the diminish return in the bottom left of figure 35, which is caused by the less and less amount of interest one has to pay. The percentage of the interest to the

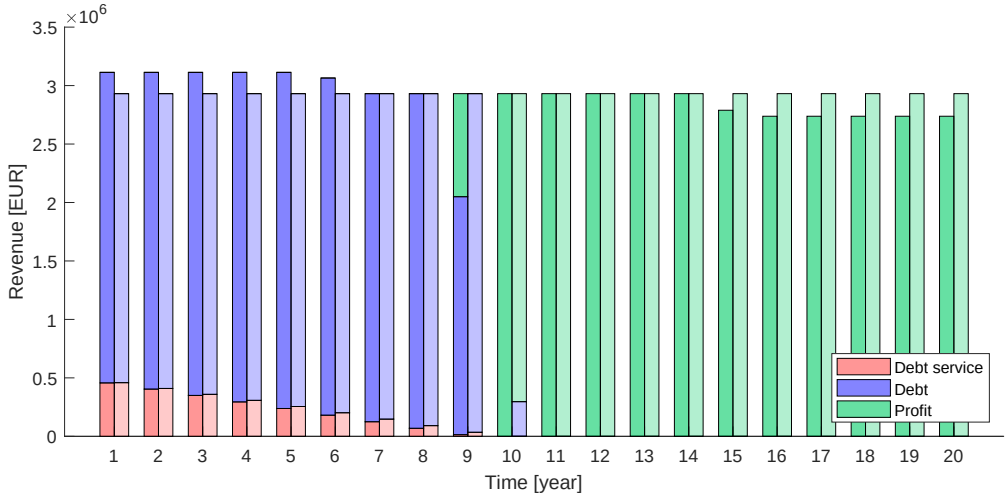

Figure 36: Yearly Distribution of Optimal Scheme (dark in color) and Baseline Scheme (light in color)

CapEx for the baseline scheme is 9.28% and 8.73% for the optimal scheme. By adopting the optimal operation schedule, the project paid less debt service by EUR 132,600 for each turbine.

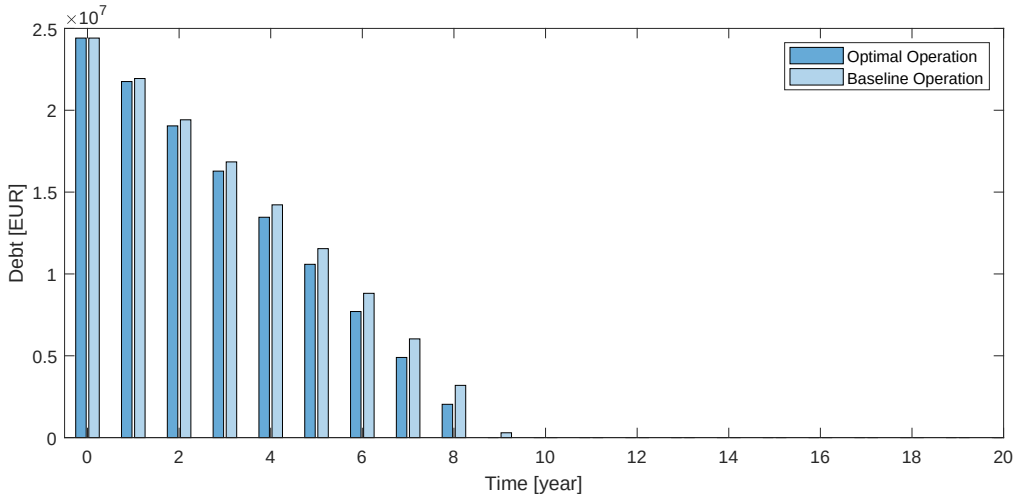

Figure 37: Yearly Debt Distribution of the two Schedules

Profit

As for profit, the green color labeled in figure 36, indicated when and how much does the project start making profit from the turbine.
As shown in the figure, the optimal scheme start earning money at year 9 and year 10 for the baseline scheme. However it should be noticed that the two schemes do not earn the same revenue every year. As the optimal scheme would be operating in the de-rated mode proportion to the length of the up-rated operation mode, the turbine in fact earn

less during the de-rated mode, where the less revenue every year might contribute to less profit overall for the turbine.
However, refer back to the upper left of figure 35, the final profit of the optimal scheme is higher than the baseline scheme. The baseline and optimal scheme has EUR 31,937,000 and EUR 32,010,000 profit. There is a 0.2% profit, EUR 70,000, increase in the optimal scheme for each turbine.

The advantage of the optimal scheme is that, the scheme took care of the debt service at the beginning and prevent it from snowballing through out the years. And the margin created by reducing the debt service can compensate the lost in operating a de-rated turbine under the defined period. The optimal scheme can not only reduce the amount of interest have to be paid, but also taking into account the downfall of the de-reated operation to maximize the profit for the turbine project over the 20 years.

7.5.2 Comparison between Upfront and Optimal Schedule

In this section, two operation schemes would be compared. An upfront operation schedule, of which the turbine is operated under frontloaded power mode for the fist 10 years, would be compared with the optimal scheme. This comparison is different than the previous example, which is the comparison between the optimal and the baseline. The previous example showcases most of the logical relationships between the operation schedule with the debt and total debt service incurred. However, this example would demonstrate more as a special case and aim to illustrate some more decision thinking behind the optimization model developed. In fact, this example aims to demonstrate that even if the debt service is minimized, the life-time profit might not be the highest.

Similar to the previous example, some of the general numerical information are shown below.
For simplicity, the two schemes would be represented with their state, optimizing parameters, x_b and x_{opt} respectively.

$$x_{upfront} = \begin{bmatrix} 10 \\ 0 \\ 10 \end{bmatrix}$$

$$x_{opt} = \begin{bmatrix} 5.7 \\ 8.5 \\ 5.7 \end{bmatrix}$$

where we have x_{opt} optimal scheme, which is the same mode as mentioned in previous example. And the upfront operation mode which operate at the up-rated (11MW) mode for the first 10 years and de-rated (9MW) mode for the remaining 10 years.
Their payback period are 8.7 and 8.5 years respectively for optimal and Upfront operation.
It is interesting that one would find the upfront mode actually achieve a faster payback period of 8.5 years. By judging through the payback period, one could imagine the upfront scheme is a better scheme for the turbine operation. However, the optimal scheme

shown otherwise. A detail explanation in this would be discuss in the sections below.

Result Comparison

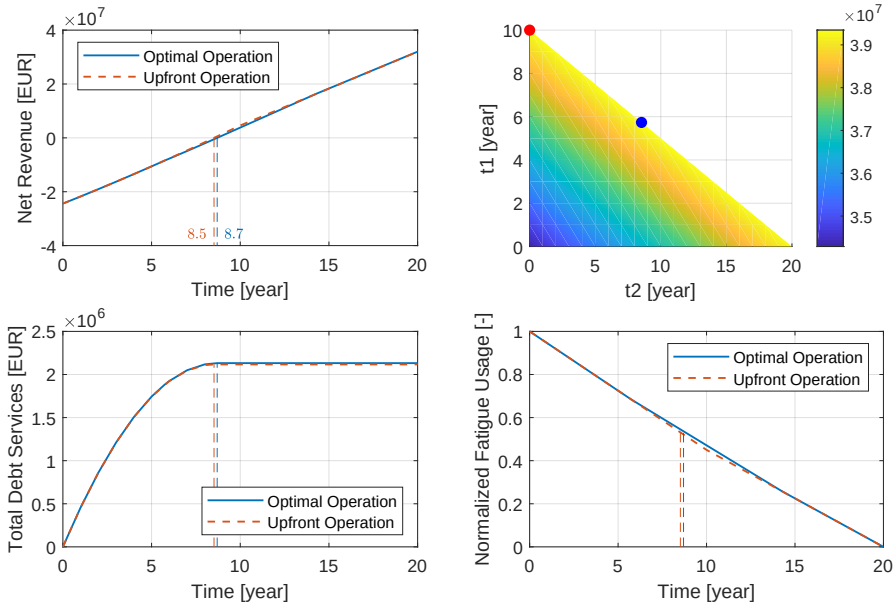

Figure 38: Optimal and Upfront scheme result comparison

The brief result comparison is conducted for the two schemes as shown in figure 38. As shown in figure 38 in the upper right figure, the comparison is made for the two cases between optimal (blue dot) and upfront (red dot) schemes.

From the net revenue (upper left) and total debt service (lower left) in figure 38, it could be seen that two nearly identical trend and values are plotted. A magnified plot of the revenue and the total debt service are plotted in figure 39 and 40 respectively. It can be seen that the total profit of the optimal operation is slight superior than the upfront operation from figure 39. The profit made at the end of the project life-time is EUR 32,010,000 and EUR 31,970,000 for the optimal and upfront scheme.
On the other hand, figure 40 shown that the upfront operation payback earlier and less debt service has to be paid compare to the optimal scheme. The upfront mode has to pay worth of EUR 2.116,000 for the debt service, which is EUR 15,220 less than the optimal scheme, which has to pay back EUR 2,132,000 worth of debt service through out the 20 years.
This demonstrated that even if less interest has to be paid, in this case 0.7% less interest for the upfront operation, the final profit of the project can be different. An this example demonstrated an improved profit of 0.1%, equivalent to EUR 31,700, for the optimal scheme than the fastest pay back operation scheme, upfront mode.
Some detailed elaboration between the two schemes are discussed in the next section.

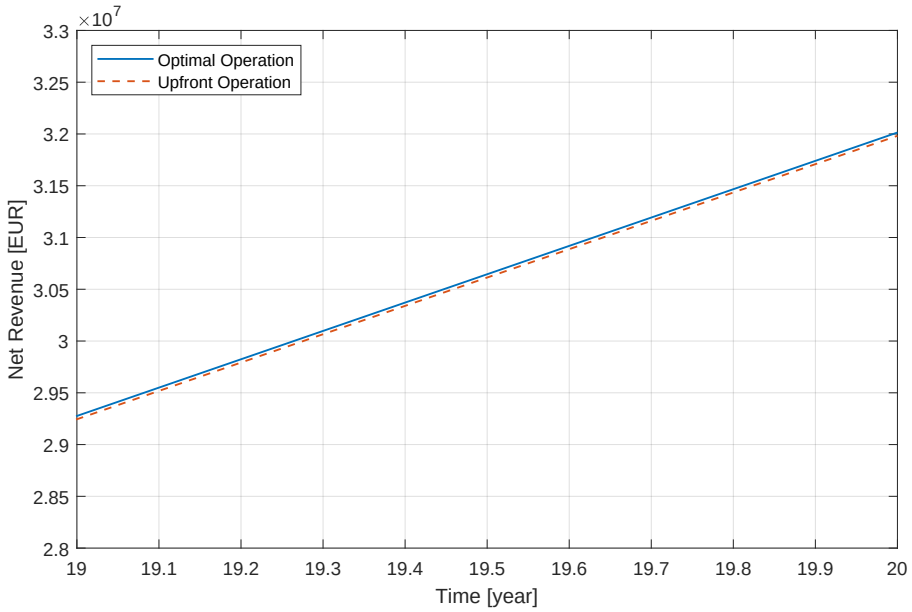

Figure 39: Optimal and baseline result comparison

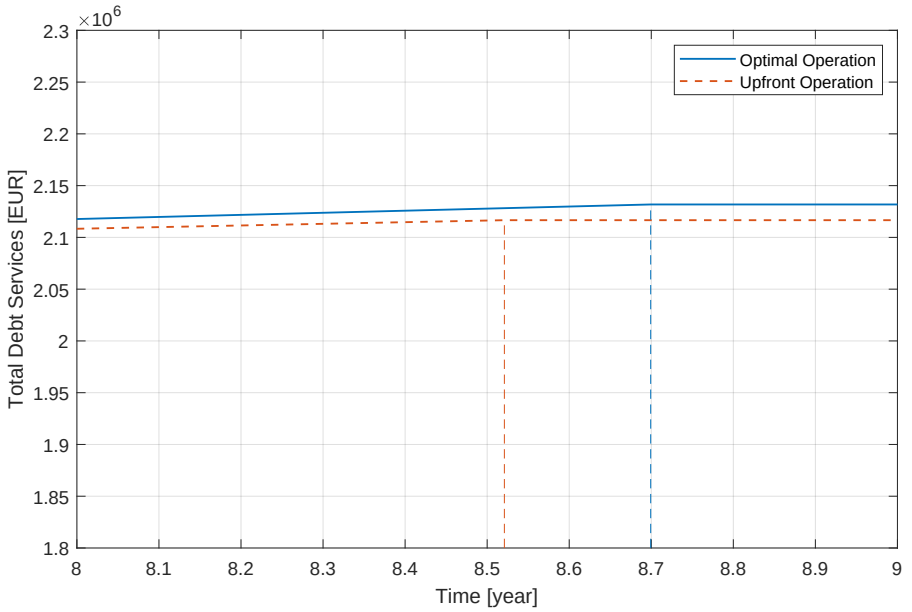

Figure 40: Optimal and baseline result comparison

Operation

The two different operation schedules can be observed from figure 41. Figure 41 describes how the revenue are being used yearly between the two case in this example. In the figure, the optimal and upfront operation are illustrated in darker and lighter color respectively.

The optimal operation in the figure is the same to the previous example, as a result, it would not be discussed in this section again. For the detailed explanation for the optimal operation trend, one could find it from the previous section.

As for the upfront operation, it could be seen that the up-rated (11MW) operation mode has run for the first 10 years, with yearly revenue production of EUR 3,108,000. And starting from year 11, the operation translated to the de-rated (9MW) mode, due to the remaining available fatigue usage, with yearly revenue production of EUR 2,734,000. And the bar chart results agree with the x_{opt} and $x_{upfront}$ as mentioned previously.

As mentioned, the upfront mode has to switch back to the de-rated mode in the 11th year due to the available fatigue usage. This is also illustrated from the (lower right) figure 38, where it could be seen that the normalized fatigue usage for the upfront mode consume the fatigue aggressively for the first 10 years. Based on the structural constraint developed in the optimizer, in order for the turbine to run for the remaining years, it has to be ran under the de-rated mode.

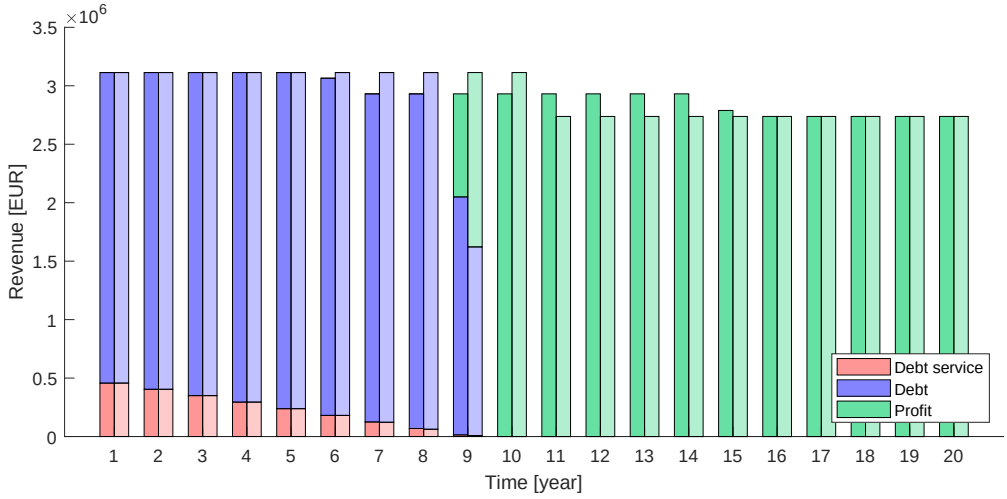

Figure 41: Yearly Distribution of Optimal Scheme (dark in color) and Upfront Scheme (light in color)

Debt and Debt Service

In terms of debt and debt service between the optimal and upfront schemes, the red and blue color which represent the debt service and debt as shown in figure 41 are studied. It can be seen that for the first 5 years, the debt service and the corresponding debt contribution in each each is the same. It is because the initial debt and the yearly revenue production of the first 5 years are the same for the two schemes. However, when the optimal scheme start to operate differently in year 6, the debt service start to behave differently in year 7. The debt service incurred for the optimal mode becomes larger than the upfront mode, since less debt is being paid off at the end of the year 6.
In figure 42, which shows the remaining debt for each operation scheme, also shows that more debt is being paid off for the upfront mode from year 6.

Subsequently, less debt service is generated for the upfront scheme every year afterward. And debt is paid off earlier in 8.5 years.
The percentage of the interest to the CapEx is 8.73% and 8.67% for the optimal and upfront scheme, which means the project paid less debt service by 0.67%, EUR 15,100, for each turbine by adopting the upfront operation schedule.

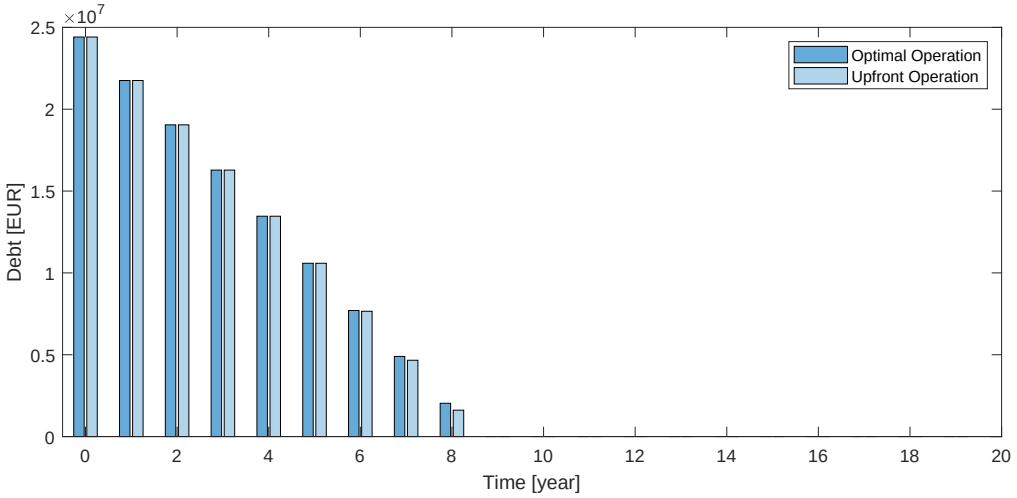

Figure 42: Yearly Debt Distribution of the two Schedules

Profit

As mentioned, even if the upfront scheme succeed in reducing the total debt service, the total profit is more superior in the optimal scheme. As for profit, the green color labeled in figure 42, indicated when and how much does the project start making profit from the turbine.
It can be seen that both operation start to make profit in year 9. While the upfront scheme operate at the up-rated (11MW) mode in year 9 and 10, it has to be switched to the de-rated (9MW) mode since year 11. And by switch to the de-rated mode, it also represent less revenue production for the next 10 years. On the other hand, the optimal scheme although operate at the normal (10MW) operation, it maintained until year 14. This is believed to be the reason why optimal scheme generate more profit at the end of the project.
The advantage of the optimal scheme is that, the scheme aims to maximize the end goal, final profit. Although the upfront mode created a profit margin in the debt service, by paying off the interest as soon as possible, it constraints itself due to turbine structural integrity and has to operate in a de-rated operation for much longer time and cost it less profitable. In another word, the optimal scheme paid EUR 15,130 more debt service by gained EUR 31,700 more profit at the end.

7.6 Electricity price uncertainty

The deterministic model of the optimizer and few examples have been discussed from previous section, where most of the calculation and optimization computation are being conducted with a certain electricity price. The electricity price that was used in the computation was chosen to be a constant Chinese price, EUR 73.72/MWh, for the deterministic model. This means that the electricity price for all the electricity produced from the turbine for its life-time 20 years are assumed to be able to be sold under the price of EUR 73.72/MWh. Even though the price value is slightly higher compares to the European value the payback period and the financial calculation outcome is realistic for the give operating expenses and capital expenditure.
However, one should be reminded that capital expenditure and the operating expenses used in this project are generic numbers collected from literature that describe the general trend of the industry. For specific numbers for individual project, the number shall be collected site specifically. Few factors could affect the capital expenditure and operating expenses, for example, the accessibility of the site, grid connection or even wind resources. Detail explanation between the price and different factors would not be discussed in this project. The general idea is that the price would always goes up if the construction is more complicated.
In terms of the electricity price, this section is dedicated in showcasing how the uncertainty is being tackled in the project. The uncertainty in the electricity price would be treated statistically and some anticipated profit with certain confident interval would be computed. These number could tell users what profit margin they are looking into under specific price uncertainty and how likely the profit could be made under the optimal operation computed from the optimizer. The trend of the electricity price would first be discussed, follow with formulating its distribution and finally determine the confident interval for different profits.

7.6.1 Electricity Price in Denmark and China

In this project, we are interested in both the price range in Denmark and China. As a result, this section would look into the available data from different organizations to conclude different price range and uncertainty that project developer would face when operating wind turbines or farm in different continents.

Denmark

The first set of data would be discussed is the electricity price in Denmark. The electricity price in Denmark is collected from the Nord Pool AS, which is the company that runs the largest market for electricity energy in Northern Europe. A lot of the electrical energy produced in the Nordic market is traded with this platform. This platform is currently operating in Norway, Denmark, Sweden and many other countries in Europe. A demonstration of the available market from Nord Pool is shown in the map in figure 43.
It could be seen that different location has different market price. Reasons could be due

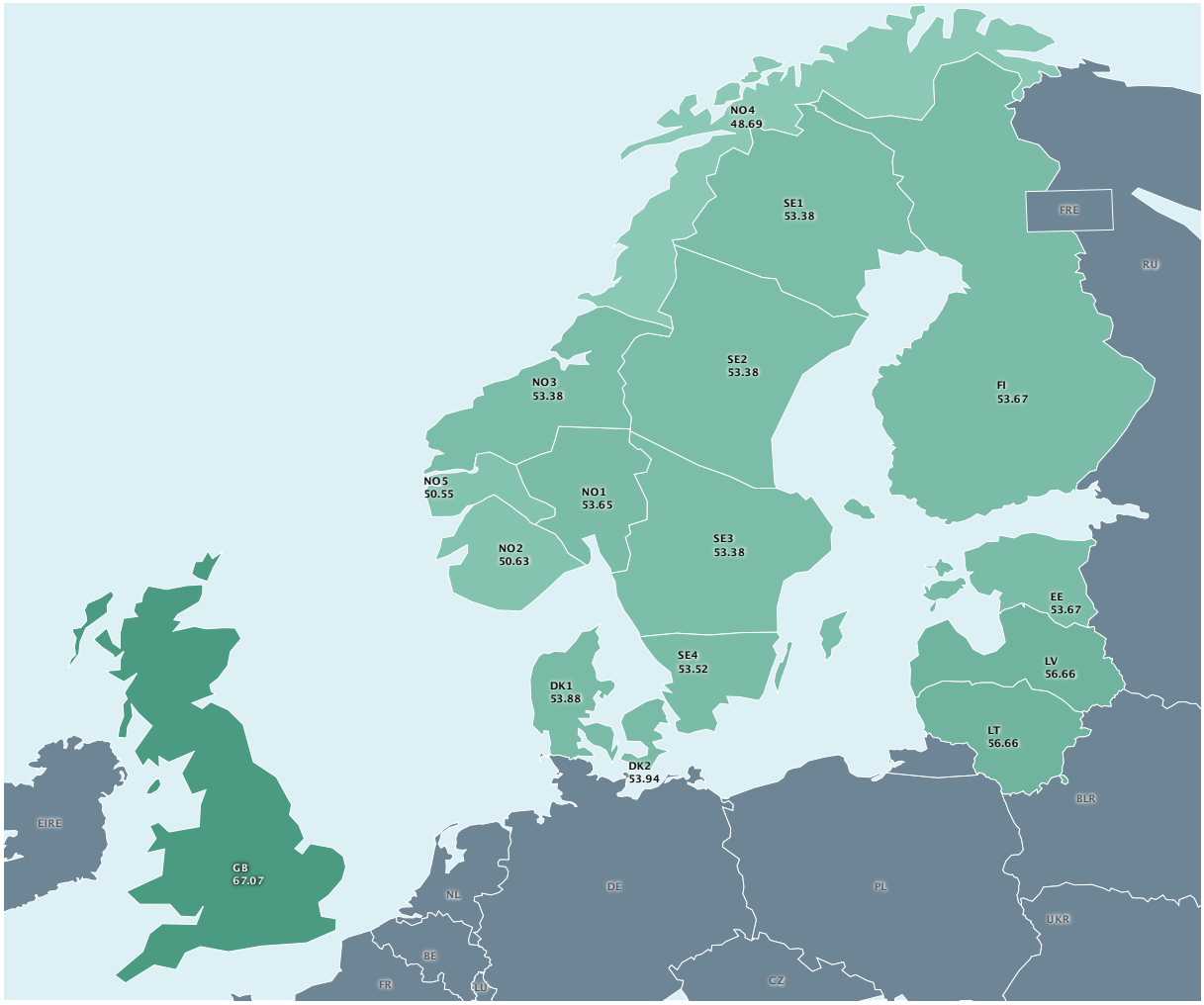

Figure 43: Map of trading market within Nord Pool (Euro)

to the market trading trend of electricity accessibility in different location, however they would not be discussed in this project. The market price that the project is interested in is the price in Denmark. For the electricity in Denmark, it separates into two regions, namely DK1 and DK2, which represent Jylland and Sjælland in Denmark. Price in Jylland is chosen for this study as more projects located in Jylland. The electricity price data farom the start of June 2017 were collected until the end of May 2018 and plotted below in figure 44. The annual data was collected and intended to take the annual fluctuation into account when calculating the price uncertainty. Further data could be collected and determine the uncertainty of the electricity price, which could make the model more realistic.
By further plotting the distribution of the data set, figure 45 shows that the distribution is similar to a normal distribution.

As a result, by assuming it is a normal distribution, the mean of the data set is calculated to be EUR 33.0/ MWh with a standard deviation of 9.1. Wind Power that are being sold in Nord Pool will receive a premium on top of the price, which regard to each of the project agreement made with the government. As a result, usually there is a extra

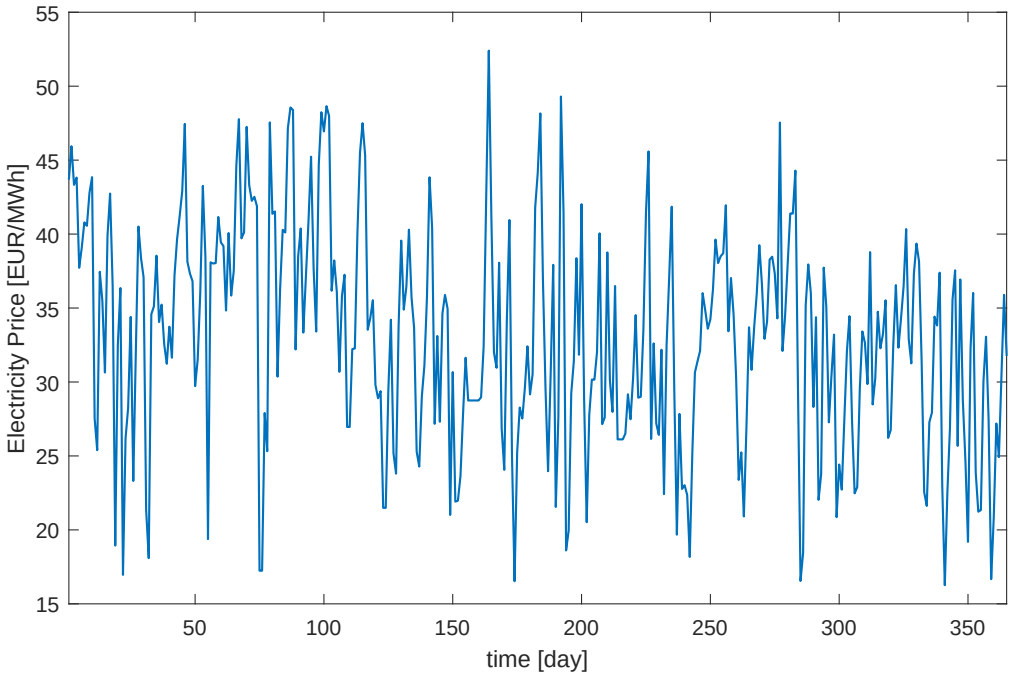

Figure 44: Time Series of Electricity Price in Denmark (6/17-5/18)

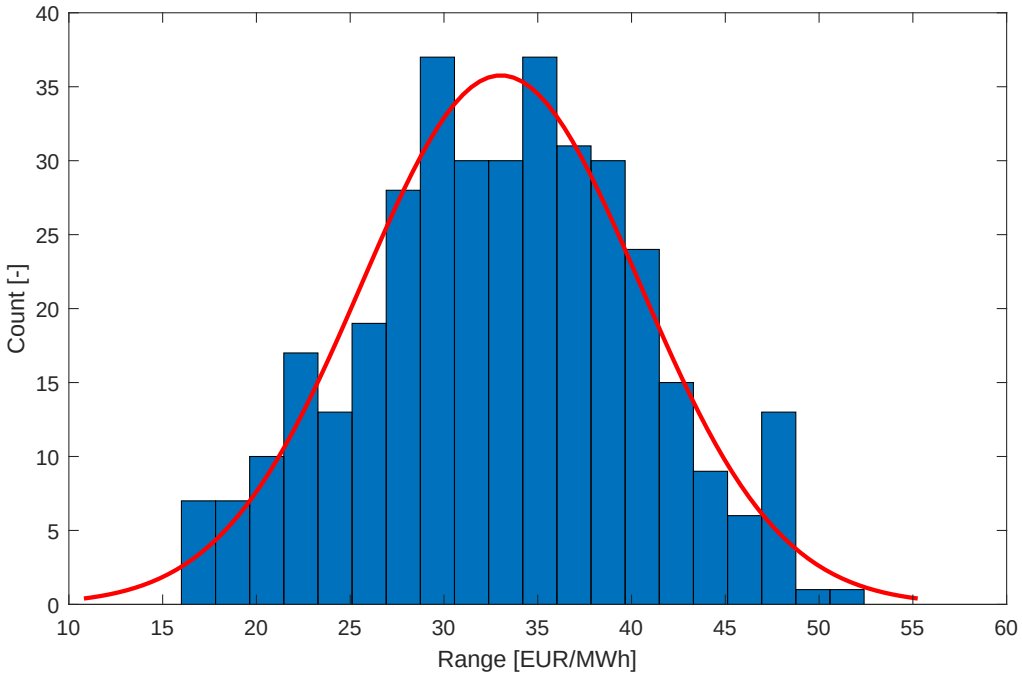

Figure 45: Distribution of Electricity Price in Denmark (6/17-5/18)

premium for wind energy for approximate extra EUR 20/ MWh.

China

In China, the electricity price for wind power selling to the grid has recently been updated and would be unified as high as approximate EUR 73.72/ MWh depending on the region of the project. The official document could be found in the appendix in figure 55. The document suggested that starting from 2018, all on-shore wind turbine electricity would have a unified price in selling electricity to the grid and are divided into four group. The document specified different price categories ranging from group 1 to 4 with electricity price range from approximate EUR 49.0/MWh to EUR 73.72/MWh. The reason for the different groups is due to different region geographically. The geographic difference in each group represents the saturation of the market as well as the availability of the wind resources. Group 1, which is the lowest electricity selling price, consist of all the well developed market in the country and mostly located at the northern part, where wind resources and accessibility are better than other groups. Group 2 and 3 represents few developing wind turbine market regions in China. And for all other regions unmentioned in the document would receive the highest electricity price, Group 4, when they are sold to the grid. It is expected that the government wish to encourage wind farm development all over the country with the extra premium incentive. Knowing that there are several Goldwind projects planning on developing in the Group 4 region, the Group 4 electricity price is chosen for this project.

7.6.2 Distribution for the project

As mentioned in previous section, the electricity price that were collected are shown in table 7.

Location	Mean [EUR]	Standard Deviation
Denmark	33.0 + premium	9.1
China	73.72	n/a

Table 7: Summary of Electricity Price in Denmark and China

Since the electricity price in China is not fluctuating at the moment and this project would like to investigate the influence under the price uncertainty. The mean value of Denmark is replaced with the Chinese value. So that it could mimic as if the Chinese electricity price is an open market with daily fluctuation like Nord Pool.
With the assumption of normal distribution, the probability density function and cumulative density function with mean and standard deviation value of EUR 73.72/MWh and EUR 9.1/MWh is plotted in figure 46.

7.6.3 Guaranteed Profit under uncertainty

Under the price uncertainty, the guaranteed profit could be further narrow down by specifying which percentile of the electricity price is focused. For example, when one is interested in the guarantee profit for the top 10% under the price uncertainty in the price distribution in figure 46 the 90 percentile of the electricity price will first be looked up

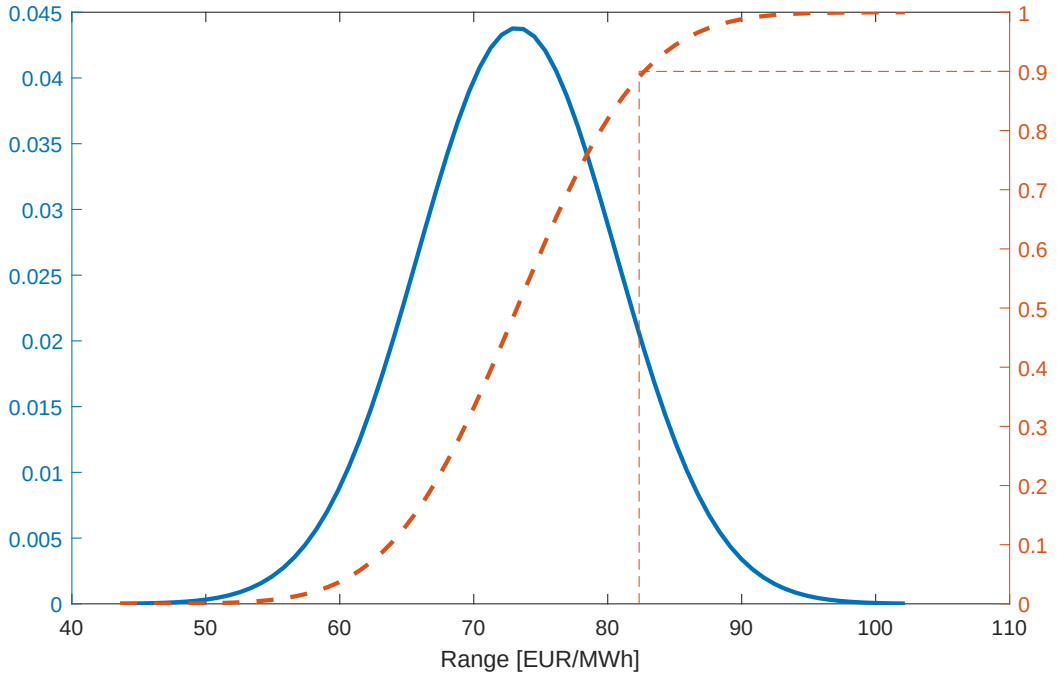

Figure 46: PDF (blue) and CDF (orange) of the electricity price uncertainty

from the CDF plot as shown with the orange dotted line in figure 46. Where the top 10 percentile of the price would be corresponding to EUR 82.75 /MWh price level. By putting this new electricity price into the deterministic optimizer as a constant electricity price, the guarantee profit could be computed. In this case the guaranteed profit for the top 10% under this price uncertainty is calculated to be EUR 41,253,000 at the end of the 20 years. Alternatively, if the lower 10 percentile is interested, which is the case where 90% of the electricity price would be higher, the corresponding price would be EUR 63.73 /MWh and the guaranteed profit would be EUR 21,263,000 at the end of the 20 years.

7.7 Optimal Operation under Electricity Price Fluctuation

Previous sections have described the model behaviors and different operation results under a constant electricity price, where optimal operating schedule is computed to maximize the end project profit. Furthermore, by assuming the electricity price as a normal distribution, confident interval of the potential profits are able to be computed. However, the model is similar to an open loop computation for the operation, when electricity price prediction is changed on daily basis, the model has to compute the optimal result again. In order to address both the daily fluctuation of electricity price as well as reflecting the optimal operation under the daily uncertainty of the electricity price. The optimization model has adopted new logic and computation to handle the electricity price uncertainty. And this section would explain step by step in how it is handled by the optimization model.

7.7.1 Model Computational Process for Electricity Price Fluctuation

In handling the fluctuation of the electricity price, the optimization model has adopted the steps listed from figure 47. The model would first receive the input of the electricity price profile for the period during the operation of the turbine, from users. After the optimization model fed with the input, the model would calculate the threshold, in electricity price, for different operation modes of the turbine. The calculation of the threshold is based on the objective to maximize the project final profit. As a result, the exact payback time of the turbine could be calculated as well as the final profit. If there is an new estimation of the electricity price uncertainty, the model would then take into account of the current turbine operation data, to further compute the new optimal operation as well as threshold for the turbine. Each of the steps taken by the model is further discussed in sections below.

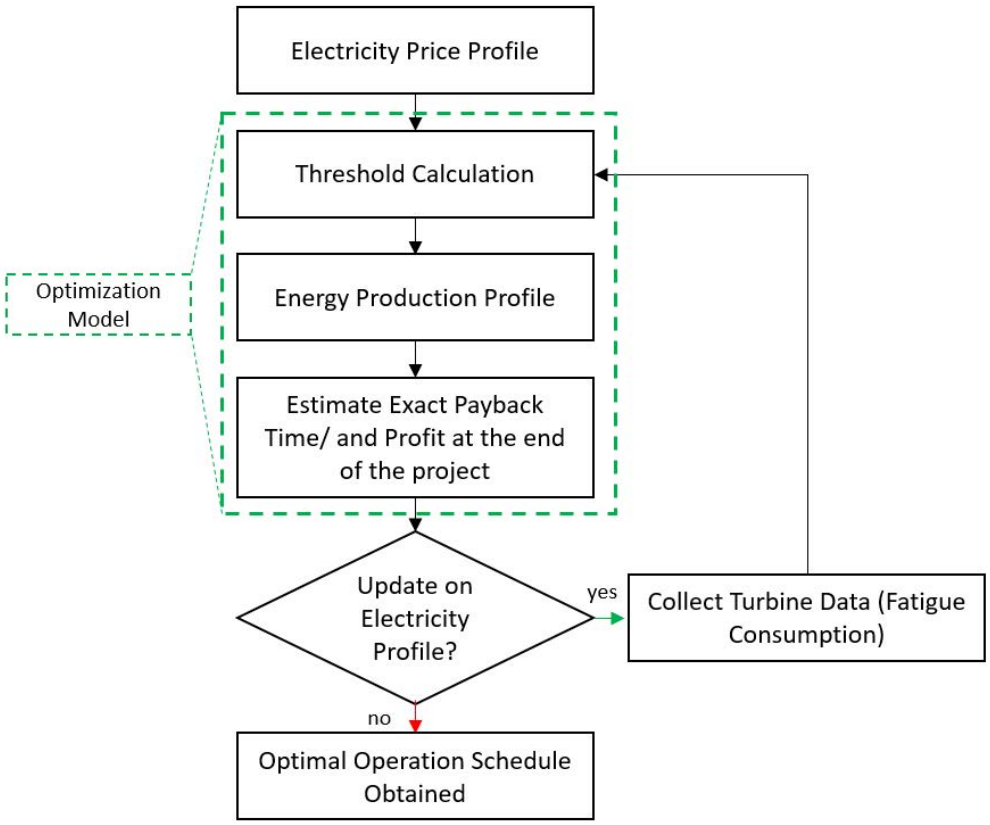

Figure 47: Logic Diagram of the Optimization Model under Fluctuating Electricity Price

Electricity Price Profile

The electricity price profile is a daily time series of the electricity price starting from the first day of operation until the last day of the turbine operation, the period is presumably 20 years. An example of the time series is shown in figure 44, however one should be reminded that the time series shown in figure 44 only has one year of data, and the

electricity price profile to be used in the optimization model must be of 20 years.
The electricity profile is one of the vital parts for the optimization, and the trend of the price could varies. One way to estimate the price profile is to assume that the electricity price is correlated with the annual wind resources under the four seasons. Based on this assumption, one example is to duplicate the electricity price obtained from one year into a 20 years long time series. Other methods could be more statistical and financial prediction similar to market prediction. Based on the economic transaction and energy market trend, economic scientist could forecast the trend.
There are several insights provided from the electricity price profile, that would be useful for the optimizer. The range of the electricity price and the frequencies of each of the price would enable the optimizer to compute the threshold value for the optimization process.

Threshold Calculation

Since the developed optimization model separate the operation into three regions and period, namely up-rated mode, normal mode and de-rated mode under the t_1, t_2 and t_3 state. The model were not able to optimize the operation schedule by producing a schedule that would allow switching operation mode other than the designated time period. However, this limitation could be lifted when the threshold calculation is adopted.
When the electricity profile is fed into the model, using figure 44 as an example, a descending order of the electricity price profile is computed. Figure 48 is the descending order profile of the electricity price in figure 44. The purpose of computing the descending order of the electricity price is to couple this descending electricity price profile with the developed optimization model. By optimizing under the descending profile, a new optimal operation schedule is obtained, of which can indicate two important values. From the new optimal solution, t_1, t_2 and t_3 are compute and they represent which operation modes should be used under different price ranges. For instance, price range included within the t_1 should be operated under the up-rated operation mode. As a result, a upper threshold value is obtained that indicate when the operation should switch between up-rated and normal operation modes based on the electricity price. Alternatively, a lower threshold value is obtained with t_2 that indicate the electricity price value that should switch between normal and de-rated operation mode for the purpose of maximizing final profit.

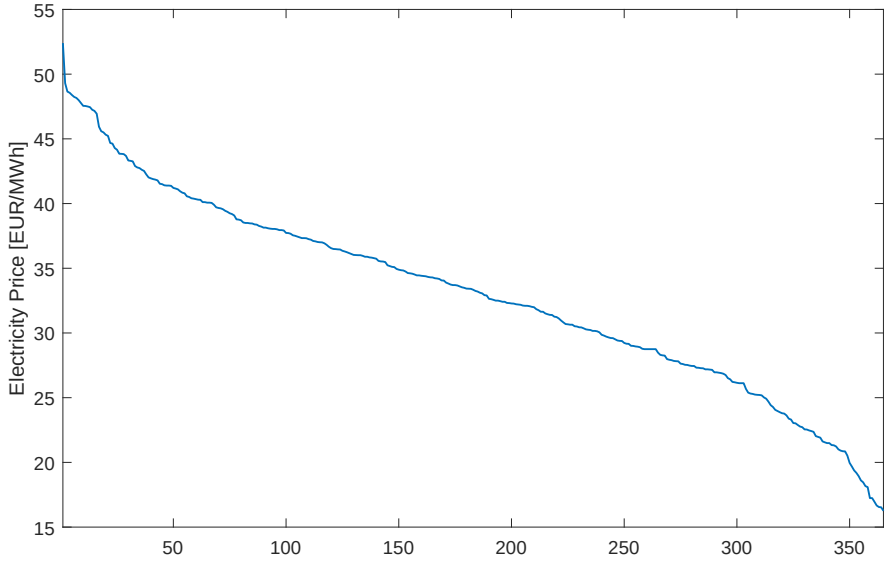

Figure 48: Descending order of the electricity price profile within the year

Energy Production Profile

As the thresholds that governs which operation modes should be used are computed from previous step. By putting the threshold into the daily electricity profile, the daily operation mode could be computed. As a result, we know exactly which operation should be used everyday for the rest of the turbine life-time, based on the input from the electricity price profile. As we know how much energy are being produced under each of the operation mode, an energy production profile, which indicate the daily energy production, are computed as the next step after the thresholds calculation.

Estimation of Payback and Final Profit

Since a detailed daily energy production profile was computed, based on the initial debt, an estimate of the exact payback time of the turbine can be calculated under this optimization framework. Furthermore, the final profit of the project could also be calculated given that the model computed the energy production profile.

7.7.2 Closed Loop Optimization

It is not surprising that the electricity price would change everyday, so as to the prediction of the electricity price. The new prediction could be an outcome of different government policies or market behaviors. As a result, the optimization model offers an continuous optimization as long as new electricity price prediction is fed into the model as an new input. Whenever the model receives a new electricity price profile, the model will transfer some of the important data into the optimizer to recalculate the new thresholds, payback time and final profit. The important data are turbine related data such as the length of the turbine operation before the update and the current accumulated fatigue consumption.

These important data could reflect the current structural status of the turbine in order to allow the optimizer to compute the optimal solution for the remaining time of the turbine.

7.8 Results of the Closed Loop Optimization

In this section, the closed loop optimization process previously described and the outcome of the model will be demonstrated with an example. The purpose of the example is to provide a benchmark for each of the steps taken in the model as well as illustrating the effectiveness of the model in bring up with the optimal solution.

7.8.1 Electricity Price Profile

As one of the objective for this model is to deal with the uncertainty in the electricity price throughout the operation period, an electricity price profile with an appropriate uncertainty is used for this example. A harmonic electricity price level is assumed for each year, where the electricity price is lower during summer time and more expensive during winter based on the assumption of more wind energy production during summer, which drive the electricity price to be lower in the market. As a result the price level fluctuate from high price during the summer to lower price when the project enters the winter while keeping the cycle every year. Figure 49 shows the time series of the electricity price profile for a project that started in summer, where the electricity price started with a high value. The profile has a mean of EUR 0.07/MWh, with EUR 0.02/MWh range across the price spectrum. This profile provide a periodic electricity price with similar mean and range of the normal distribution described previously.
It could be seen that the price level start with EUR 0.9/MWh at the beginning and dropped to EUR 0.056/MWh after passing half a year. The price later on climbs back on EUR 0.09/MWh level when one year cycle is reached. This cycle keeps on repeating itself for 20 years until the end of the project.
One should be aware that the mini-fluctuation of the electricity price everyday is assumed not to be present such that the price level smoothly translate the annual behavior for demonstration. While there are price volatility in real life as well as other aspects that could affect the electricity profile.

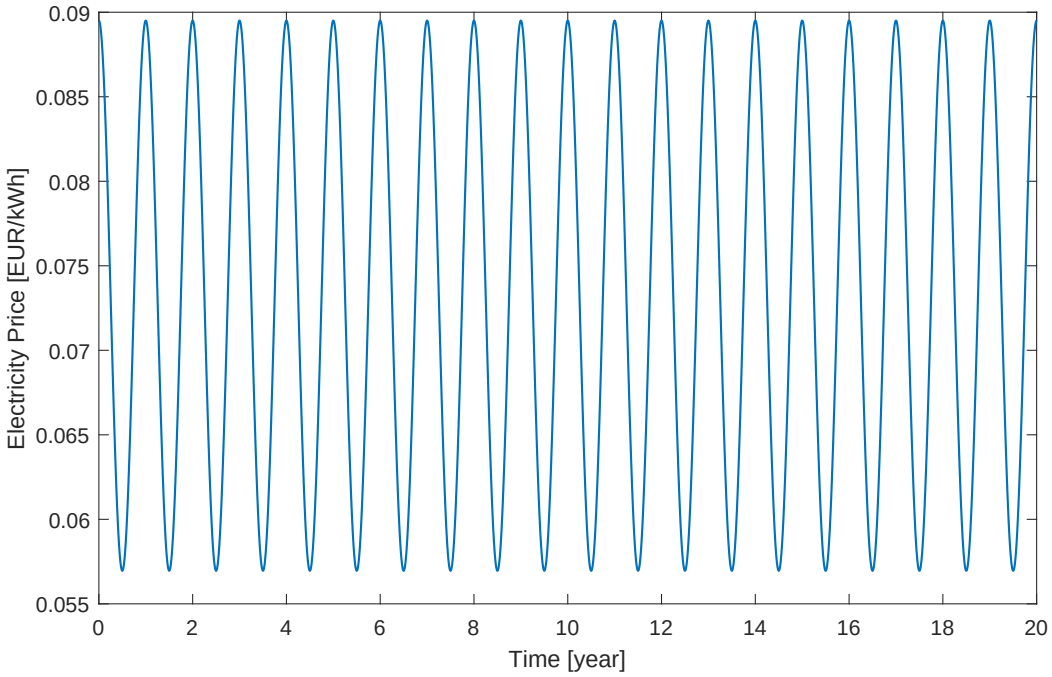

Figure 49: Electricity Price over 20 years

7.8.2 Threshold Calculation

With the electricity price profile, the optimizer would be able to calculate the threshold for different operation modes.
As the profile is being imported to the optimizer, the electricity price level is sorted in a descending order as shown in figure 50. The descending order profile would then allow the model to determine how long should each operation modes to operate in order to maximize the profit at the end of the project. It is because by sorting the electricity price in a descending order, the high electricity price value would always be allocated for the up-rated operation model and vice versa under the optimization model. In another word, the optimizer would allocate the highest possible electricity price for the up-rated operation mode until the up-rated mode is not as economic as operating in normal operation model due to finance and structural concern.
As shown in figure 50, the optimizer resolved the operation schedule, which indicate that the up-rated and the de-rated mode should run for 9.32 years while the normal operation mode should run for 1.35 years. This mean that the up-rate mode is allocated to operate under all the electricity price under the descending order of the electricity price until year 9.32, which is equivalent to price EUR 0.0749/ MWh in figure 50. This value is the upper threshold that indicate the turbine should be operating under up-rated mode. Additionally, the normal mode was optimized to run for 1.35 years after the up-rated mode, which means that the price range within the 1.35 years should be operated under the normal mode. As a result, the lower threshold for the de-rated mode operation is the electricity price at year 10.67, EUR 0.0715/MWh, under the descending order electricity price profile.
The general idea for this optimization process is to optimize the operation such that more

energy production under up-rated mode when the electricity price is high and switch operation mode by maintaining balance between financial benefits and structural integrity. As a result, the operation can prevent potential lost in revenue due to excess energy production when their price is lower.

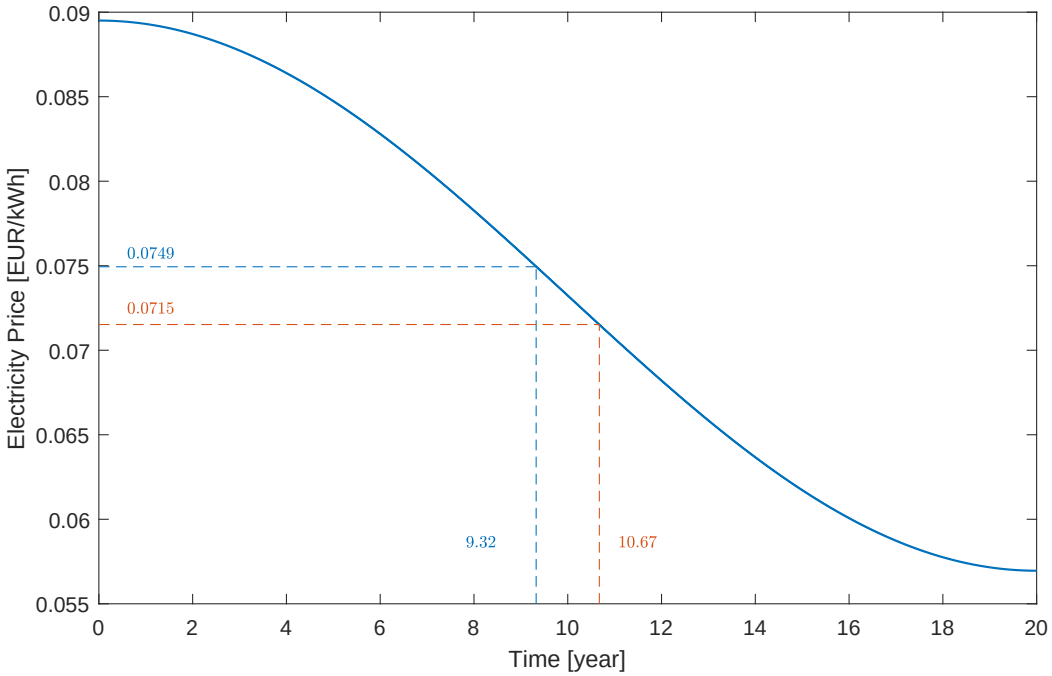

Figure 50: Descending order of the electricity price profile

If we put the lower and upper threshold into the electricity profile, we could visualize how the turbine operate throughout the 20 years. According to figure 51, where each color filled area represent different operation modes the turbine should operate at. The green area represents the turbine should operate at the up-rated mode, because the price level is above the upper threshold and vice versa for the de-rated mode, red in color, where the electricity price is lower than the lower threshold. While blue color denotes the normal operation mode when the electricity price is lower than the upper threshold but higher than the lower threshold.

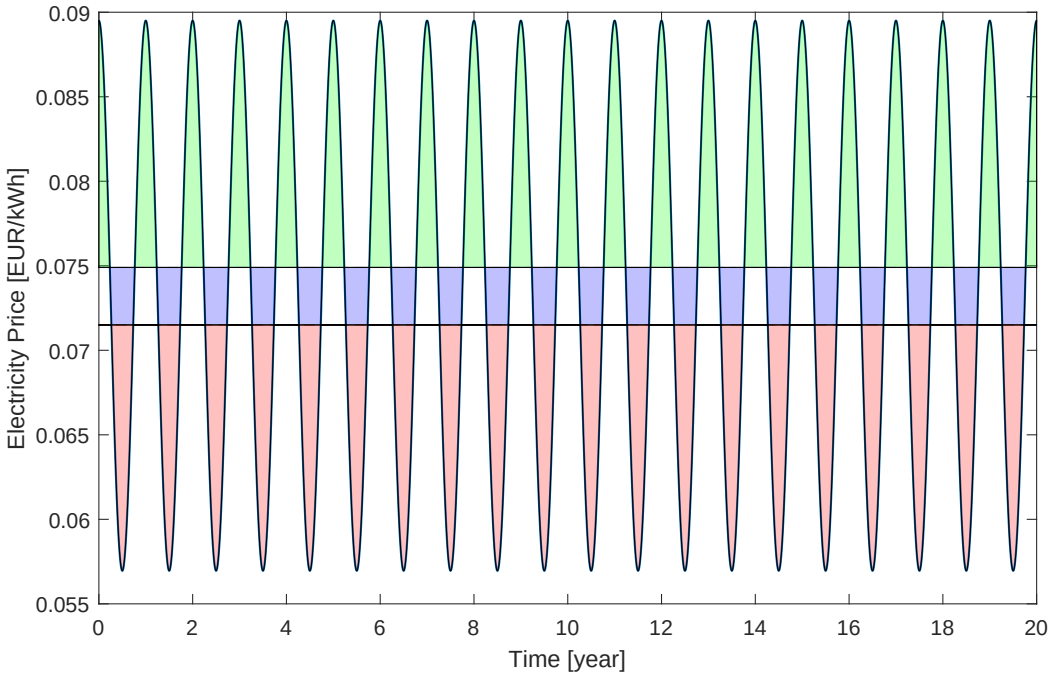

Figure 51: Operation Mode under Electricity Price Profile; Up-rated (Green), Normal (Blue); De-rated mode (Red)

7.8.3 Results

As shown in figure 51, which shows the operation schedule of the turbine over the 20 year. In this section, the optimal solution, which defined the lower and upper threshold for different operation modes, is compared to a baseline solution, of which is a 20 years normal operation schedule. It is a similar comparison we have made in previous section. The only difference is the variation of the electricity price profile.
As shown from the results, the payback period of the optimal solution is 9.06 years, where it is 9.15 for the baseline solution. It is shown in the figure 52 upper left plot. The plot also shows that the final profit of the optimal solution is higher than the baseline solution. The exact number of the final profit of the optimal solution is EUR 32,059,000 while the baseline solution has a profit of EUR 31,407,000. The optimal solution has a 1.8% higher profit, equivalent to EUR 585,840.
At the same time, the optimal solution also pay less interest than the baseline solution by 1.1%, equivalent of EUR 24,410. The optimal solution pays a EUR 2,262,000 interests for the whole project, while the baseline solution pays up to EUR 2,286,000 for the debt service. The interest trend could also be observed from the lower left plot in figure 52.

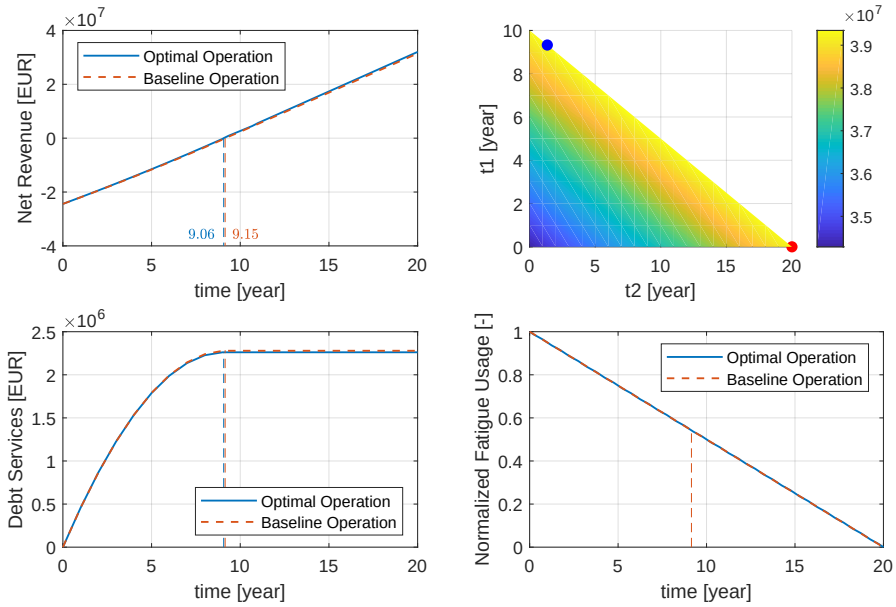

Figure 52: Comparison between the Optimal and the Baseline Schedule

The main reason for the optimal solution to succeed in maximizing profit is the way how the upper and lower threshold changes the operation schedule of the turbine. The changes in the operation schedule captures all the possibility for a higher revenue generation under the uncertainty in price range. From figure 53, it could be observed that the yearly revenue of the optimal solution is constantly higher than the baseline solution. It is because the threshold capture the higher revenue generation with the up-rated operation when the electricity price is high while smartly handle the dilemma of structural and fatigue consumption. The constant higher yearly revenue results a faster process in paying back the debt service and as a result maximized the final profit as well as having an earlier payback time.

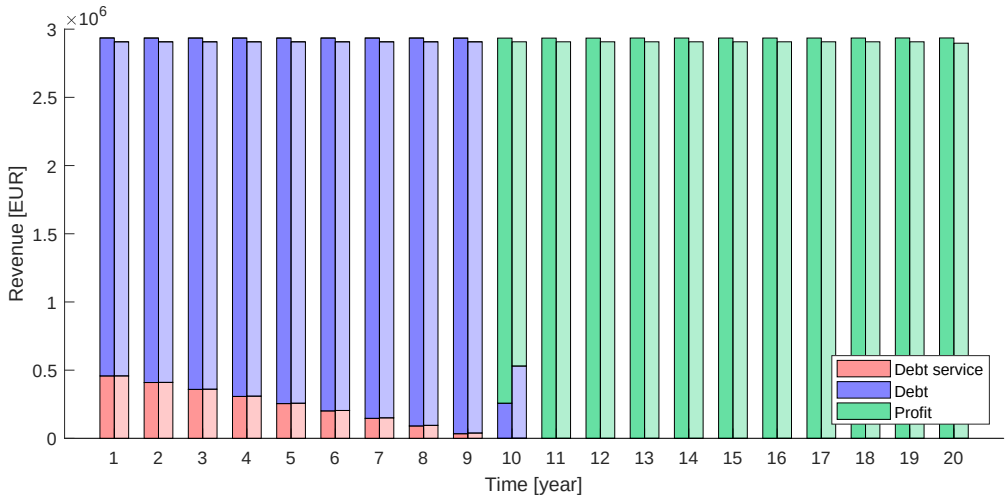

Figure 53: Yearly Distribution of Optimal Scheme (dark in color) and Upfront Scheme (light in color)

From figure 54, it also demonstrated the rate of debt are being paid of each of the year under the two solutions. It can be seen that the optimal solution is able to payback the debt faster, thanks to the constantly higher revenue generation.

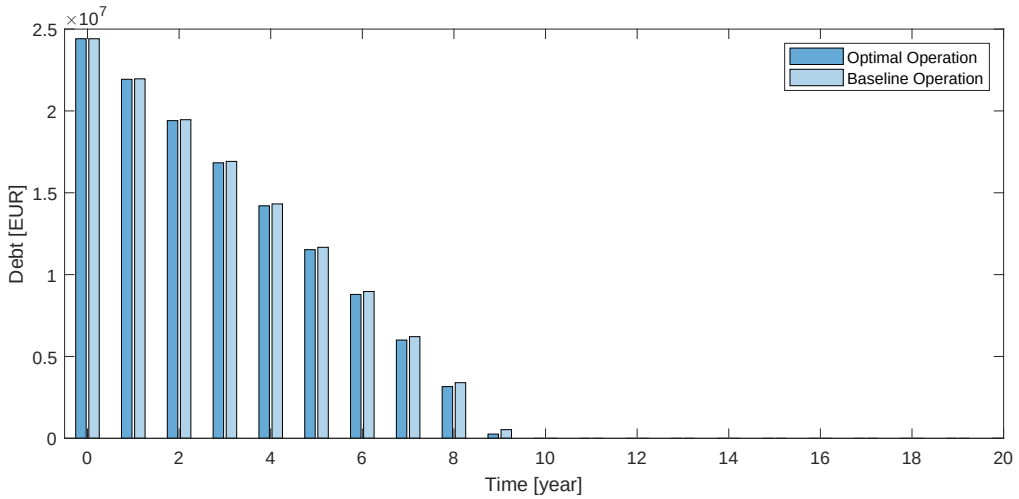

Figure 54: Yearly Debt Distribution of the Two Schemes

Benefit of the model

One should be reminded that the model could update the operation based on an updated electricity price profile anytime throughout the project operation. As long as a new profile is inputted, the thresholds would be recalculated to obtain a optimal solution.

7.9 Sensitivity Analysis

The optimization process was done with a mathematical model, where are lot of decision and logic are developed implicitly computationally. In order to improve the overall understanding of the relationships between each of the input and output variables in the model, this section would focus on the sensitivity analysis for the model developed in the project.
The purpose of the sensitivity analysis is to test the robustness of the optimizer as the model developer and also enhance users credibility of making the suitable changes the the model for each of their individual use of the optimizer. Such that it could provide a benchmark to identify important connections between the users inputs and the outputs. Furthermore, it could provide a more complete picture of the model and to provide insights in further model development.

For the sensitivity analysis, one of the most common approach, changing one-factor-at-a-time (OAT/OFAT) is used. This method explain its methodology fairly well with its name, and it changes one input variable and keep others at their baseline or nominal values for comparison. Afterward, the changed input variable returns to its nominal value. By repeating doing so to different input variables, the sensitivity analysis would be illustrated by the changes in output values under the different inputs.

7.9.1 Distinguish Input Parameters

First, the "baseline" for the sensitivity analysis has to be defined before each parameters are to be changed for the OFAT approach. As the optimal scheme was computed from the deterministic model in previous section, it makes sense by adopting the optimal operation scheme as the "baseline" for the sensitivity analysis.
Different parameters are shown in table 8. The parameters are divided into three categories, input, output and constant parameters.

Input Parameters	-CapEx -Interest rate -Electricity Price -OpEx -Fatigue Factor for 11MW -Fatigue Factor for 9MW
Output Parameters	-Payback time -Profit -Paid debt service
Constant Parameters	-Operation mode (9MW & 11MW) -Turbine life-time

Table 8: Summary of Input and Output Parameters for Sensitivity Analysis

For the input parameters, the model objective equation, equation 7.4, 7.5 and 7.6, are revisited. By looking into the three equations, the first term on the RHS is the compound interest of the debt, of which is calculating the debt has to be paid, and both the initial debt (CapEx) and the interest rate are used in the calculation. As a result both parameters are considered the input parameters. On the second term on the RHS from the objective equation, Electricity price, OpEx and interest rate are used to calculate the future value of revenue production. These values would determine the final debt/profit at the end of the 20 years. As a result, the electricity price and OpEx are also considered as the input parameters.
In addition, the fatigue consumption factor that was assumed in equation 7.12, are also part of the input parameters due to their significant influence to the output as a constraint in the optimizer.

For output parameters, payback time, profit and paid debt service are the three important parameters for operation comparison. As a result, they are easily considered as the output parameters.

Last but not least, few parameters are considered constant in the model. P, electricity production, from equation 7.4, 7.5 and 7.6, are considered as part of the constant parameters as this was part of the turbine operation mode design and not maneuverable under the model mathematically. Another parameter that is considered as constant is the turbine lift-time as shown in constraint equation 7.13, due to the normal life span of wind turbine.

7.9.2 Results

Each of the input parameters listed in table 8 are modified by ± 10%, which is a common practice in sensitivity analysis [Mouida and Alaa, 2011].
Each parameter has been tested individually and their corresponding optimization result are computed and results are plotted in Appendix D from figure 66 to 71.
A result summary of the sensitivity analysis is shown below in table 9

		Modifier	Output Parameters		
			Payback	Profit	Paid Debt Service
Input Parameters	CapEx	+10%	+10.8%	-9.1%	+22.3%
		-10%	-10.6%	+9.0%	-19.8%
	Interest Rate	+10%	+0.7%	-0.7%	+11.1%
		-10%	-0.6%	+0.7%	-10.8%
	Electricity Price	+10%	-11.7%	+23.6%	-12.1%
		-10%	+15.4%	-23.9%	+16%
	OpEx	+10%	+2.7%	-4.7%	+2.8%
		-10%	-2.6%	+4.7%	-2.6%
	Fatigue Factor for 11MW	+5%	+4.6%	-0.2%	+6.2%
		-5%	-2.1%	+4.4%	-0.7%
	Fatigue Factor for 9MW	+5%	+4.6%	-0.2%	+6.2%
		-5%	-2.1%	+2.1%	-0.7%

Table 9: Summary of Sensitivity Analysis Result

One should be reminded that for most of the cases, the t_1 and t_3 has the same value due to the linear behavior of fatigue weighting factor. However, t_1 and t_3 could be different when the weighting factors are different as shown in figure 70 and 71. This also explain the absent of surf plot in figures, since each surf plot represents the optimization schedule under two designated fatigue weighting factors. When the weighting factor changes, the optimization surf plot also chagnes.

8 Conclusion and Discussion

The thesis has successfully investigated the feasibility in frontloading wind turbine and bring early stage financial benefits to the project. A simulator has been developed in order to calculate the optimal operation schedule to reduce the amount of interest that has to be paid. From the analysis, it has shown that roughly 5% of the interest, would be able to waived by adopting the optimal operation schedule for each turbine. Furthermore, the thesis also steps up and focus in maximizing the profit at the end of the project with optimization, such that the optimal operation schedule would not only reduce the interest incurred as much as possible but also to maximize the end-game profit of the project. The results has also shown that the total profit would increase by 1.8%, if the optimal solution is adopted during the whole operation for each turbine. The exact financial gain in interest and profit are correlated to the electricity price profile.

During the course of the simulator development, several disciplines, including engineering, financial and optimization , of a wind turbine project has been studied. These three sections are also clearly discussed in the thesis work.

The first section, engineering, has discussed extensively the procedures and strategies in load calculations, wind turbine characteristic as well as tuning the controller to reproduce different operation modes for our maneuver. Few designs in the operation modes has been discussed, where their advantages has been compared. The final design for the operation modes has chosen to change the pitch controller setting such that different torques and power levels of the turbine could reproduce. And three operation modes are designed and named by the baseline 10MW, proposed 9MW and proposed 11MW operation.
The three operations are further validated against high-fidelity code, HAWC2, with their operation behaviors. In addition, the fatigue loads for the three modes are calculated , where the results have shown that the proposed 11MW and 9MW operation modes has some level of fatigue loads increase and decrease compared to the baseline results. These values allow us to make the optimization process possible and meaning in determining the benefit of running a frontloaded turbine.

The second section, financial, has gone through the state-of-the-art financial calculation as well as some of the assumption for wind turbine projects. The section has not only try to realize the simulator with realistic and suitable financial index, but also looked into the fluctuation in electricity price. An example for the project financial calculation are demonstrated in the thesis, which set the foundation for the next section, optimization.

The last section, optimization, has developed the financial, engineering and operation schedules relationship into a mathematical model, where one can choose the optimize the model to reproduce the optimal schedule for maximum profit. Few examples has demonstrated in the section to show that both mathematically and intuitive what advantage the optimal operation process compares to other scenarios. Some important figures, for example, the confident level of a profit under the fluctuation electricity price are also calculated under the section.

The three sections come hands in hands in to develop the optimizer. The operation modes design and the loads calculation brings in the weighting factor used in the optimizer; The financial formulation helps to compute the revenue and debt paid at different stage of the project; The optimization process produced the best operation schedule for the turbine to operate under the uncertainty of electricity price.

Future Studies

The optimizer works fine in maximizing revenue generation based on few assumptions for both the fatigue load calculation sides as well as the turbine operation modes design. The project would like to stress on few assumptions and approaches that were used in this project which are important to the optimization solver, such that the solver could improve ranging from its applicability on different turbine models to continuous wind farm monitoring system.

During the design stage of the different turbine operation modes being used in this project, the approach of up-rating and de-rating the turbine to 11MW and 9MW from normal 10MW operation mode is done by pitch controller. This represents that the energy production between the three modes would only be difference when the turbine runs above the rated wind speed. In the project the wind speed were not taken into account during the optimization process, which means that the turbine could be generating exactly the same amount of energy while running at the up-rated mode comparing to the normal mode due to the wind speed lower that rated. The impact of this situation would be a wrong estimation of the revenue generation in each period or the calculation of accumulated fatigue life-time. However, the project has assumed that the different operation modes would operate at rated wind speed, such that each designed operation mode would produce different rated power. Having said that, by coupling the wind speed to the optimization system could be done by creating a time series of the wind speed, which would in turn formulate the energy production profile. Making the optimization model even more realistic.

Secondly, the consumption of the equivalent fatigue loads for the up-rated and de-rated modes are being calculated referencing to the normal operation life-time equivalent fatigue loads. And the correlation between the fatigue loads were assumed to be linear. This is different in real scenario where linear relationship is not the best relationship between the fatigue loads and the rated power. Future studies that focus on determining the life-time fatigue load on the same turbine under different rated power operations could prove influential to the weighting parameter used during the inequality constraint construction in the optimization process.

Furthermore, to provide continuous monitoring of the turbine performance and the final profit estimation, inputs from the blades root bending moment sensors could help simultaneously determine the fatigue consumption of the turbine. This value could be different than the constraint set up under the optimizer because there are some other factors that could affect the life-time equivalent fatigue loads except the operation mode. For example, the turbine has operated under a storm the fatigue consumption would definitely be higher than an up-rated mode. If the turbine data could be updated continuously for the

optimizer, not only could the life-time of the turbine be guaranteed, but the final profit of the turbine could also be more realistic.

Lastly, since the optimizer here has only taken into account of the fatigue load consumption, the model could actually couple with other requirements, design load basis, as constraints during the optimization. For example, the extreme loads could be added to the optimizer, which specify when the turbine should not be operated under extreme wind speeds. By building up more coupling with the requirements for a certified turbine, the optimizer could enhance its capability and be even more ready for industrial application.

9 Appendix

A Chinese Electricity Price Document

附件2

全国陆上风力发电标杆上网电价表

单位：元/千瓦时（含税）

资源区	2018年新建陆上风电标杆上网电价	各资源区所包括的地区
Ⅰ类资源区	0.40	内蒙古自治区除赤峰市、通辽市、兴安盟、呼伦贝尔市以外其他地区；新疆维吾尔自治区乌鲁木齐市、伊犁哈萨克族自治州、克拉玛依市、石河子市
Ⅱ类资源区	0.45	河北省张家口市、承德市；内蒙古自治区赤峰市、通辽市、兴安盟、呼伦贝尔市；甘肃省嘉峪关市、酒泉市；云南省
Ⅲ类资源区	0.49	吉林省白城市、松原市；黑龙江省鸡西市、双鸭山市、七台河市、绥化市，伊春市，大兴安岭地区；甘肃省除嘉峪关市、酒泉市以外其他地区；新疆维吾尔自治区除乌鲁木齐市、伊犁哈萨克族自治州、克拉玛依市、石河子市以外其他地区；宁夏回族自治区
Ⅳ类资源区	0.57	除Ⅰ类、Ⅱ类、Ⅲ类资源区以外的其他地区

注：2018年1月1日以后核准并纳入财政补贴年度规模管理的陆上风电项目执行2018年的标杆上网电价。2年核准期内未开工建设的项目不得执行该核准期对应的标杆电价。2018年以前核准并纳入以前年份财政补贴规模管理的陆上风电项目但于2019年底前仍未开工建设的，执行2018年标杆上网电价。2018年以前核准但纳入2018年1月1日之后财政补贴年度规模管理的陆上风电项目，执行2018年标杆上网电价。

Figure 55: Chinese Official Document on Electricity Price for Wind Energy

B Extreme Load

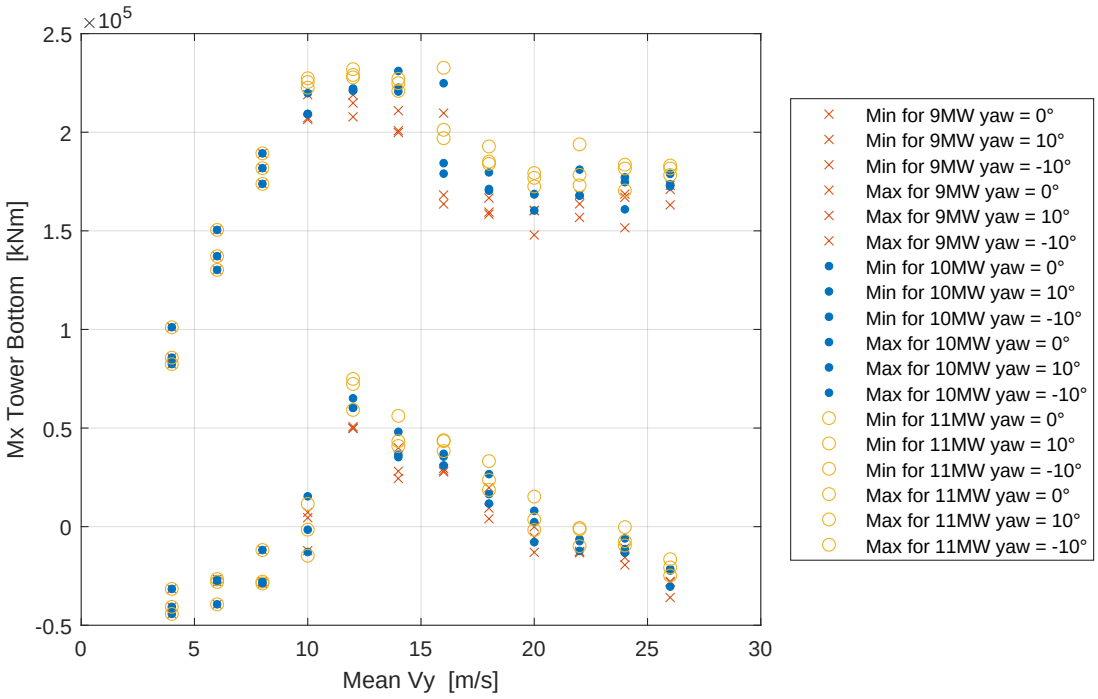

Figure 56: Ultimate Load of Mx tower bottom

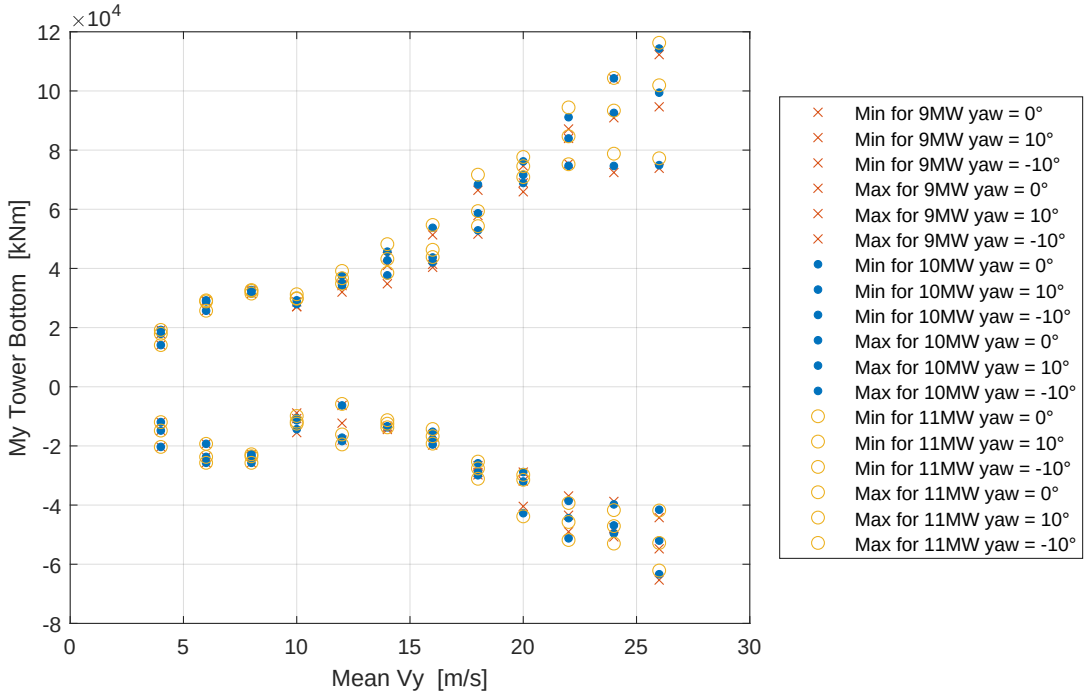

Figure 57: Ultimate Load of My tower bottom

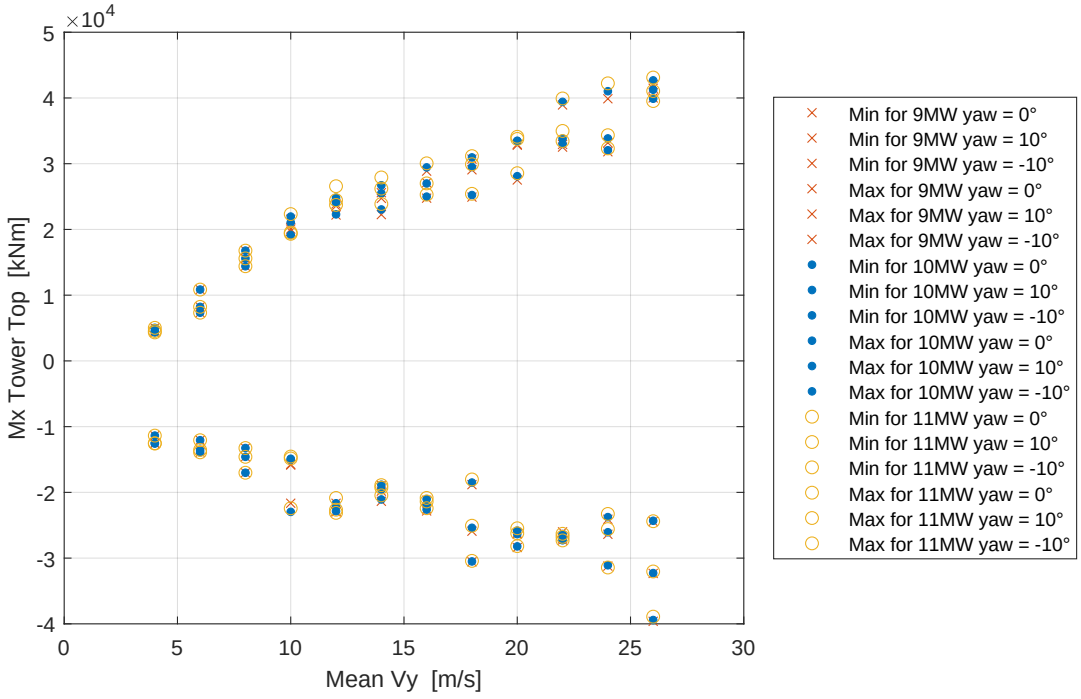

Figure 58: Ultimate Load of Mx tower top

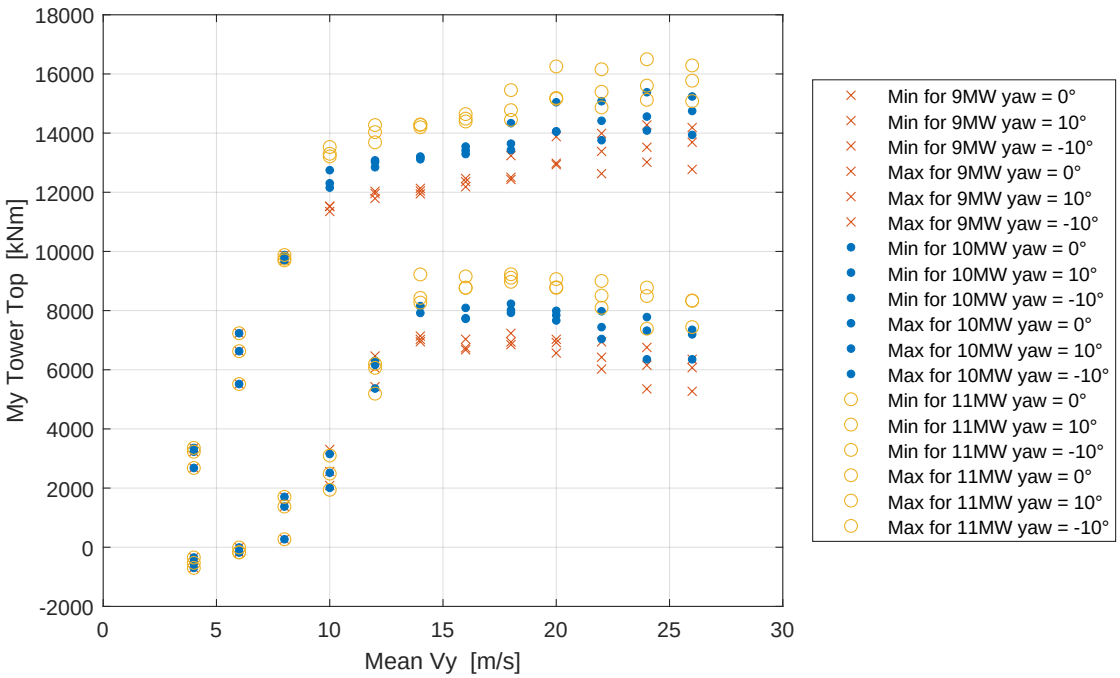

Figure 59: Ultimate Load of My tower top

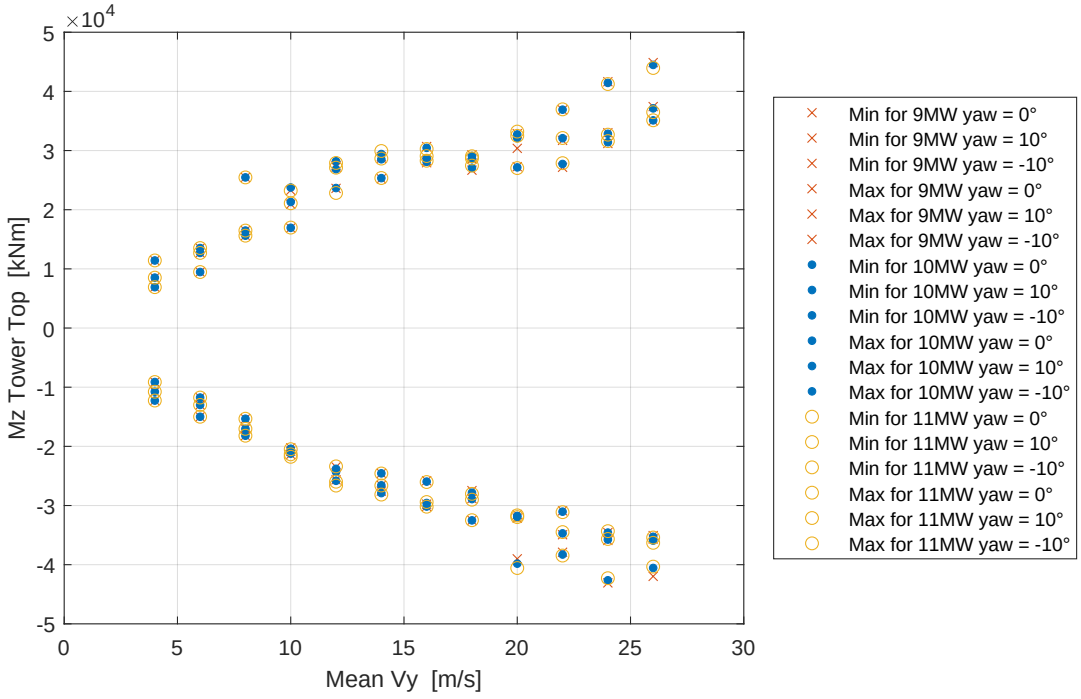

Figure 60: Ultimate Load of Mz tower top

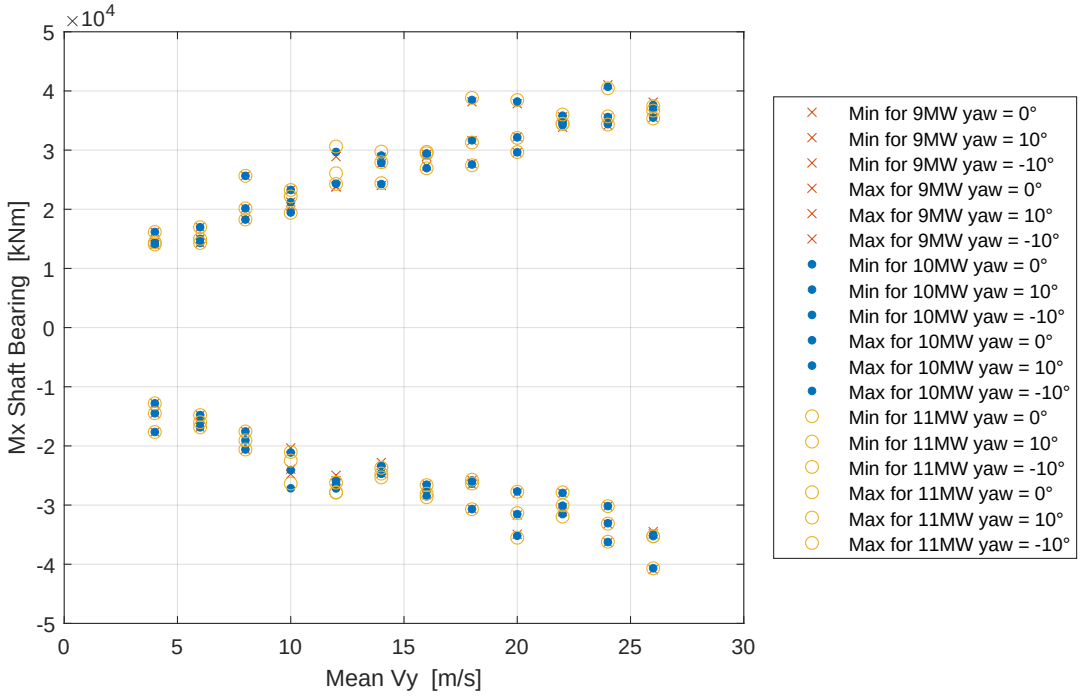

Figure 61: Ultimate Load of Mx shaft bearing

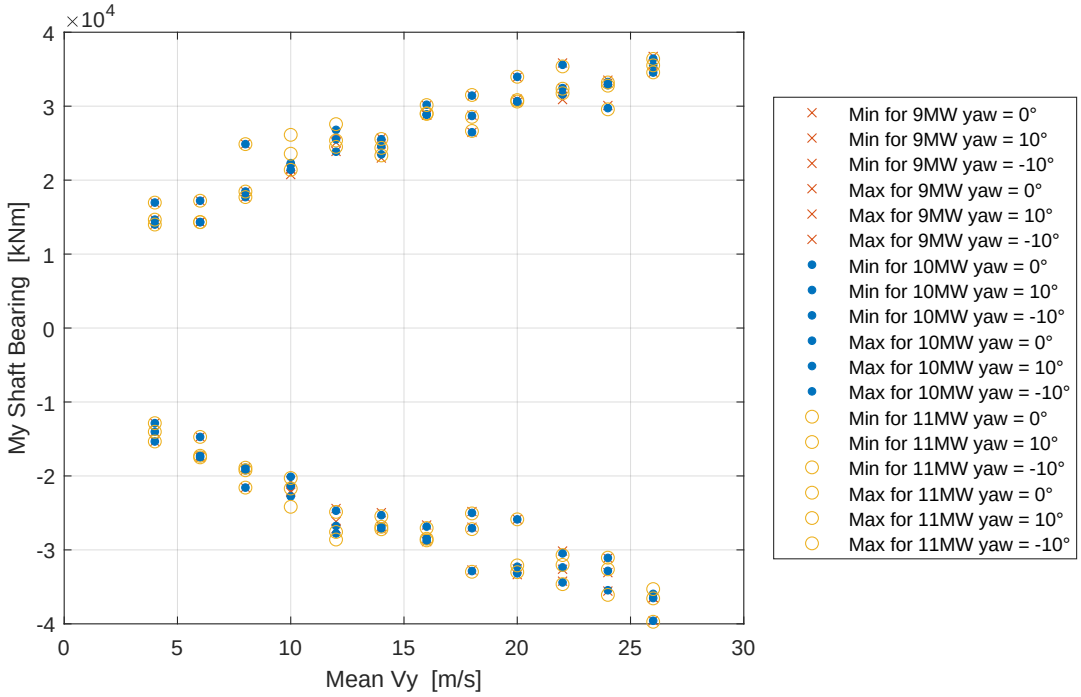

Figure 62: Ultimate Load of My shaft bearing

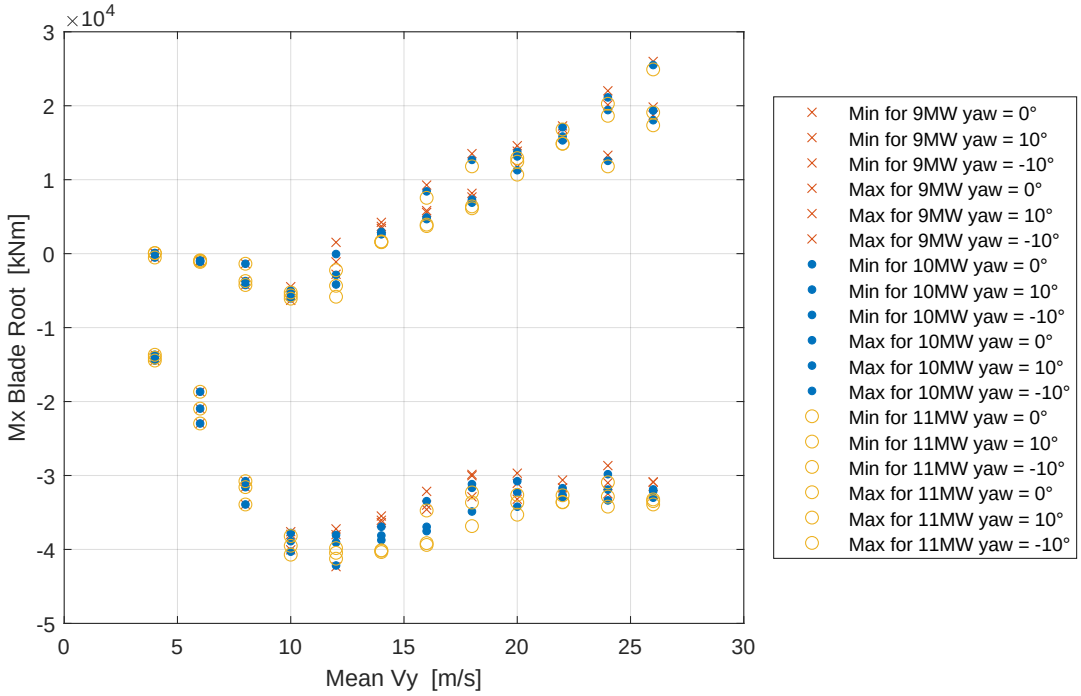

Figure 63: Ultimate Load of Mx blade root

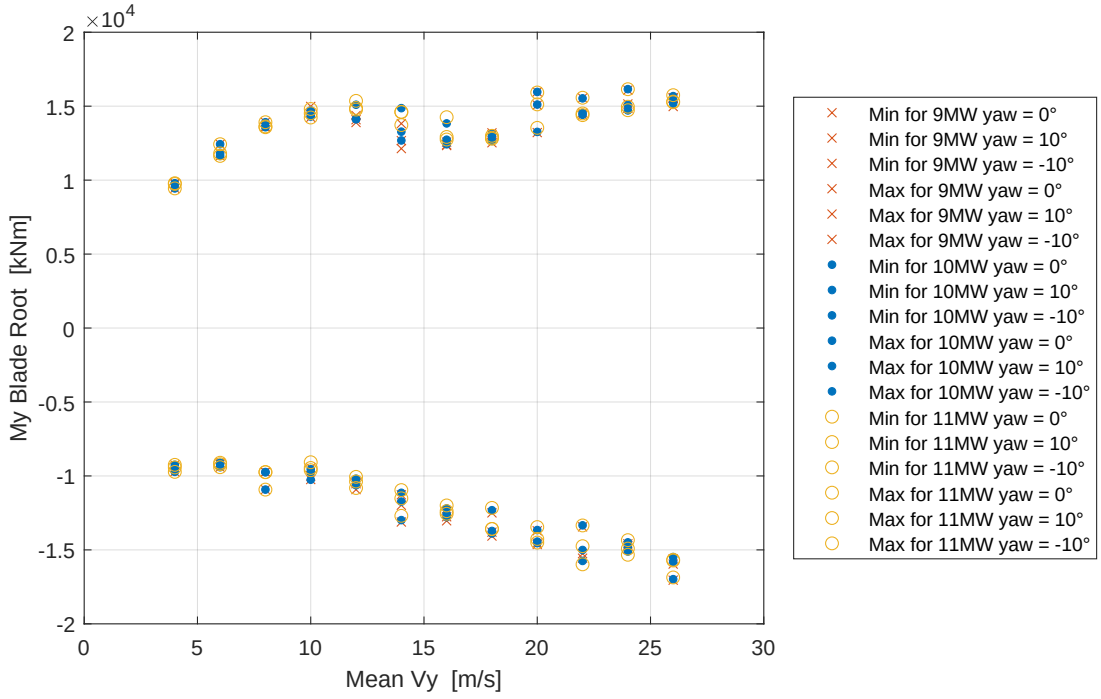

Figure 64: Ultimate Load of My blade root

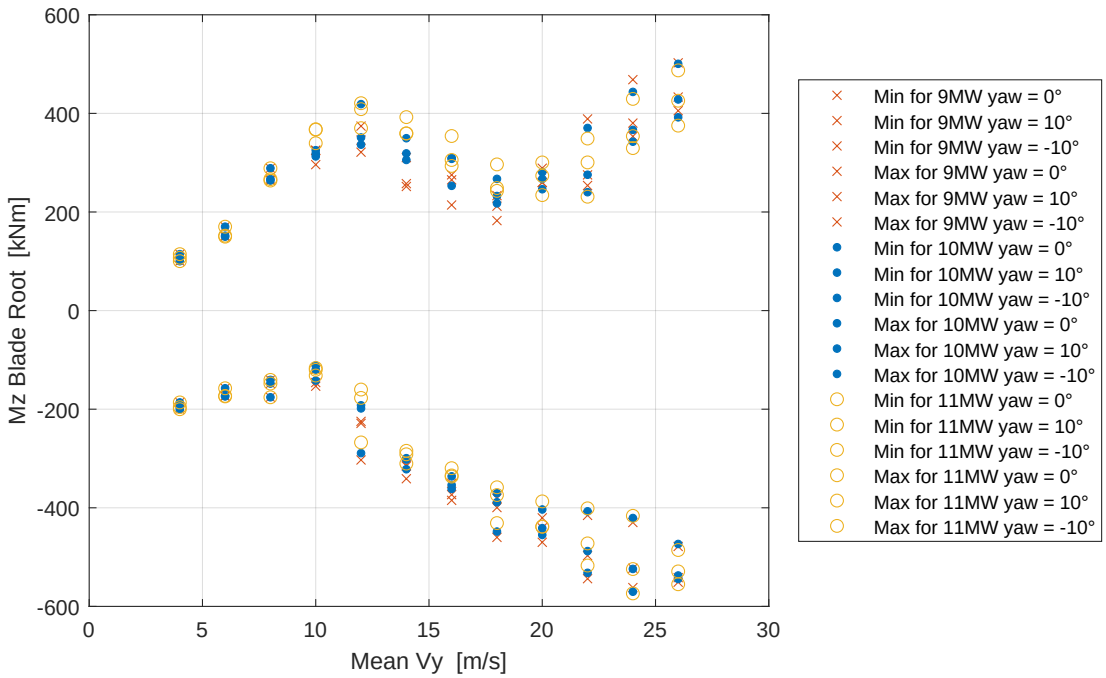

Figure 65: Ultimate Load of Mz blade root

C Derivation of Periodic Payment for an Annuity (PMT)

The calculation of the periodic payment for an annuity is based on the sum of geometric sequence. As revenue generated each year has their future value computed with the interest rate. So the sum of all future yearly revenue value would be the total revenue at specified year.
The equation for the sum of geometric sequence is shown below,

$$\sum_{k=0}^{n-1}(ar^k) = a(\frac{1-r^n}{1-r})$$

where a is the first term, r is the common ratio between terms, n is the number of terms. By putting the values into the equation of the sum of geometric sequence. The $\sum_{k=0}^{n-1}(ar^k)$ as the FV. a, the first term, as $pmt/cdot(1+i)$. And the r, common ratio, as 1+i, where i is the interest rate. The equation will transform into calculating the future value of periodic payment.

$$FV = pmt \cdot (1+i) \cdot \frac{(1+i)^n - 1}{i}$$

D Sensitivity Analysis Results

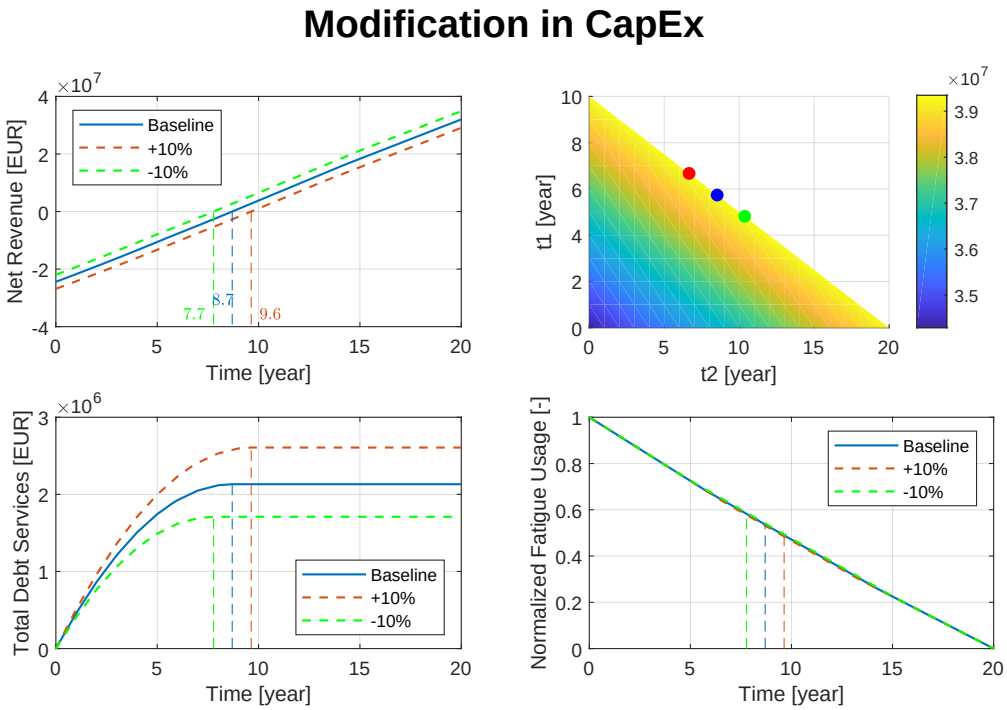

Figure 66: Sensitivity Analysis of CapEx

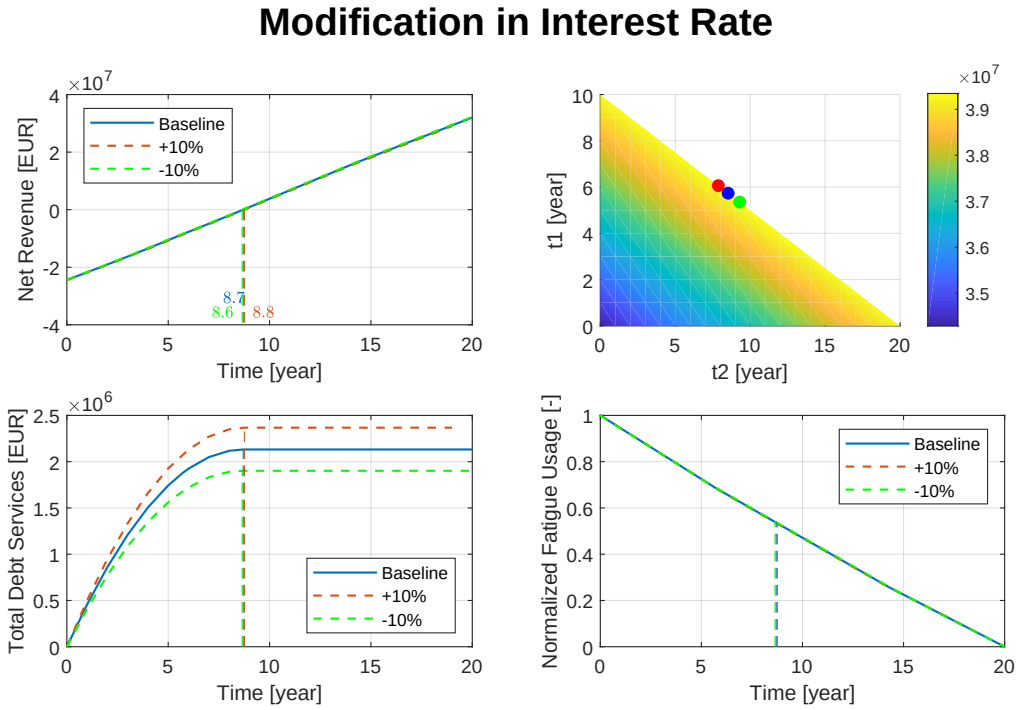

Figure 67: Sensitivity Analysis of Interest Rate

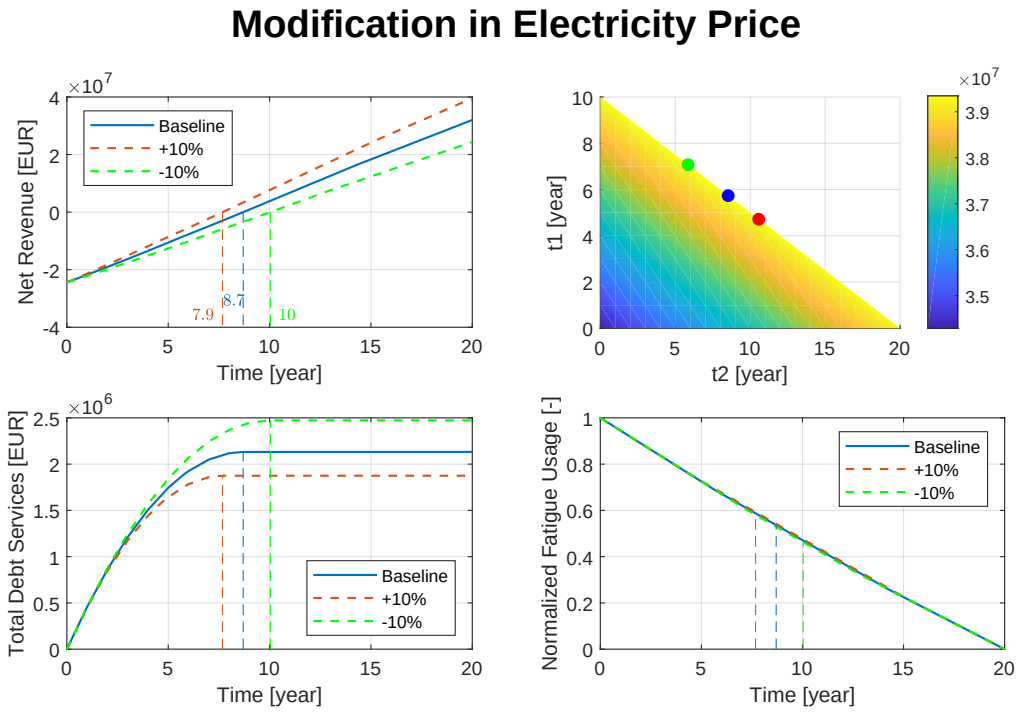

Figure 68: Sensitivity Analysis of Electricity Price

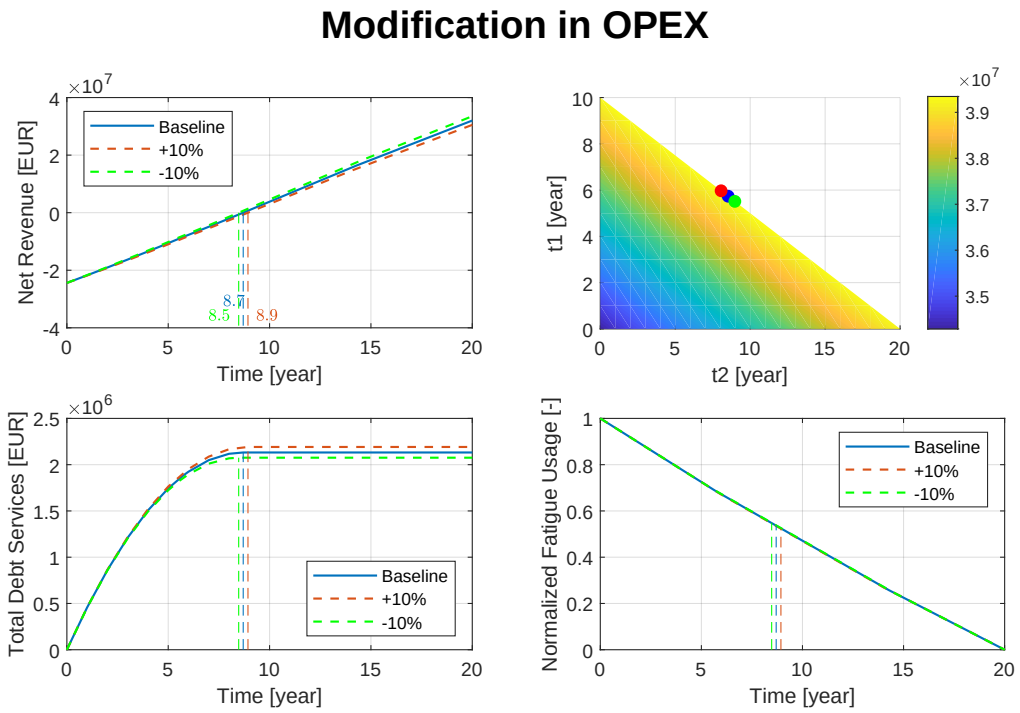

Figure 69: Sensitivity Analysis of OpEx

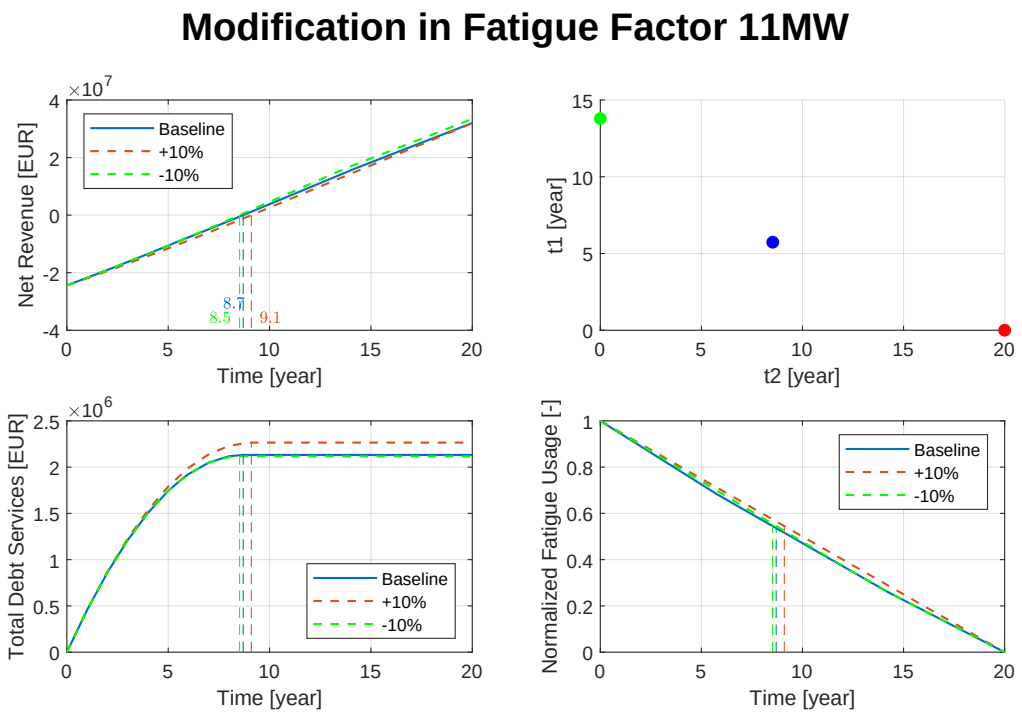

Figure 70: Sensitivity Analysis of Fatigue Factor for 11MW

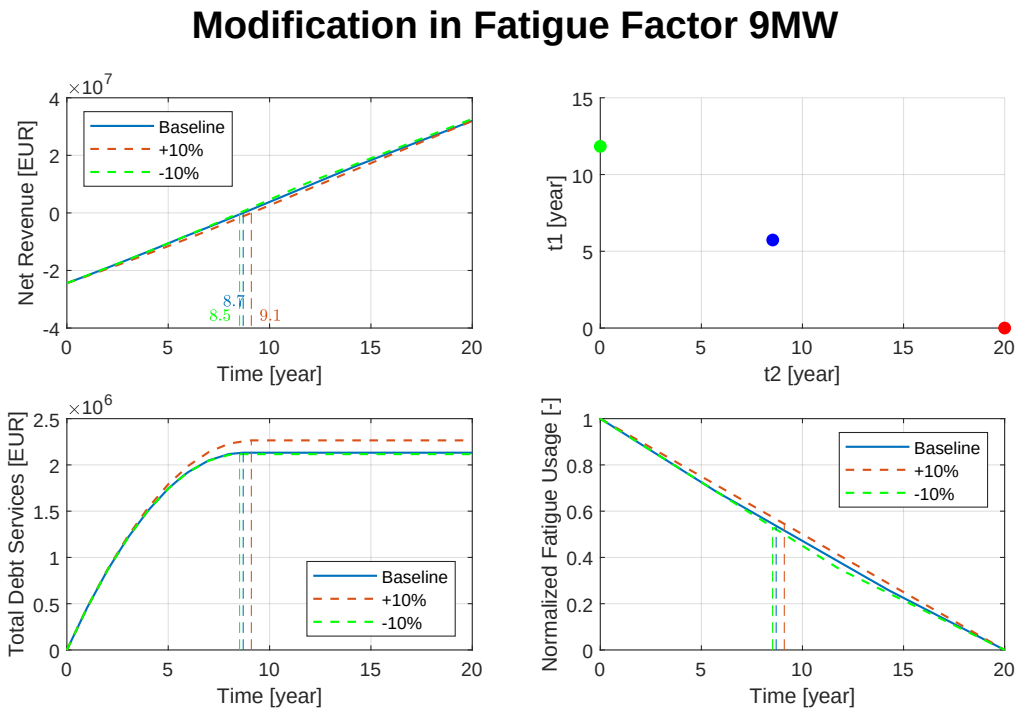

Figure 71: Sensitivity Analysis of Fatigue Factor for 9MW

E Matlab Code Demonstration

```
21 %% Debt Calculation
22
23 % Calculation done from 0 to t_1
24 % Condition 1: payback did not happen in t_1.
25 if D0 >0
26     D_t1 = D0*(1+i_365/100)^(t1*365);
27     Income_t1 = P(1)*(E-OPEX)*((1+i_365/100)*((1+i_365/100)^(t1*365)-1)/↙
(i_365/100));
28     Debt_remaining_t1 = D_t1 - Income_t1;
29     Paid_debt_t1 = D0-Debt_remaining_t1;
30     D_interest_t1 = P(1)*(E-OPEX)*(t1*365) - Paid_debt_t1;
31
32 % Condition 2: payback happened during t_1 and find t_payback. (Earning
33 % money in t_1 already)
34     if Debt_remaining_t1 <=0
35         t_payback_t1 = log(1/(1-(D0/(P(1)*(E-OPEX)))*(i_365/100/(1+i_365/100))))↙
/...
36             log(1+i_365/100);
37         t_payback = t_payback_t1/365;
38         t_temp = t1-t_payback;
39         D_interest_t1 = P(1)*(E-OPEX)*(t_payback_t1/365*365) - D0;
40         Debt_remaining_t1 = -P(1)*(E-OPEX)*(t_temp*365);
41     end
42 else
43 % Condition 3: payback happend in previous operation, OR not in debt at the
44 % start of the operation.
45     D_interest_t1 = 0;
46     Debt_remaining_t1 = D0-AEP(3)*(E-OPEX)*(t1*365);
47 end
48
```

Figure 72: Matlab Script for demonstration

```
54 %% FMINCON
55 A = [1.1 1 0.9];
56 b = 20;
57 Aeq = [1 1 1];
58 beq = 20;
59 lb = 0*ones(3);
60 ub = 20*ones(3);
61 nonlincon = [];
62
63 x = fmincon(@Debt_Objective_Function,x0,A,b,Aeq,beq,lb,ub,nonlincon);
```

Figure 73: Matlab Script for optimization demonstration

References

Markus Abel. Time dependent linear scalar equations. Report, 2011.

Lars O Bernhammer, van Kuik Gijs A M, and Roeland De Breuker. Fatigue and extreme load reduction of wind turbine components using smart rotors. *Journal of Wind Engineering and Industrial Aerodynamics*, 154:84–95, 2016. ISSN 0167-6105. doi: https://doi.org/10.1016/j.jweia.2016.04.001. URL http://www.sciencedirect.com/science/article/pii/S0167610516301970.

Corantin Bouty, Sebastian Schafhirt, Lisa Ziegler, and Michael Muskulus. Lifetime extension for large offshore wind farms: Is it enough to reassess fatigue for selected design positions? *Energy Procedia*, 137:523–530, 2017. ISSN 1876-6102. doi: https://doi.org/10.1016/j.egypro.2017.10.381. URL https://www.sciencedirect.com/science/article/pii/S187661021735364X.

Howared E Boyer. *Atlas of Fatigue Curves*. 1985.

Chinese Development Reform Commission China. Electricity price for chinese onshore wind turbine, 2017.

Deloitte. Establishing the wind investment case 2014. Report, Deloitte, 2014.

L Fingersh, M Hand, and A Laxson. Wind turbine design cost and scaling model. Report, National Renewable Energy Laboratory, 2006.

Peter Fuglsang and Kenneth Thomsen. Cost optimization of wind turbines for large-scale off-shore wind farms. Report, Riso National Laboratory, 1998.

J Harper, M Karcher, and M Bolinger. Wind project financing structures: A review and comparative analysis. Report, Lawrence Berkeley National Laboratory, 2007.

Kim Soo Hyun, Shin Hyung Ki, Joo Young Chul, and Kim Keon Hoon. A study of the wake effects on the wind characteristics and fatigue loads for the turbines in a wind farm. *Renewable Energy*, 74:536–543, 2015. ISSN 0960-1481. doi: https://doi.org/10.1016/j.renene.2014.08.054. URL http://www.sciencedirect.com/science/article/pii/S0960148114005242.

IRENA. Renewable energy technologies cost analysis series wind power. Report, International Renewable Energy Agency, 2012.

IRENA. Renewable power generation costs in 2017. Report, International Renewable Energy Agency, 2017.

Njiri Jackson and Söffker Dirk. State-of-the-art in wind turbine control: Trends and challenges. *Renewable and Sustainable Energy Reviews*, 60:377–393, 2016. ISSN 1364-0321. doi: https://doi.org/10.1016/j.rser.2016.01.110. URL http://www.sciencedirect.com/science/article/pii/S1364032116001404.

Peter Kall and Janos Mayer. *Stochastic Linear Programming Models Theory and Computation*, volume Second Edition. Springer, Zurich, 2010.

Wai Hou Lio, J.A. Rossiter, and Bryn L. Jones. A review on applications of model predictive control to wind turbines. *IEEE*, 2014. URL http://eprints.whiterose.ac.uk/80307/.

Mirzaei Mahmood, Göçmen Bozkurt Tuhfe, Giebel Gregor, Sørensen Poul Ejnar, and Poulsen Niels Kjølstad. Turbine control strategies for wind farm power optimization, 2015.

Rachit R Mathur, Jennifer A Rice, Andrew Swift, and Jamie Chapman. Economic analysis of lidar-based proactively controlled wind turbines. *Renewable Energy*, 103(Supplement C):156–170, 2017. ISSN 0960-1481. doi: https://doi.org/10.1016/j.renene.2016.10.069. URL http://www.sciencedirect.com/science/article/pii/S0960148116309466.

Ariola Mbistrova. Financing and investment trends 2016. Report, Wind Europe, 2017.

Angus McCrone. If interest rates turn, clean energy will find it tougher, 2016. URL https://about.bnef.com/blog/mccrone-interest-rates-turn-clean-energy-will-find-tougher/.

Eduardo José Novaes Menezes, Maurício Araújo Alex, and Bouchonneau da Silva Nadège Sophie. A review on wind turbine control and its associated methods. *Journal of Cleaner Production*, 174(Supplement C):945–953, 2018. ISSN 0959-6526. doi: https://doi.org/10.1016/j.jclepro.2017.10.297. URL http://www.sciencedirect.com/science/article/pii/S0959652617326021.

Zhang Mingming, Tan Bin, and Xu Jianzhong. Smart fatigue load control on the large-scale wind turbine blades using different sensing signals. *Renewable Energy*, 87:111–119, 2016. ISSN 0960-1481. doi: https://doi.org/10.1016/j.renene.2015.10.011. URL http://www.sciencedirect.com/science/article/pii/S0960148115303633.

Abdelhaq Mouida and Noureddine Alaa. Sensitivity analysis of tseb model by one-factor-at-a-time in irrigated olive orchard. *International Journal of Computer Science*, 8(3), 2011.

Adam Niesłony. Determination of fragments of multiaxial service loading strongly influencing the fatigue of machine components. *Mechanical Systems and Signal Processing*, 23(8):2712–2721, 2009. ISSN 0888-3270. doi: https://doi.org/10.1016/j.ymssp.2009.05.010. URL http://www.sciencedirect.com/science/article/pii/S0888327009001551.

M. Noda and R. G. J. Flay. A simulation model for wind turbine blade fatigue loads. *Journal of Wind Engineering and Industrial Aerodynamics*, 83(1):527–540, 1999. ISSN 0167-6105. doi: https://doi.org/10.1016/S0167-6105(99)00099-9. URL http://www.sciencedirect.com/science/article/pii/S0167610599000999.

Peter Elsborg Obling. Valuation models for wind farms under development. Report, Copenhagen Business School 2010, 2010.

Thomas Petru. *Modeling of Wind Turbines for Power System Studies*. Thesis, 2001.

Odgaard PF and Thogersen PB. Method for controlling a wind power park and a wind power park controlled by such method, 2013. URL http://www.google.sr/patents/US20130038060.

Wais Piotr. A review of weibull functions in wind sector. *Renewable and Sustainable Energy Reviews*, 70:1099–1107, 2017. ISSN 1364-0321. doi: https://doi.org/10.1016/j.rser.2016.12.014. URL http://www.sciencedirect.com/science/article/pii/S1364032116310565.

Kazacoks Romans and Jamieson Peter. Evaluation of fatigue loads of horizontal up-scaled wind turbines. *Energy Procedia*, 80:13–20, 2015. ISSN 1876-6102. doi: https://doi.org/10.1016/j.egypro.2015.11.401. URL http://www.sciencedirect.com/science/article/pii/S1876610215021335.

Nikolaos V Sahinidis. Optimization under uncertainty: state-of-the-art and opportunities. *Computers and Chemical Engineering*, 2003.

Hector Sanchez, Teresa Escobet, Vicenc Puig, and Peter Fogh Odgaard. Health-aware model predictive control of wind turbines using fatigue prognosis. *IFAC*, 2015. URL https://www.sciencedirect.com/science/article/pii/S2405896315018443.

Hector Sanchez, Teresa Escobet, Vicenc Puig, and Peter Fogh Odgaard. Health-aware model predictive control of wind turbines using fatigue prognosis. *Wiley*, 2017.

C Schram and P Vyas. Windpark turbine control system and method for wind condition estimation and performance optimization, 2007. URL https://www.google.ch/patents/US20070124025.

Dongran Song, Jian Yang, Xinyu Fan, Yao Liu, Anfeng Liu, Guo Chen, and Young Hoon Joo. Maximum power extraction for wind turbines through a novel yaw control solution using predicted wind directions. *Energy Conversion and Management*, 157:587–599, 2018. ISSN 0196-8904. doi: https://doi.org/10.1016/j.enconman.2017.12.019. URL https://www.sciencedirect.com/science/article/pii/S0196890417311676.

Tyler Stehly, Donna Heimiller, and George Scott. 2016 cost of wind energy reveiw. Report, National Renewable Energy Laboratory, 2017.

David Toke. Wind power costs 'could plunge below wholesale electricity prices', 2017. URL http://www.owjonline.com/news/view,wind-power-costs-could-plunge-below-wholesale-electricity-prices_50232.htm.

Petrović Vlaho and Bottasso Carlo L. Wind turbine envelope protection control over the full wind speed range. *Renewable Energy*, 111(Supplement C):836–848, 2017. ISSN 0960-1481. doi: https://doi.org/10.1016/j.renene.2017.04.021. URL http://www.sciencedirect.com/science/article/pii/S0960148117303269.

Petrović Vlaho, Jelavić Mate, and Baotić Mato. Advanced control algorithms for reduction of wind turbine structural loads. *Renewable Energy*, 76:418–431, 2015. ISSN 0960-1481. doi: https://doi.org/10.1016/j.renene.2014.11.051. URL http://www.sciencedirect.com/science/article/pii/S0960148114007812.

Liu Weipeng, Li Changgang, Liu Yutian, and Wu Qiuwei. Predictive control of wind turbine for load reduction during ramping events. *International Journal of Electrical Power and Energy Systems*, 93:135–145, 2017. ISSN 0142-0615. doi: https://doi.org/10.1016/j.ijepes.2017.05.025. URL `http://www.sciencedirect.com/science/article/pii/S0142061517300406`.

Alessandro Zanon, Michele De Gennaro, and Helmut Kühnelt. Wind energy harnessing of the nrel 5 mw reference wind turbine in icing conditions under different operational strategies. *Renewable Energy*, 115(Supplement C):760–772, 2018. ISSN 0960-1481. doi: https://doi.org/10.1016/j.renene.2017.08.076. URL `http://www.sciencedirect.com/science/article/pii/S0960148117308376`.